



University of Pennsylvania  
ScholarlyCommons

---

Publicly Accessible Penn Dissertations

---

Summer 8-14-2009

# Changes in Oxygen Tension Rapidly and Reversibly Regulate Macrophage Nitric Oxide Production

Mary A. Robinson

University of Pennsylvania Philadelphia, [marobins@vet.upenn.edu](mailto:marobins@vet.upenn.edu)

Follow this and additional works at: <http://repository.upenn.edu/edissertations>

 Part of the [Cell Biology Commons](#), and the [Cellular and Molecular Physiology Commons](#)

---

## Recommended Citation

Robinson, Mary A., "Changes in Oxygen Tension Rapidly and Reversibly Regulate Macrophage Nitric Oxide Production" (2009).  
*Publicly Accessible Penn Dissertations*. 17.  
<http://repository.upenn.edu/edissertations/17>

This paper is posted at ScholarlyCommons. <http://repository.upenn.edu/edissertations/17>  
For more information, please contact [libraryrepository@pobox.upenn.edu](mailto:libraryrepository@pobox.upenn.edu).

---

# Changes in Oxygen Tension Rapidly and Reversibly Regulate Macrophage Nitric Oxide Production

## **Abstract**

Macrophage nitric oxide (NO) production and hypoxia coexist during wound healing, and have been implicated in the pathogenesis and pathophysiology of multiple disease states including sepsis and cancer. Macrophages stimulated with pathogen associated molecular patterns (PAMPs) produce NO via inducible nitric oxide synthase (iNOS) from molecular O<sub>2</sub>, L-arginine, and NADPH. The first aim of this research was to characterize the degree and duration of hypoxia which would limit NO production by PAMPs stimulated macrophages. The second aim was to identify the contributing mechanism(s). Using a novel forced convection cell culture system, we demonstrated that NO production was rapidly (within seconds) and reversibly regulated by physiological and pathophysiological O<sub>2</sub> tensions (pO<sub>2</sub>). The effect of pO<sub>2</sub> on NO production was not mediated by changes in iNOS protein concentration or iNOS dimerization, implicating limitation of the reactant(s) as the predominant causative mechanism. In addition to O<sub>2</sub> limitation, hypoxia has the potential to affect NADPH and L-arginine availability. In PAMPs stimulated macrophages, NADPH is predominantly produced by the oxidative pentose phosphate cycle (OPPC). NO production directly correlated with OPPC activity over a wide range of pO<sub>2</sub>, and inhibition of NO production with the specific iNOS inhibitor, 1400W, significantly decreased OPPC activity. OPPC activity increased significantly in response to chemically mediated oxidative stress irrespective of pO<sub>2</sub>, and NO production was unaffected by increasing cellular oxidative stress, indicating that NADPH availability for NO production was not limited by hypoxia. L-arginine is required for iNOS dimerization, and iNOS dimerization was maintained or increased during hypoxic exposure, suggesting sufficient L-arginine was available. Furthermore, the effect of L-arginine depletion on NO production was much slower than the response observed due to changes in pO<sub>2</sub>. In conclusion, decreased O<sub>2</sub> availability is the predominant mechanism responsible for rapidly and reversibly limiting NO production by PAMPs stimulated macrophages exposed to acute hypoxia.

## **Degree Type**

Dissertation

## **Degree Name**

Doctor of Philosophy (PhD)

## **First Advisor**

Cynthia M. Otto

## **Second Advisor**

Cameron J. Koch

## **Keywords**

inducible nitric oxide synthase, substrate limitation, NO consumption, reactive nitrogen mediated stress, oxidative stress, inflammation

---

**Subject Categories**

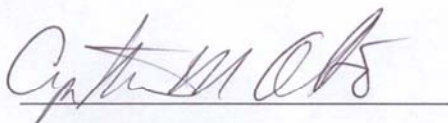
Cell Biology | Cellular and Molecular Physiology

**CHANGES IN OXYGEN TENSION  
RAPIDLY AND REVERSIBLY REGULATE  
MACROPHAGE NITRIC OXIDE PRODUCTION**

Mary Elissa Alles Robinson

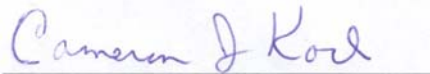
A DISSERTATION  
in  
Pharmacological Sciences

Presented to the Faculties of the University of Pennsylvania  
in Partial Fulfillment of the Requirements for the Degree  
of Doctor of Philosophy

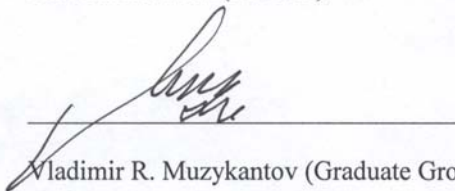


2009

Cynthia M. Otto (Advisor)



Cameron J. Koch (Advisor)



Vladimir R. Muzykantov (Graduate Group Chairperson)

## **DEDICATION**

I dedicate this thesis to my grandmother,

Ms. Dorothy Matern

whose battle with breast cancer ended too soon,  
and who inspired me to pursue biomedical research.

And

To my family and friends for all of their love and support.

## ACKNOWLEDGEMENTS

This work would not have been possible without the guidance and support of Dr. Cynthia M. Otto, Dr. James E. Baumgardner, Dr. Cameron J. Koch, Dr. Stephen W. Tuttle, Dr. Sydney Evans, Dr. Harry Ischiropoulos, Dr. Vladimir Muzykantov, Dr. Andrew Gow, Dr. Michael Atchison, Ms. Julia Fox, and Ms. Virginia Good. Financial support was provided by the VMSTP program at the University of Pennsylvania, the American Heart Association (AHA 0515359U), and the National Institutes of Health (NIH CA92108 and NIH T32 CA009677-17).

## ABSTRACT

### CHANGES IN OXYGEN TENSION RAPIDLY AND REVERSIBLY REGULATE MACROPHAGE NITRIC OXIDE PRODUCTION

Mary A. Robinson

Advisors: Cynthia M. Otto and Cameron J. Koch

Macrophage nitric oxide (NO) production and hypoxia coexist during wound healing, and have been implicated in the pathogenesis and pathophysiology of multiple disease states including sepsis and cancer. Macrophages stimulated with pathogen associated molecular patterns (PAMPs) produce NO via inducible nitric oxide synthase (iNOS) from molecular O<sub>2</sub>, L-arginine, and NADPH. The first aim of this research was to characterize the degree and duration of hypoxia which would limit NO production by PAMPs stimulated macrophages. The second aim was to identify the contributing mechanism(s). Using a novel forced convection cell culture system, we demonstrated that NO production was rapidly (within seconds) and reversibly regulated by physiological and pathophysiological O<sub>2</sub> tensions (pO<sub>2</sub>). The effect of pO<sub>2</sub> on NO production was not mediated by changes in iNOS protein concentration or iNOS dimerization, implicating limitation of the reactant(s) as the predominant causative mechanism. In addition to O<sub>2</sub> limitation, hypoxia has the potential to affect NADPH and L-arginine availability. In PAMPs stimulated macrophages, NADPH is predominantly produced by the oxidative pentose phosphate cycle (OPPC). NO production directly correlated with OPPC activity over a wide range of pO<sub>2</sub>, and inhibition of NO production with the specific iNOS inhibitor, 1400W, significantly decreased OPPC activity. OPPC activity increased significantly in response to chemically mediated oxidative stress

irrespective of  $pO_2$ , and NO production was unaffected by increasing cellular oxidative stress, indicating that NADPH availability for NO production was not limited by hypoxia. L-arginine is required for iNOS dimerization, and iNOS dimerization was maintained or increased during hypoxic exposure, suggesting sufficient L-arginine was available. Furthermore, the effect of L-arginine depletion on NO production was much slower than the response observed due to changes in  $pO_2$ . In conclusion, decreased  $O_2$  availability is the predominant mechanism responsible for rapidly and reversibly limiting NO production by PAMPs stimulated macrophages exposed to acute hypoxia.



## TABLE OF CONTENTS

Introduction	Macrophage NO Production Coexistence of NO Production and Hypoxia <i>in vivo</i> Hypoxic Affects on iNOS and NO production <i>in vitro</i> Hypoxic Affects on NADPH and L-Arginine Availability Specific Aims
Chapter 1.	Physiological and Hypoxic O <sub>2</sub> Tensions Rapidly Regulate NO production by Stimulated Macrophages
Chapter 2.	pO <sub>2</sub> Dependent NO Production Determines OPPC Activity in Macrophages
Chapter 3.	Effect of Changing Extracellular L-Arginine Concentration on Macrophage NO Production
Discussion	Acute Hypoxic Regulation of NO Production Implications for NO Physiology and Pathology Conclusions
Appendix	Hypoxic Cell Culture
Bibliography	

## LIST OF TABLES

- Chapter 1. Table 1. NO Consumption in DMEM.  
Table 2. Cell survival in DMEM and JBMEM.
- Chapter 2. Table 1. Effect of 1400W on RAW 264.7 NO<sub>x</sub> Production, OPPC activity, and TCA activity.

## LIST OF ILLUSTRATIONS

- Chapter 1. Figure 1. Forced Convection Cell Culture System.  
Figure 2. NO Consumption by Media  
Figure 3. Effect of PO<sub>2</sub> on NO Production.  
Figure 4. Effect of O<sub>2</sub> tension on iNOS protein concentration.  
Figure 5. Effect of O<sub>2</sub> tension on iNOS dimerization.  
Figure 6. Effect of NO and O<sub>2</sub> tension on cellular NO consumption.  
Figure S1. Dependence of cellular NO consumption on NO tension.  
Figure S2. Dependence of cellular NO consumption on PO<sub>2</sub>.
- Chapter 2. Figure 1. Schematic of the relationship investigated between NO<sub>x</sub> production and OPPC activity.  
Figure 2. EF5 binding in Glass Dishes versus Vials.  
Figure 3. NO<sub>x</sub> production, iNOS protein concentration, and iNOS dimerization in LPS and IFN $\gamma$  stimulated RAW 264.7 cells cultured with Thin Film Cell Culture.  
Figure 4. Correlation between OPPC activity and NO<sub>x</sub> production.  
Figure 5. OPPC Challenge with HEDS and PIMO.  
Figure 6. NO<sub>x</sub> production during OPPC challenge with HEDS and PIMO.
- Chapter 3. Figure 1. Effect of Changing Extracellular L-Arginine Concentration on Macrophage NO production.

## INTRODUCTION

### **Macrophage NO Production**

Macrophages are found throughout vertebrate and invertebrate tissues at all stages of life. They mediate tissue development and maintenance, and innate (pathogen pattern recognition) and adaptive (antigen presentation to T cells) immunity, but are also implicated in many disease states (208). The mononuclear phagocytic system classifies adult vertebrate macrophages based on their tissue phenotype and currently includes: inflammatory macrophages (M1 macrophages, aka classically activated macrophages), alternatively activated macrophages (M2 macrophages), dendritic cells, and tissue-resident macrophages such as alveolar macrophages (lung), osteoclasts and bone marrow macrophages (bone), microglia (brain), Langerhans cells (dendritic cells in the skin), crypt macrophages (intestine), Kupffer cells (liver), uterine dendritic cells and uterine macrophages (208).

Macrophages are bone marrow derived myeloid cells, and are continuously repopulated (84). Repopulation commonly occurs by extravasation and differentiation of monocytes from systemic circulation; half of the blood monocytes leave systemic circulation daily (84). Two populations of monocytes have been identified in circulation, one which responds to inflammation (M1 and M2 macrophages, dendritic cells), and one which repopulates noninflamed tissues (resident macrophages, some dendritic cells eg. Langerhans cells) (84). Thus, the monocyte lineage and the tissue microenvironment dictate monocyte extravasation, differentiation, and macrophage phenotype.

Macrophages exposed to bacterial and parasitic components, collectively termed pathogen associated molecular patterns (PAMPs), and to cytokines such as interferon  $\gamma$  (IFN $\gamma$ ), were among the first macrophages to be investigated as part of the innate immune system, and are referred to as classically activated or M1 macrophages (123, 208). A key component of the M1 macrophage phenotype is the production of nitric oxide (NO) by inducible nitric oxide synthase (iNOS) from molecular O<sub>2</sub>, L-arginine, and NADPH (148, 155, 245). The ability of M1 macrophages to produce NO is essential for the effective elimination of several types of infections (6, 94, 96, 215, 265). However, dendritic cells (233), microglia cells (14, 210, 234), and some tumor associated macrophages (typically thought to be M2 macrophages) (102), have also been demonstrated to upregulate iNOS, suggesting NO production and its effects may not be limited to M1 macrophages. In our studies of NO production, two stimuli known to induce macrophage iNOS were utilized: lipopolysaccharide (LPS) and IFN $\gamma$ .

LPS is the primary component of the outer membrane of gram-negative bacteria (5). LPS binding to CD14 and TLR4/MD2 on the macrophage cell surface results in signaling through multiple adaptor proteins including Src kinases, protein kinase C, PI3-kinase, mitogen activated protein kinases, phospholipase D, Gi/Go proteins, protein kinase A, FKBP12-rapamycin-associated protein, MyD88, IRAK, and TRAF6 (5, 25). Signaling through these proteins activates the transcription factors, NF $\kappa$ B, C/EBP, AP-1 (5, 25), and even HIF1 in normoxic differentiated macrophages (31, 195). NF $\kappa$ B, NF-IL6 (a C/EBP transcription factor), and HIF1 have been shown to bind to regions in the iNOS promoter and upregulate iNOS transcription (63, 95, 126, 163, 170, 181, 205, 288).

IFN $\gamma$  is produced by activated T lymphocytes and natural killer cells, and acts in a paracrine manner on macrophages (19, 60). IFN $\gamma$  binds to the IFN $\gamma$  receptor, which signals through the adaptor proteins JAK2, MEK1/2, and Erk1/Erk2 to activate the transcription factor STAT1 $\alpha$  (19, 29). STAT1 $\alpha$  binds to the iNOS promoter (80, 170, 288), and to the IRF-1 promoter (146), at the gamma-interferon activated site. STAT1 $\alpha$  and IRF-1 binding to the iNOS promoter is necessary for IFN $\gamma$  mediated upregulation of iNOS transcription (80, 139, 170, 174).

LPS and IFN $\gamma$  treatment of macrophages results in the upregulation of iNOS mRNA by 3 hours, and protein by 6 hours, with maximal protein concentration and activity observed at 24 hours (4, 61). NO production continues for up to 2 days (9), at which point the cells die via apoptosis (8, 224), most likely mediated by the continued exposure to nitrosative stress (103, 173). iNOS cleavage and degradation by calpain 1 (267, 268) and the ubiquitin-proteasome pathway (189) occurs with a half life of 1 ½ hours in atmospheric O<sub>2</sub> (145), suggesting continuous production of the enzyme is necessary to enable this prolonged NO production. For the experiments described herein, we chose to investigate the effects of acute hypoxia at 24 hours after LPS and IFN $\gamma$  stimulation of RAW 264.7 cells, a macrophage-like transformed cell line, to ensure robust and reproducible NO production.

### **Coexistence of Macrophage NO Production and Hypoxia *in vivo***

Molecular O<sub>2</sub> is a cosubstrate for NO production (148, 155), thus the partial pressure of oxygen (pO<sub>2</sub>) has the potential to affect macrophage function *in vivo*.

Physiological tissue pO<sub>2</sub> measurements are 5 to 71 Torr (23, 32, 37, 42, 87, 88, 124, 129,

159, 253, 254, 263, 266, 281, 282), indicating that even in the absence of hypoxia ( $pO_2 <$  the normal  $pO_2$  for the tissue), macrophages are exposed to a wide range of  $pO_2$ .

Macrophages are exposed to hypoxia when tissue  $pO_2$  decreases due to cardiovascular compromise and/or overwhelming metabolic demand, such as in the wound environment (116, 194, 213, 236) and in multiple inflammatory diseases: sepsis (118, 122), cancer (37, 38, 69, 70, 79, 111, 166), hypoxia-mediated pulmonary hypertension (154, 225), hypoxic brain injury (125, 196, 220), congenital heart defects (72), necrotizing enterocolitis (45), sleep apnea (75, 119, 295), asthma (17, 132, 289), cerebrovascular stroke (160), and atherosclerosis (28, 34, 43). Three examples will be discussed: wound healing, sepsis, and cancer.

The  $pO_2$  measured in the center of the wound environment can be as low as 0 to 2 Torr (225). Wound healing is typically thought to occur in three stages: inflammation, proliferation, and maturation (285). Consistent with this model, macrophages have been shown to express iNOS for the first 24 to 72 hours of healing, and to become the predominant cell type within the wound on days 3 to 5 (211). iNOS knockout mice have delayed wound healing, which can be improved with gene transfer of the human iNOS gene via an adenoviral vector (293), indicating that the presence of iNOS influences wound healing. Nitrite and nitrate, metabolites of NO, are increased in the wound fluid isolated from a sponge model of wound healing during the first 24 to 48 hours (177). However, hypoxia ( $\sim 0$  Torr) has been shown to limit wound macrophage NO production *in vitro*, and to result in the redirection of L-arginine metabolism to arginase (7). Further investigation of NO production by macrophages expressing iNOS in a hypoxic

environment is required to better understand how macrophages produces NO during wound healing.

Improper wound healing and bacterial invasion into systemic circulation can lead to the development of sepsis, a systemic inflammatory response (36). The progression of sepsis to acute respiratory distress syndrome (ARDS) and multiorgan failure (MOF) is one of the most frustrating syndromes to treat in human and animal emergency rooms and intensive care units due to the rapidity of its progression (within 24 to 48 hours), and to the high mortality rate in this patient population (20 to 50% in humans, 60% in dogs) (24, 64, 76, 175, 185, 228, 248). Patients initially become locally hypoxic due to the redirection of blood flow to the vital organs and increased metabolic demand, and subsequently become systemically hypoxic due to circulatory and pulmonary collapse (118). NO production by PAMPs stimulated macrophages has been implicated in this progression (44, 252).

Excessive amounts of nitrosylated and nitrated proteins, markers of endogenous NO production (91, 262), have been detected in urine, plasma, and affected organs from septic patients (86, 89, 140, 197, 243). iNOS has been demonstrated to directly bind, nitrosylate, and increase the activity of cyclooxygenase-2, even in the presence of oxyhemoglobin, an extracellular NO scavenger (137). Alternatively, some nitrated proteins have impaired function e.g. surfactant protein A can no longer aggregate lipids (101). The NO metabolite, peroxynitrite, inhibits oxygen consumption by alveolar type II cells (113), and mediates pulmonary cell damage and death (90). The ensuing hypoxia due to impaired pulmonary gas exchange is exacerbated by the concurrent circulatory dysfunction due to macrophage NO production. iNOS has a  $V_{max}$  that is 5 fold greater



than the  $V_{\max}$  for endothelial NOS (eNOS) and neuronal NOS (nNOS) (214). Thus, one of the major mechanisms contributing to generalized vasodilatation and septic shock is the larger amount of NO produced by macrophages in similar tissue microenvironments as endothelial cells (118, 252).

Because of these negative effects of NO production, nonspecific NOS inhibitors (i.e. inhibition of iNOS, eNOS, and nNOS) were tested in animal models of sepsis (55, 77, 133-135, 183, 198, 244, 256, 257), and in human Phase I (97, 117), II (21, 272), and III (167) clinical trials. Although effective in preventing the decrease in blood pressure observed due to septic shock (21, 55, 97, 133-135, 167, 244, 272), in the Phase III clinical trial patient mortality was ultimately increased, and the trial was terminated prior to completion (167). Specific inhibitors of iNOS have been shown to have some benefit in animal models (151, 161, 176, 199, 221, 249). However, bacterial sepsis in iNOS knockouts results in increased mortality (54), or no survival advantage (152, 193), probably due to the role of macrophage NO production in innate and adaptive immunity (6, 94, 96, 215, 265). Thus, even specific inhibition of iNOS needs to be carefully evaluated for its utility in treating septic patients. Macrophage NO production may already be limited due to the tissue hypoxia, and more information is needed to enable the development of NO targeted therapeutic strategies for sepsis.

A third example of macrophage exposure to hypoxia is within tumors. Hypoxia has been documented in 50 to 60% of all solid tumors (166), and has been shown to correlate with poor clinical outcome (37, 38, 69, 70, 79, 111, 166). Chronic inflammation has been linked to the development of cancer (162), and while tumor associated macrophages (TAM) are predominantly thought to have an M2 phenotype,

they have been demonstrated to express iNOS (235). Tumor cells themselves can also express iNOS (12, 104, 261), and increased serum nitrite and nitrate levels correlated with poor survival in lung cancer patients (56). However, some studies have shown that NO can inhibit tumorigenesis and metastasis, and whether NO is beneficial or detrimental has been proposed to depend on the location, degree, and timing of NO production (283, 284).

Anti-tumorigenic properties of NO include inhibition of mitochondrial respiration (65, 246) and the induction of apoptosis (103, 173). Pro-tumorigenic properties include genotoxic effects (71), increased iron uptake (66, 106, 255), promotion of angiogenesis (12, 261), and promotion of tumor growth and metastasis (50, 83, 207, 291). The p53 status of the tumor is one mechanism which appears to determine whether NO is pro- or anti-tumorigenic. p53 positive tumor cells typically undergo apoptosis due to NO exposure, whereas p53 negative cells have increased VEGF production, resulting in the promotion of angiogenesis (283).

In normoxic cells, NO increases VEGF production via HIF-1 $\alpha$  stabilization, DNA binding, and transcriptional activity (138, 204, 222, 223). However, in hypoxic cells, NO decreased HIF-1 $\alpha$  stabilization and HIF-1 activity (3, 114, 165, 238, 269), suggesting the presence of hypoxia can affect the pro- versus anti-tumorigenic status of NO. Hypoxia also stimulates VEGF production via HIF1 activation (15, 231, 274) and increases iron uptake (51, 255). A better understanding of the hypoxic effects on macrophage NO production is needed to elucidate how hypoxia and NO interact and contribute to cancer development and progression.

In summary, NO producing macrophages are exposed to a wide range of pO<sub>2</sub>, and the requirement of molecular O<sub>2</sub> for NO production (148, 155) suggests that tissue pO<sub>2</sub> has the potential to influence macrophage NO generation. The presence of macrophage NO production is a double edged sword for most diseases: some effects are beneficial while others are detrimental to the host. The affect of macrophage NO production on patient outcome (quality of life, and life vs. death) often seems to depend on the location, timing, and degree of NO production, all of which will be affected by tissue pO<sub>2</sub>. Thus, understanding the effects of pO<sub>2</sub> on macrophage NO production is essential to understanding the pathogenesis of multiple diseases.

### **Hypoxic Affects on NO production and iNOS *in vitro***

The effect of hypoxia on iNOS activity has been investigated in numerous models (1, 2, 13, 46, 67, 110, 136, 179, 182, 202, 214, 296). Consistent with the role of molecular O<sub>2</sub> as a cosubstrate (148, 155), NO production uniformly was decreased during hypoxia. However, the degree and duration of hypoxia required for this decrease, and the mechanisms mediating this effect, have not been clearly defined.

The apparent  $K_mO_2$  for isolated iNOS has been reported to be  $6.3 \pm 0.9 \mu\text{M}$  ( $5 \pm 0.6$  Torr) (214),  $130 \mu\text{M}$  (93 Torr) (1), and  $135 \mu\text{M}$  (96 Torr) (67). There are three possible mechanisms explaining the differences between the studies: 1) the source of iNOS, 2) the method of measurement, and 3) the method of pO<sub>2</sub> control. When NO was scavenged with oxyhemoglobin, the apparent  $K_mO_2$  was reduced approximately 4 fold from  $130 \mu\text{M}$  (93 Torr) to  $42 \mu\text{M}$  (30 Torr) (1). Abu-Soud et al. propose that the removal of NO feedback inhibition by the scavenging of NO with oxyhemoglobin mediates the

shift they measured in the apparent  $K_mO_2$  (1, 247). However, details regarding the contribution of additional  $O_2$  by oxyhemoglobin, a factor which could also cause a shift toward a lower apparent  $K_mO_2$ , are not available.

The apparent  $K_mO_2$  in stimulated macrophages has been investigated in two studies. In one study, nitrite was measured following treatment with LPS and IFN $\gamma$  for 24 hours at various  $pO_2$ , and a calculated apparent  $K_mO_2$  of  $10.8 \pm 2.0 \%$  ( $77 \pm 1.4$  Torr) was reported (179). Under similar culture conditions, Otto and Baumgardner measured a hypoxia mediated decrease in iNOS activity at the conclusion of the exposure period (18 hours) via the citrulline assay in cell lysates at atmospheric  $O_2$ , suggesting an effect of  $pO_2$  on the specific activity and/or the amount of active iNOS, in addition to reactant limitation (202). After normalizing nitrite production for changes in iNOS activity, and accounting for the  $O_2$  diffusion gradient from the headspace gas to the cell surface, their estimate for the apparent  $K_mO_2$  at the cell surface was 14 Torr (202). Thus, the reported apparent  $K_mO_2$  for iNOS spans a wide range (5 Torr to 96 Torr), making it difficult to assess which  $pO_2$  could regulate NO production *in vivo*.

The duration of hypoxia required for decreased macrophage NO production has not been previously investigated. Prior studies relied on indirect measurement of NO after 18 to 24 hours of concurrent exposure to LPS, IFN $\gamma$ , and hypoxia (179, 202). Therefore, the effects of hypoxia on iNOS upregulation could not be separated from the effects due to reactant limitation. The amount of active iNOS, and the iNOS velocity, during the 24 hour period may vary tremendously because of hypoxic effects on iNOS mRNA, iNOS protein concentration, iNOS dimerization, and reactant availability.

Hypoxic induction of iNOS is mediated by the transcription factor, HIF-1 (126, 205). HIF-1 is a dimer composed of HIF-1 $\alpha$  and HIF-1 $\beta$  subunits. Both subunits are constitutively expressed in most tissues (280). However, the HIF-1 $\alpha$  protein is rapidly degraded via the ubiquitin-proteasome pathway in the presence of O<sub>2</sub> (59, 229, 230). Hypoxia increases HIF-1 DNA binding to the iNOS hypoxia responsive element (HRE), which upregulates iNOS transcription (126), (205). Upregulation of iNOS in rat primary cardiac myocytes was measured at 12 hours (126). In contrast, hypoxic exposure durations  $\leq$  24 hours did not increase iNOS mRNA in the CRL-2192 alveolar macrophage cell line or in rat lungs (4). Exposure of rats to hypoxia (10% inspired pO<sub>2</sub>) for 3 weeks increased iNOS mRNA in the lung (147, 198). These results suggest the temporal effects of hypoxia on iNOS mRNA depends on the cell type. Co-stimulation of CRL-2192 alveolar macrophages with LPS or IFN $\gamma$  and hypoxia, or treatment of rats with LPS immediately prior to hypoxia (9% inspired pO<sub>2</sub>), expedited the upregulation of iNOS mRNA in the macrophages and in the lung, respectively, with an observed effect as early as 3 hours (4).

Hypoxic upregulation of iNOS mRNA has not always resulted in increased iNOS protein concentration. iNOS protein was decreased in LPS, IFN $\gamma$ , and hypoxia stimulated RAW 264.7 cells (24 hours (202)), and in TNF $\alpha$ , IL1 $\beta$ , and hypoxia stimulated rat pulmonary artery cells (296). In contrast, iNOS protein was increased in LPS or IFN $\gamma$  and hypoxia stimulated CRL-2192 macrophages (4) and ANA-1 macrophages (182), and in the lungs of rats treated with LPS, and then with 3, 6, or 12 hours of hypoxia (9% O<sub>2</sub>) (4). Rats maintained in hypoxia (10% O<sub>2</sub>) for 3 weeks were also shown to have increased iNOS protein in their lungs (154). Thus, the degree and duration of hypoxia, cytokine

concentration, combination of cytokines, and/or cell type appear to determine whether upregulated iNOS mRNA correlates with increased iNOS protein concentration.

Following the upregulation of iNOS mRNA and protein expression, dimerization is necessary for NO production (20). Dimerization requires BH<sub>4</sub> (20, 147, 209, 260, 275), heme (20, 239), and L-arginine (20). Preliminary data in our laboratory measured a decrease in the iNOS dimer:monomer ratio in RAW 264.7 cells costimulated with LPS, IFN $\gamma$ , and hypoxia (24 hours), which was fully reversible by L-sepiapterin, a pharmacologic source of BH<sub>4</sub> (201). Cytokine stimulation increases macrophage BH<sub>4</sub> concentration via increased activity of the rate limiting enzyme, GTP cyclohydrolase I (85, 276-278). Thus, these preliminary results suggest hypoxia may limit BH<sub>4</sub> availability despite increased activity of GTP cyclohydrolase I.

### **Hypoxic Affects on NADPH and L-arginine availability**

In addition to O<sub>2</sub> substrate limitation, hypoxia has been reported to affect NADPH and L-arginine availability. NADPH is produced by the oxidative pentose phosphate cycle (OPPC) in LPS and IFN $\gamma$  stimulated macrophages (58). An association between NADPH production by glucose 6 phosphate dehydrogenase (G6PD), the rate limiting enzyme of the OPPC, and NO production has previously been demonstrated in macrophages (57, 112, 180, 258), and pharmacologic inhibition of OPPC activity or G6PD deficiency was shown to significantly impair NO production (112, 180, 258). Classical studies have measured increased [NADPH] in response to short term hypoxia due to the absence of oxidizing agents (99, 127, 227, 259). More recently, however, decreased [NADPH] was measured in denuded bovine coronary arteries following brief

exposure to hypoxia (~ 8 to 10 Torr, 20 minutes (100)). The effect of hypoxia on macrophage OPPC activity and [NADPH] has not been investigated.

The concentration of L-arginine in cell culture media (JBMEM: 300  $\mu$ M, MEM: 700  $\mu$ M) is well above the apparent  $K_m$  for arginine (2.8  $\mu$ M; (245)), and is not expected to be limiting for these studies. In addition, LPS and hypoxia increase the mRNA of the arginine transporter, MCAT-2B (169), suggesting cellular L-arginine import is increased. However, hypoxia (24 hours) alone and in combination with LPS has also been shown to upregulate macrophage arginase (7, 169), which has been proposed to compete with iNOS for L-arginine as a substrate (48, 108, 250). Inhibition of arginase can increase NO production by stimulated macrophages, and vice versa (109). However, the interplay between iNOS and arginase is cell specific (226), cytokine specific (107, 270), and time dependent (270).

### **Specific Aims**

In summary, hypoxia has the potential to alter macrophage NO production by multiple mechanisms. Due to the difficulties of culturing cells at defined  $pO_2$ , and the difficulties of measuring NO production directly, previous studies were not able to evaluate the effects of an abrupt change in  $pO_2$  on NO production. Therefore, the first aim of this work was to measure macrophage NO production directly, and in real time, during precise and accurate step changes in  $pO_2$  using a novel forced convection cell culture system (Chapter 1). A decrease in NO production could be mediated by limitation of the reactant(s) or an effect on iNOS itself. Limitation of molecular  $O_2$  is the most intuitive mechanism. However, hypoxic exposure has also been documented to

affect the amount of active iNOS, and the availability of NADPH and L-arginine.

Therefore, the second specific aim of this work was to investigate the contribution of these alternate mechanisms to the regulation of NO production during acute hypoxia (Chapters 1, 2, and 3).



## CHAPTER 1.

### PHYSIOLOGICAL AND HYPOXIC O<sub>2</sub> TENSIONS RAPIDLY REGULATE NO PRODUCTION BY STIMULATED MACROPHAGES

Mary A. Robinson<sup>1,2,3</sup>, James E. Baumgardner<sup>4,5</sup>, Virginia P. Good<sup>2</sup>, and Cynthia M. Otto<sup>1,2</sup>.

<sup>1</sup>Department of Clinical Studies-Philadelphia, School of Veterinary Medicine, University of Pennsylvania Philadelphia PA 19104; <sup>2</sup>Center for Sleep and Respiratory Neurobiology, University of Pennsylvania Philadelphia PA 19104; <sup>3</sup>Department of Radiation Biology, School of Medicine, University of Pennsylvania Philadelphia PA 19104; <sup>4</sup>Department of Anesthesiology and Critical Care, School of Medicine, University of Pennsylvania Philadelphia PA 19104; <sup>5</sup>Oscillogy, LLC Folsom PA 19033.

Published on February 13<sup>th</sup>, 2008 in the American Journal of Physiology Cell Physiology  
Volume 294, Pages 1079 – 1087

## ABSTRACT

NO production by inducible nitric oxide synthase (iNOS) is dependent on O<sub>2</sub> availability. The duration and degree of hypoxia which limit NO production are poorly defined in cultured cells. To investigate short term O<sub>2</sub>-mediated regulation of NO production, we used a novel forced convection cell culture system to rapidly (response time = 1.6 seconds) and accurately ( $\pm 1$  Torr) deliver specific O<sub>2</sub> tensions (from  $< 1$  to 157 Torr) directly to a monolayer of LPS and IFN $\gamma$  stimulated RAW 264.7 cells while simultaneously measuring NO production via an electrochemical probe. Decreased O<sub>2</sub> availability rapidly ( $\leq 30$  seconds) and reversibly decreased NO production with an apparent  $K_mO_2$  of 22 (SD 6) Torr (31  $\mu$ M) and a  $V_{max}$  of 4.9 (SD 0.4) nmol/min $\cdot 10^6$  cells. To explore potential mechanisms of decreased NO production during hypoxia, we investigated O<sub>2</sub>-dependent changes in iNOS protein concentration, iNOS dimerization, and cellular NO consumption. iNOS protein concentration was not affected ( $p = 0.895$ ). iNOS dimerization appeared to be biphasic (6 Torr ( $p \leq 0.008$ ) and 157 Torr ( $p \leq 0.258$ )  $> 36$  Torr), but did not predict NO production. NO consumption was minimal at high O<sub>2</sub> and NO tensions and negligible at low O<sub>2</sub> and NO tensions. These results are consistent with O<sub>2</sub> substrate limitation as a regulatory mechanism during brief hypoxic exposure. The rapid and reversible effects of physiological and pathophysiological O<sub>2</sub> tensions suggest that O<sub>2</sub> tension has the potential to regulate NO production *in vivo*.

## INTRODUCTION

Macrophage NO production via inducible nitric oxide synthase (iNOS) is a key component of the cellular inflammatory response (33, 172). *In vivo*, *in vitro*, and isolated enzyme experiments have clearly demonstrated the dependence of NO production on O<sub>2</sub> tension for all 3 of the NOS isoforms (1, 2, 13, 46, 67, 110, 136, 179, 182, 202, 214, 296). Normal non-pulmonary tissue O<sub>2</sub> tensions range from 5 to 71 Torr (23, 37, 42, 124, 129, 263, 282), and systemic and/or tissue hypoxia develops during several inflammatory diseases (42, 75, 122), extending the range for tissue macrophages to even lower levels. Alveolar macrophages can be exposed to O<sub>2</sub> tensions ranging from approximately 30 Torr (mixed venous O<sub>2</sub> tension with atelectasis) to over 650 Torr (with O<sub>2</sub> therapy) (279). Thus, macrophages must function over a wide range of physiologic and pathophysiological O<sub>2</sub> tensions, and O<sub>2</sub> tension has the potential to regulate macrophage NO production (67, 179, 202, 214). It is currently unknown, however, if the macrophage response to changing O<sub>2</sub> tension is rapid enough for O<sub>2</sub> to play a role in the regulation of NO production.

Prior studies have explored the long-term effects (18 and 24 hours) of culture PO<sub>2</sub> (partial pressure of O<sub>2</sub>) on nitrite production in LPS and IFN $\gamma$  stimulated RAW 264.7 cells, but estimates of the apparent  $K_mO_2$  have varied considerably. McCormick et al. reported an apparent  $K_mO_2$  of 10.8% (77 Torr) for the PO<sub>2</sub> in the headspace gas (179). In contrast, Otto and Baumgardner estimated the apparent  $K_mO_2$  at the cell surface to be 14 Torr, after normalizing to iNOS activity and accounting for the O<sub>2</sub> diffusion gradient through the media layer (202). This wide range of reported  $K_mO_2$  may be in part due to

difficulties in accurately controlling headspace (202, 242) and cellular (22, 202) PO<sub>2</sub> in conventional cell culture.

No prior studies of macrophage NO production explored the effects of short-term exposure to different O<sub>2</sub> tensions, primarily due to the limitations of conventional cell culture and NO analysis methods. First, diffusion of O<sub>2</sub> through the media covering cells cultured in dishes can be slow, requiring as long as 30 minutes for a change in headspace PO<sub>2</sub> to be translated to the cell surface (10, 22). Second, the sensitivity of nitrite measurement via the Griess method, which integrates NO production over the period of the experiment, is not adequate for short time periods with less NO accumulation (121, 179, 202).

Forced convection cell culture utilizes a continuous flow of media to deliver O<sub>2</sub> and nutrients directly to the cell monolayer, and to remove waste products (22). Because this method of cell culture overcomes the limitations of extracellular O<sub>2</sub> diffusion, it is ideally suited for measuring the effects of rapid changes in O<sub>2</sub> tension. In addition, the system used for the present study controls O<sub>2</sub> tensions with an accuracy of about 1 Torr, and permits rapid, direct measurement of changes in NO in the effluent using a sensitive electrochemical probe (216, 217). Thus, the first goal of our current study was to use this recently developed method to accurately define the PO<sub>2</sub> dependence of NO production by LPS and IFN $\gamma$  stimulated RAW 264.7 cells, after brief exposures to a range of physiological and hypoxic O<sub>2</sub> tensions.

The second goal of our study was to evaluate three mechanisms that could alter NO production after brief hypoxic exposures. The oxygen atom in NO is derived from molecular O<sub>2</sub> (148, 155). Prior cell culture studies which used long term exposures to

varying O<sub>2</sub> tensions, and studies with isolated nitric oxide synthases (NOS), have emphasized the potential role of O<sub>2</sub> as a rate-limiting substrate (67, 179, 202, 214). O<sub>2</sub> has also been shown to participate in more complex interactions with the NOS enzyme than simple substrate dependence (247). These mechanisms could operate on a short enough time scale to alter NO production after brief hypoxic exposures. There are, however, several additional opportunities for changes in PO<sub>2</sub> to rapidly influence NO production. Our goal was to evaluate three of these additional mechanisms: changes in the cellular levels of inducible NOS (iNOS) protein, changes in iNOS dimerization, and changes in cellular NO consumption. We hypothesized that: 1) brief hypoxic exposures would reduce NO production by reducing iNOS protein; 2) brief hypoxic exposures would reduce NO production by reducing iNOS dimerization; and 3) brief hypoxic exposures would reduce NO production and release from the cell by increasing intracellular consumption of NO.

## **MATERIALS AND METHODS**

### **Forced Convection Cell Culture.**

RAW 264.7 cells (American Type Culture Collection, Manassas, VA) were cultured using a novel forced convection cell culture system as described previously (22). Briefly, cells were aspirated through a ProNectin<sup>®</sup> F-coated (0.1mg/ml; Sigma, St Louis, MO) 0.53 mm diameter, 10 cm long fused-silica capillary column (Alltech, Deerfield, IL), allowed to adhere for 15 minutes, and cultured with forced convection in air with 5% CO<sub>2</sub> for 18 to 22 hours in the presence of 1 µg/ml LPS (E. coli O111:B4; Sigma) and 100

U/ml CHO-derived recombinant mouse IFN $\gamma$  (Cell Sciences, Canton, MA) in DMEM (Gibco, Carlsbad, CA) supplemented with 5% heat-inactivated FBS (LONZA, Visp, Valais, Switzerland) and 1% antibiotic/antimycotic (penicillin, streptomycin, fungizone; Life Technologies, Gaithersburg, MD). Following stimulation, the column of cells was transferred to the forced convection cell culture system (Figure 1).

Experiments were performed in a minimal essential media (JBMEM: 140 mM NaCl, 1.4 mM CaCl<sub>2</sub>, 5.3 mM KCl, 4.4 mM Dextrose, 25 mM HEPES, 0.3 mM L-arginine, and 0.1% heat-inactivated FBS (LONZA)) equilibrated with 0, 0.7, 3.6, 8.4, 15.2, 25.8, 38.0, 85.3, or 159.6 Torr O<sub>2</sub> (5% CO<sub>2</sub>, balance N<sub>2</sub>) from certified premixed compressed gas cylinders (AirGas, Allentown, PA). Corresponding estimates of average cellular PO<sub>2</sub>, after accounting for cellular O<sub>2</sub> consumption, were 0, < 1, 1, 6, 13, 24, 36, 83, or 157 Torr O<sub>2</sub> (22). Upon completion of experiments, the fluid was briefly switched to PBS equilibrated with the experimental O<sub>2</sub> tension, and then the column of cells was removed from the system and immediately frozen at -70°C.

### **Measurement of Effluent NO Tension.**

NO was detected using a 2 mm NO electrode (NOP, World Precision Instruments, Sarasota, FL) filled with a CO<sub>2</sub> insensitive electrolyte (World Precision Instruments). To enable calibration of the NO electrode, the forced convection cell culture system was adapted to allow defined amounts of NO (input NO) to be added to the fluid stream (Figure 1). Deionized H<sub>2</sub>O (dH<sub>2</sub>O) was deoxygenated via a membrane equilibrator with certified ultra high purity N<sub>2</sub> (AirGas), then equilibrated via a second membrane equilibrator with 2000 ppm NO in N<sub>2</sub> (AirGas). As in our prior report (6), function of all

membrane equilibrators was tested by confirming flow independence of the measured gas partial pressure in the equilibrator effluent. Defined amounts of 2000 ppm NO-containing dH<sub>2</sub>O were injected into the fluid stream using a syringe pump (Harvard Apparatus, Holliston, MA). The electrode was calibrated with input P<sub>NO</sub> of 19, 40, 79, 160, 319, and 500 ppm at the beginning of each day. In the forced convection system, the measured 0-95% time constant for the probe was 27 seconds. Due to NO probe baseline drift during experiments, the NO probe baseline was measured regularly (i.e. ≤ 5 minute intervals) to allow for manual baseline correction of the data.

All NO measurements were performed in JBMEM, which was designed to minimize media NO consumption while maintaining cell viability. To evaluate NO consumption by JBMEM, the forced convection system depicted in Figure 1 was modified by inserting two lengths of fused silica (13 cm and 30 cm) between the NO input site (labeled T in Figure 1) and the outlet valve (labeled B in Figure 1), resulting in exposure of NO to the media for 9 and 18 seconds, respectively. The NO signal was recorded for each exposure duration at two input P<sub>NO</sub> (160 and 320 ppm), and at three PO<sub>2</sub> (0, 40 and 80 Torr). PO<sub>2</sub> dependence of NO consumption in JBMEM was further investigated after restoring the system to the configuration of Figure 1 (i.e. 16 cm of tubing between the NO input and the inlet valve, labeled A in Figure 1, and 10 cm of tubing between the inlet valve and the outlet valve) in the absence of cells at five P<sub>NO</sub> (40, 79, 160, 319, 500 ppm) and six PO<sub>2</sub> (0, 15, 26, 38, 85, 160 Torr). To test if JBMEM was sufficient to support cell viability, RAW 264.7 cells were seeded onto 6 well plates (9.5 cm<sup>2</sup>) and cultured in a humidified incubator (room air, 37°C, 5% CO<sub>2</sub>) in either DMEM or JBMEM. Viability was measured by Trypan blue staining after 2, 6 or 18 hours of

culture. Cells were evaluated with and without stimulation (1 µg/ml LPS and 100 U/ml IFN $\gamma$  initiated 18 hours prior to seeding).

### **Electrophoresis and Immunoblotting.**

Cell lysates were prepared from columns by aspirating ice cold protease-inhibitor containing hypotonic lysis buffer (PIB: 10 µM phenylmethylsulfonyl fluoride (ICN Biochemical, Aurora, OH), 5 µg/ml aprotinin (Sigma), and 5 µg/ml pepstatin (Amresco, Solon, OH) in dH<sub>2</sub>O) through each column. Cell lysate protein concentrations were measured using the Biorad DC protein assay (Hercules, CA).

Proteins (10 µg) were separated on a 7.5% Tris-HCl gel using SDS PAGE or low temperature SDS PAGE (LT SDS PAGE) as previously described (287), except the final  $\beta$ -mercaptoethanol concentration for samples subjected to LT SDS PAGE was 0.1% (v/v). Proteins were transferred to polyvinylidene fluoride (Immobilon<sup>TM</sup>-FL 0.2µm; Millipore, Bedford, MA) and immunoblotted for iNOS (1:1000 to 1:2000; NOS2 M19 sc650, Santa Cruz Biotechnology, Inc., Santa Cruz, CA) and the loading control, Raf-1 (1:200 to 1:500; Raf-1 sc227, Santa Cruz Biotechnology, Inc.). Primary antibodies were immunocomplexed with IRDye<sup>TM</sup> 800 goat anti-rabbit (1:20,000; Rockland, Gilbertsville, PA). Proteins were detected, documented, and analyzed using an Odyssey Imaging System and software (LiCor Biosciences, Lincoln, NE).

### **Cellular NO Consumption.**

Endogenous NO production by LPS and IFN $\gamma$  stimulated RAW 264.7 cells cultured in the forced convection system was inhibited by a 36 to 48 minute exposure to



100  $\mu$ M N-[[3-(aminomethyl)phenyl]methyl]-ethanimidamide, dihydrochloride (1400W; Cayman Chemical, Ann Arbor, MI) in JBMEM lacking L-arginine. Maximal NO inhibition by 1400W (86 SD 7 % of basal NO production;  $n = 8$ ), was expedited by 3 to 4 periods of stopped flow for 5 minutes followed by 7 minutes of flow. Once maximal inhibition of endogenous NO production was achieved, cells were returned to JBMEM with L-arginine and were sequentially exposed to input  $P_{NO}$  of 40, 79, 160, 319, 500, and 0 ppm in the presence of 6, 36, or 83 Torr  $O_2$ . Average effluent  $P_{NO}$  was recorded for each input  $P_{NO}$  once steady state was achieved, and was compared to average effluent  $P_{NO}$  recorded on the same day for the same input  $P_{NO}$  in the absence of cells. The difference between effluent  $P_{NO}$  with cells and without cells for each input  $P_{NO}$  was assumed to be due to the net result of NO consumption and residual endogenous NO production. Testing for zero order, first order, or higher order dependence of NO consumption on  $P_{NO}$  and  $PO_2$  was performed, and the data were analyzed, by considering a mass balance on the cell column:

$$(\text{NO entering the column}) - (\text{NO leaving the column}) = \text{consumption} - \text{production}$$

Production represents the small amount of residual cellular NO production that was not inhibited by 1400W treatment. Consumption represents overall cellular degradation of NO from all irreversible and slowly reversible reactions, for example reaction with superoxide to form peroxynitrite (30, 115), conversion to nitrate via the iNOS futile pathway (247), nitrosylation, nitration and oxidation of proteins (92), autoxidation (74, 164), and other reactions (74, 212).

Our analysis assumes that NO production is independent of NO concentration, since the range of NO concentrations we studied is below the range associated with NO feedback inhibition of inducible nitric oxide synthase (iNOS) (1). Consumption is modeled, as a starting point, as first order in both NO and O<sub>2</sub> (251). It is known that autoxidation is second order in NO and first order in O<sub>2</sub> (74), but the reaction is too slow to consume NO before it reaches the electrode. Additionally, our data were calibrated to the effluent P<sub>NO</sub> detected for the five input P<sub>NO</sub> in JBMEM in the absence of cells and O<sub>2</sub>. Therefore, the detected NO consumption in our experiments is expected to be dominated by intracellular consumption reactions. The mass balance on the column of cells becomes

$$Q\alpha_{NO}(P_{NOi}-P_{NOe}) = k_cN (PO_2)(P_{NO}) - f(PO_2)k_pN$$

Where:

- Q is the media flow rate through the column (4.27x10<sup>-6</sup> L/sec)
- $\alpha_{NO}$  is the NO solubility in media at 37°C (2.13x10<sup>6</sup> pM/Torr) (271)
- P<sub>NOi</sub> is the NO partial pressure in media entering the column (Torr)
- P<sub>NOe</sub> is the NO partial pressure in media leaving the column (Torr)
- k<sub>c</sub> is the consumption rate constant (pmol NO/ cell·sec·Torr<sup>2</sup>)
- PO<sub>2</sub> is the average oxygen partial pressure for cells in the column
- P<sub>NO</sub> is the average NO partial pressure for cells in the column
- f(PO<sub>2</sub>) is the functional dependence of NO production on PO<sub>2</sub>
- k<sub>p</sub> is the maximal NO production for each column at high PO<sub>2</sub> (pmol NO/ cell·sec)

N is the number of cells in the column

### **Statistics.**

Comparison of means were tested by a one way ANOVA for each  $P_{NO}$  for  $PO_2$  dependent NO consumption in the absence of cells (Figure 2), a two way ANOVA for the effects of DMEM versus JBMEM over time on cell survival (Table 2), and a three way ANOVA for the effects of input  $P_{NO}$ ,  $PO_2$  and exposure time on NO degradation in JBMEM using SigmaStat version 3.1. All other statistics were performed using GraphPad InStat version 3.06 for Windows 95, GraphPad Software, San Diego, CA, [www.graphpad.com](http://www.graphpad.com). Changes in NO production with repeated cycling between 0 and 36 Torr  $O_2$  (Figure 3A) were tested by linear regression. The apparent  $K_m$  and  $V_{max}$  were calculated by SigmaPlot Enzyme Kinetics Module 1.1 using a Michaelis-Menten non-linear analysis (Figure 3C). Comparison of means for iNOS protein concentration data (Figure 4) were tested by one-way ANOVA. Comparison of means for iNOS dimerization data (Figure 5) were tested by pair-wise t-tests with a Bonferroni correction. Testing of the NO consumption model was performed with linear regression as described in Appendix A.

## RESULTS

### Characteristics of JBMEM.

In the absence of O<sub>2</sub> and cells, NO was rapidly consumed in DMEM by many of its components (Table 1), consistent with previous reports(39, 47, 131). Consumption of 160 and 320 ppm NO in JBMEM was investigated in the absence of cells at 0, 40, and 80 Torr O<sub>2</sub> by varying exposure duration. Exposure duration (9 versus 18 seconds) and PO<sub>2</sub> had no effect on the measured NO signal ( $n \geq 2$ ;  $p = 0.516$  and  $p = 0.201$ , respectively), indicating negligible consumption by the media for exposures less than 18 seconds. Consistent with these observations, PO<sub>2</sub> dependent NO consumption in JBMEM was not detectable for any of the input P<sub>NO</sub> investigated with the system in its standard configuration as depicted in Figure 1, with a 15 second transit time from the NO input to the NO electrode (Figure 2;  $n = 3$ ; 500 ppm,  $p = 0.152$ ; 319 ppm,  $p = 0.264$ ; 160 ppm,  $p = 0.370$ ; 79 ppm,  $p = 0.951$ ; 40 ppm,  $p = 0.468$ ). For all subsequent experiments, NO consumption during the approximately 3.5 second average transit time from the cells to the NO electrode was therefore considered negligible.

In unstimulated cells, there was a small but significant reduction of cell viability with JBMEM (Table 2;  $p = 0.028$ ). There was no detectable effect of time ( $p = 0.074$ ) or interaction between media type and time ( $p = 0.601$ ). In cells cultured with LPS and IFN $\gamma$ , no significant effect of media ( $p = 0.364$ ) or time ( $p = 0.894$ ) was detected.

### Effect of O<sub>2</sub> tension on effluent P<sub>NO</sub>.

Steady-state NO release by LPS and IFN $\gamma$  stimulated RAW 264.7 cells exposed to 36 Torr O<sub>2</sub> was 3.08 (SD 1.14) nmol/min·10<sup>6</sup> cells ( $n = 5$ ). Unstimulated cells did not

produce detectable NO (data not shown). Exposure of the cells to 0 Torr O<sub>2</sub> decreased effluent P<sub>NO</sub> within 30 seconds to an undetectable amount (Figure 3A). Similarly, within 30 seconds of re-exposure to 36 Torr O<sub>2</sub>, effluent P<sub>NO</sub> was greater than or equal to the initial measured concentration. Repeated cycling between 0 Torr (2 minutes) and 36 Torr O<sub>2</sub> (3 minutes) consistently produced these rapid changes in effluent P<sub>NO</sub> with a cumulative 10% increase in effluent P<sub>NO</sub> over a period of 40 minutes ( $p < 0.0001$ ,  $n = 2$ ). Unstimulated cells subjected to identical cycling patterns between 0 Torr and 36 Torr O<sub>2</sub> for 40 minutes did not produce detectable NO (data not shown).

Exposure of LPS and IFN $\gamma$  stimulated RAW 264.7 cells to a range of O<sub>2</sub> tensions elicited corresponding changes in effluent P<sub>NO</sub>, which predominantly followed a Michaelis-Menten kinetic model (Figure 3B). A non-linear analysis computed an apparent  $K_m$ O<sub>2</sub> of 22 (SD 6) Torr and  $V_{max}$  of 4.9 (SD 0.4) nmol/min $\cdot$ 10<sup>6</sup> cells ( $n = 5$ ,  $R^2 = 0.80$ ). A slight deviation from a smooth monotonic function is apparent between 6 and 36 Torr O<sub>2</sub> (Figure 3C).

### **Effect of O<sub>2</sub> tension on iNOS.**

O<sub>2</sub> tension did not influence iNOS protein concentration (Figure 4,  $n \geq 4$ ,  $p = 0.895$ ), but did influence the bands thought to contain iNOS dimers (Figure 5,  $n = 3$ ). In the western blot derived from the partially denaturing gel, three bands were present: a band corresponding to the expected monomer molecular weight (~130 kD) (49), a band corresponding to the expected dimer molecular weight (~260 kD), and an unexpected band of much higher molecular weight ( $\geq 500$  kD). Compared to 36 Torr, the ratio of the 260 kD band to the 130 kD band was significantly increased in lysates from samples at 6

Torr ( $p = 0.003$ ). A similar finding was observed for the ratio of the 500 kD band to the 130 kD band ( $p = 0.008$ ). The ratios also appeared to increase in lysates from samples at 157 Torr, but the increase did not achieve statistical significance (260 kD ratio  $p = 0.258$ , 500 kD ratio  $p = 0.129$ ).

### **Effect of NO and O<sub>2</sub> tension on cellular NO consumption.**

Following 1400W inhibition of endogenous NO production (Figure 6A), LPS and IFN $\gamma$  stimulated RAW 264.7 cells at 6, 36, or 83 Torr O<sub>2</sub> were exposed to five input P<sub>NO</sub> (Figure 6B). Data are presented in Figure 6C as the ratio of effluent P<sub>NO</sub> with cells to effluent P<sub>NO</sub> without cells. Net cellular NO consumption, as indicated by a ratio less than 1, was evident at input P<sub>NO</sub> of 160, 319, and 500 ppm in PO<sub>2</sub> of 36 and 83 Torr.

Calculations based on known autoxidation rate constants (74, 164) estimated that autoxidation within the cells could account for a maximum of 3% of the measured NO consumption. Cellular consumption was negligible at a PO<sub>2</sub> of 6 Torr, regardless of the input P<sub>NO</sub>. Net cellular NO production resulted in a ratio greater than 1 for the lower two input P<sub>NO</sub> (40 and 79 ppm) delivered in the lower two PO<sub>2</sub> (36 and 83 Torr). The amount of NO production was consistent with the residual cellular NO that was not inhibited by 1400W. Immediately following 1400W treatment, mean cellular NO production was 14% (SD 7) ( $n = 8$ ) of initial NO production. By the end of the experiment, cellular production increased to 24% (SD 6) ( $n = 7$ ) of initial NO production. The relationship between net cellular NO consumption and P<sub>NO</sub> was most consistent with 1<sup>st</sup> order kinetics. NO consumption also correlated positively with PO<sub>2</sub> in a 1<sup>st</sup> order-dependent manner at all P<sub>NO</sub>. The overall consumption constant ( $k_c$ ) for the model was 0.038 pmol NO/sec $\cdot$ 10<sup>6</sup>

cells·Torr<sup>2</sup> [12.7 (mmol NO)/(sec·10<sup>6</sup> cells·M<sup>2</sup>)]. Details of the consumption model are presented in Appendix A.

## DISCUSSION

Our study examined the effects of brief exposures to O<sub>2</sub> tensions, ranging from < 1 Torr to 157 Torr, on the production and release of NO by stimulated macrophages. Decreased PO<sub>2</sub> rapidly and reversibly decreased NO production, with an apparent  $K_mO_2$  of 22 (SD 6) Torr. Short term hypoxic exposures did not affect iNOS protein levels, but did influence iNOS dimerization. Surprisingly, however, iNOS dimerization did not predict NO production. NO consumption was small at high cellular O<sub>2</sub> and NO tensions and was negligible at low O<sub>2</sub> and NO tensions.

Our measured apparent  $K_mO_2$  is within the range of values reported previously for long term exposures in macrophage cell culture (179, 202), and for the isolated iNOS enzyme (1, 67, 214). It is also well within the range of PO<sub>2</sub> that would be required for O<sub>2</sub> tension to regulate NO production *in vivo*, as has been suggested previously (1, 67, 179, 202, 214). Our study additionally demonstrated, however, that precisely controlled changes in extracellular O<sub>2</sub> tension altered NO production by intact isolated cells within seconds, and that this effect was immediately reversible. A slow response, or an irreversible response, would have argued against any role for the regulation of NO production by PO<sub>2</sub> changes in intact cells. Instead, the effect on cellular NO production was rapid and reversible, further supporting a significant regulatory role for O<sub>2</sub> tension *in vivo*.

Several studies have investigated PO<sub>2</sub> dependence of NO production in intact tissues, and *in vivo*. NO production has been shown to be rapidly decreased by hypoxia when the primary enzyme responsible for NO production was thought to be endothelial



NOS (eNOS) (110, 136), iNOS (67), or neuronal NOS (nNOS) (292). O<sub>2</sub>-mediated intracellular kinetics and regulatory mechanisms, however, are difficult to evaluate *in vivo* and in tissue models due to the complications of tissue structure and O<sub>2</sub> delivery dynamics. Tissues are by definition composed of several different cell types with the potential for expression of several different NOS isoforms, and it is often difficult to unequivocally define which isoform is primarily responsible for producing the measured NO. For example, in bronchial airways each isoform is expressed in different cells (35, 67), and in different regions of the same cells (35, 290). This could have important effects on total NO production, as the  $K_mO_2$  for each isoform varies markedly in isolated enzyme studies (1, 214). Although tissue and *in vivo* studies are not directly comparable to our cell culture study, they do support the concept that NO production can be rapidly regulated by changes in O<sub>2</sub> tension *in vivo*.

We are not aware of any prior cell culture studies of NO production during brief exposure to hypoxia for the direct comparison to our results. Two prior studies, however, investigated the effects of long term exposure ( $\geq 18$  hours) to multiple O<sub>2</sub> tensions on nitrite production by RAW 264.7 cells concurrently stimulated with LPS and IFN $\gamma$  (179, 202). McCormick et al. measured cellular nitrite production following 24 hours of exposure to various headspace O<sub>2</sub> tensions ranging from 1% to 21% (7 to 150 Torr). The decrease in nitrite production at low O<sub>2</sub> tensions was well described by a hyperbolic curve fit, and the apparent  $K_mO_2$  for the headspace gas was 10.8% (77 Torr) (179). Otto and Baumgardner measured cellular nitrite production following 18 hours of exposure to various headspace O<sub>2</sub> tensions ranging from 1 to 677 Torr. Nitrite production decreased with decreasing O<sub>2</sub> tension throughout the entire range. iNOS activity in cell lysates,

defined by citrulline production in room air at 25°C, also showed substantial dependence on cellular PO<sub>2</sub> prior to lysis, suggesting an effect of O<sub>2</sub> tension on specific activity and/or the amount of active iNOS. After normalizing nitrite production for changes in iNOS activity, and accounting for the O<sub>2</sub> diffusion gradient from the headspace gas to the cell surface, their estimate for the apparent  $K_mO_2$  at the cell surface was 14 Torr (202). Studies of long term exposures to different O<sub>2</sub> tensions are not strictly comparable to the short term exposures of the current study due to the many factors that could change slowly over time. For example, O<sub>2</sub> dependent changes in the transcription and translation of iNOS (4, 126, 179, 181, 182, 202), as well as of other relevant proteins (e.g. mediators of arginine metabolism (169)), would be expected to take several hours (4) and could substantially influence NO production in long term exposures, yet have minimal impact in short term exposures.

Three prior studies have investigated the apparent  $K_mO_2$  for isolated iNOS. Using a steady state kinetics approach, Rengasamy and Johns measured citrulline production at various PO<sub>2</sub> by iNOS within a RAW 264.7 cell lysate. In their system, O<sub>2</sub> tension was rigidly controlled in the headspace gas by use of continuous gas flows, and the reaction mixture was constantly stirred to minimize diffusion gradients. They reported an apparent  $K_mO_2$  for iNOS of 6.3 μM, for a solution temperature of 37°C (214). Using a rapid equilibrium kinetics approach, Abu-Soud et al. and Dweik et al. studied the effects of O<sub>2</sub> tension on purified recombinant mouse iNOS by measuring the rate of NADPH oxidation spectroscopically, in a closed system at 25°C (1, 67). They reported an apparent  $K_mO_2$  of 130 μM (1) and 135 μM (67). When the NO produced was scavenged with oxyhemoglobin, however, the measured  $K_mO_2$  was reduced approximately 4 fold to

42  $\mu\text{M}$  (1). The difference between these values was shown to be due to direct feedback inhibition of iNOS by NO, an effect that has been demonstrated for all 3 NOS isoforms (247).

In our experiments using forced convection cell culture, the flowing media continuously removed NO as it was produced, thereby minimizing NO accumulation. Our results, therefore, are most comparable to the isolated enzyme experiments that either continuously removed NO with flowing headspace gas in an open system (Rengasamy and Johns,  $K_m\text{O}_2$  6.3  $\mu\text{M}$  (214)), or scavenged NO with oxyhemoglobin in a closed system (Abu Soud et al.,  $K_m\text{O}_2$  42  $\mu\text{M}$  (1)). The apparent  $K_m\text{O}_2$  we measured for intact cells was 22 (SD 6) Torr (31  $\mu\text{M}$  based on an Ostwald solubility coefficient of 0.0271 ml  $\text{O}_2$  BTP/ml water-atm at 37°C (273)). Unlike the isolated enzyme, within intact cells several mechanisms in addition to substrate dependence and product feedback inhibition could acutely alter NO production after a change in  $\text{PO}_2$ . We investigated 3 potential mechanisms: changes in iNOS protein levels, iNOS dimerization, and cellular NO consumption.

iNOS protein levels were not influenced by brief hypoxic exposures. Hypoxia has been shown to induce increased expression of iNOS mRNA and protein via HIF 1 $\alpha$ -dependent regulation (126, 181, 182). Acute changes in  $\text{PO}_2$ , however, would not be expected to acutely increase iNOS protein production because transcription and translation have been shown to take up to 6 hours to change after an appropriate stimulus (4). To our knowledge, the effect of hypoxia on iNOS degradation has not been investigated. The iNOS half life in room air, however, was approximately 1.6 hours in

several cell types (145). Our results showing that brief hypoxic exposures have little impact on iNOS protein are consistent with these previous studies.

iNOS dimerization was influenced by brief exposure to various O<sub>2</sub> tensions, but surprisingly did not correlate with changes in NO production. The changes in dimerization appeared to be biphasic (6 Torr and 157 Torr > 36 Torr), and were consistent for the 260 kD band, the expected size for iNOS dimers (49), and for the 500 kD band, an undefined iNOS-containing protein complex. Our data for NO production as a function of cellular O<sub>2</sub> tension (Figure 3C), and data from a prior study on iNOS activity as a function of O<sub>2</sub> tension (202), show deviations from a smooth monotonic function in that range of PO<sub>2</sub>, that may in part be related to the biphasic changes we observed in dimerization. Decreased NO production despite a large increase in iNOS dimerization during hypoxia could be due to O<sub>2</sub> substrate limitation, limitation of another substrate or cofactor during hypoxia, and/or the generation of inactive dimers.

Cellular NO consumption was negligible at all but the highest PO<sub>2</sub> and P<sub>NO</sub>, with an overall consumption constant of 0.038 pmol NO/sec·10<sup>6</sup> cells·Torr<sup>2</sup> [12.7 (mmol NO)/(sec·10<sup>6</sup> cells·M NO·M O<sub>2</sub>)]. There are many possible intracellular reactants that can directly consume NO, and correspondingly, there are many possible reaction kinetics for cellular NO consumption (93, 150, 212). Our data is most consistent with first order dependence in NO and O<sub>2</sub>, most similar to the findings of Thomas et al. (251). Our consumption rates are at the low end of the reported range for various cell types (0.050 to 1.61 pmol NO/sec·10<sup>6</sup> cells·Torr<sup>2</sup>) (81, 251), but are consistent with a previous report of LPS and IFN $\gamma$  stimulated RAW 264.7 cells (0.011 pmol NO/sec·10<sup>6</sup> cells·Torr<sup>2</sup> (190); see Appendix B for conversion of consumption constants to comparable units).

In summary, we used a novel forced convection cell culture system to precisely regulate cellular O<sub>2</sub> tensions in the range of < 1 Torr to 157 Torr. In an LPS and IFN $\gamma$  stimulated macrophage cell line, decreases in cellular PO<sub>2</sub> reduced NO production within seconds, an effect which was immediately reversible with restoration of the original PO<sub>2</sub>. The apparent  $K_mO_2$  for this oxygen dependence was 22 (SD 6) Torr (31  $\mu$ M). The changes in NO production were not explained by the effects of cell PO<sub>2</sub> on iNOS protein levels, iNOS dimerization, or consumption of NO. The rapid effects of cellular PO<sub>2</sub> on macrophage NO production are consistent with regulation of NO production by O<sub>2</sub> substrate limitation. The apparent  $K_mO_2$  in intact cells and the kinetics of the PO<sub>2</sub> dependence suggest that O<sub>2</sub> substrate limitation could play a dynamic role in the regulation of NO production by iNOS *in vivo*.

## APPENDIX A: NO Consumption Model

For each individual column, studied at a fixed  $PO_2$ ,  $Q\alpha_{NO}(P_{NOi}-P_{NOe})$  was plotted against  $P_{NO}$  (Figure S1) to assess for linear dependence that would indicate that first order kinetics in NO are appropriate. The negative intercept on this plot is production, i.e. intercept =  $-f(PO_2)k_pN$ , which could be of any functional form (for example the Michaelis-Menten fit in Figure 3). The only assumption required about production for this analysis of NO consumption is that the production is independent of  $P_{NO}$ .

For the experiments at higher  $PO_2$  (36 and 83 Torr) in figure S1, a linear fit is clearly adequate, and the slopes were significantly different from zero. At lower  $PO_2$ , as the slope of this relationship approaches zero, the power to detect a slope significantly different from zero is reduced. As expected, the trend for a linear relationship did not result in a slope significantly different from zero ( $p \geq 0.122$ ) for the  $PO_2 = 6$  Torr data sets.

For each column, the best fit slope ( $b1$ ) of the  $Q\alpha_{NO}(P_{NOi}-P_{NOe})$  versus  $P_{NO}$  data was divided by  $PO_2$  and plotted against  $PO_2$  (Figure S2). First order dependence in  $PO_2$  predicts that  $b1/PO_2$  should be independent of  $PO_2$ . The data of figure S2 are consistent with a constant  $b1/PO_2$  that is independent of  $PO_2$ , confirmed by a best fit regression slope not significantly different from zero ( $p = 0.422$ ).

The best estimate of the overall consumption constant  $k_cN$  was estimated from a weighted average of the  $b1/PO_2$  values in figure S2 that accounts for the fact that the confidence in parameter estimates is increased at higher  $PO_2$ . The weighted average assigned weights in direct proportion to  $PO_2$ . The resulting best estimate for  $k_cN$  was  $0.0186 \text{ pmol NO/sec}\cdot\text{Torr}^2$ .

Finally, cell number for these experiments was estimated from representative measurements of total protein after lysis of cells from the columns, combined with a previously established relationship between cell number and protein for RAW 264.7 cells (202):

$$N = -1.99 \times 10^4 + 7.09 \times 10^6 (\text{protein})$$

where protein is in mg. Average cell number for these experiments was  $4.9 \times 10^5$ .

The overall NO consumption rate constant, normalized to cell number, is

$$\text{NO consumption} = 0.038 \text{ (pmol NO)} / (\text{sec} \cdot 10^6 \text{ cells} \cdot \text{Torr NO} \cdot \text{Torr O}_2)$$

$$= 12.7 \text{ (mmol NO)} / (\text{sec} \cdot 10^6 \text{ cells} \cdot \text{M NO} \cdot \text{M O}_2)$$

## APPENDIX B: Conversion of $k_c$ Units for Comparison to Previous Studies

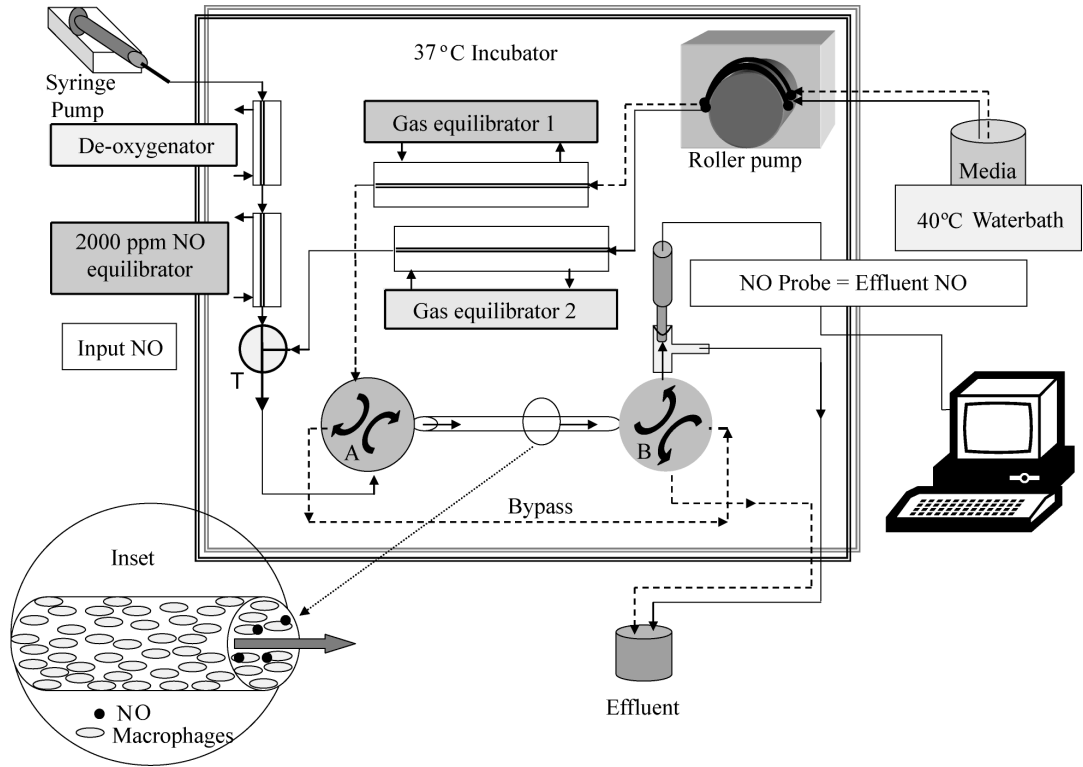
Thomas et al. reported NO consumption data for cultured rat hepatocytes (251). NO consumption was first order in both NO concentration and O<sub>2</sub> concentration, with a rate constant of  $5.38 \times 10^{-4} \text{ M}^{-1} \cdot \text{sec}^{-1} \cdot (\text{cell/ml})^{-1}$ . For an NO solubility at 37°C of 2.13 μM/Torr (271) and an O<sub>2</sub> solubility at 37°C of 1.40 μM/Torr (273), the equivalent rate constant in units compatible with our reported value is 1.61 pmol/sec·10<sup>6</sup> cells·Torr<sup>2</sup>.

Nalwaya and Deen reported NO consumption data for stimulated RAW 264.7 cells (190). NO consumption was treated as first order in NO and zero order in O<sub>2</sub>, with a rate constant of 0.6 sec<sup>-1</sup>. They measured NO consumption over a range of PO<sub>2</sub>. Taking as an approximation a PO<sub>2</sub> in the middle of this range at 100 Torr, with an NO solubility as above, and with their estimate of cell volume of  $8.8 \times 10^{-13} \text{ L/cell}$ , the equivalent rate constant is 0.011 pmol/sec·10<sup>6</sup> cells·Torr<sup>2</sup>.

Gardner et.al. reported NO consumption data for several cell types (81). NO consumption values, in compatible units, ranged from 0.050 to 0.52 pmol/sec·10<sup>6</sup> cells·Torr<sup>2</sup>.



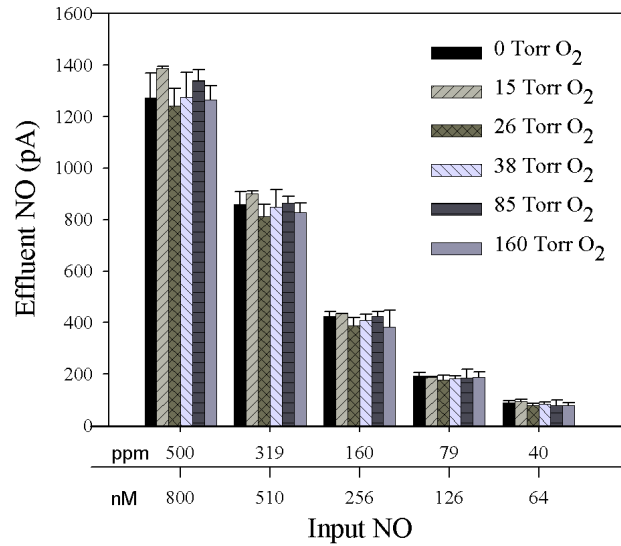
Figure 1.



Forced convection cell culture system. Adherent RAW 264.7 cells were cultured at 37°C on the inside of a fused-silica column (inset). The media, delivered by forced convection via a roller pump, was partially degassed by prewarming to 40°C, and then was equilibrated with calibrated compressed gas mixtures ranging from 0 to 157 Torr O<sub>2</sub> (5% CO<sub>2</sub>, balance N<sub>2</sub>) inside one of two gas equilibrators (labeled Gas Equilibrator 1 and 2). Rapid changes in O<sub>2</sub> tension or media components were enabled by a switching valve upstream from the column of adherent cells (labeled A). NO in the media stream (effluent NO) was measured by an NO electrode (WPI) located downstream from a second switching valve (labeled B) that permitted assay of media from the cells or a

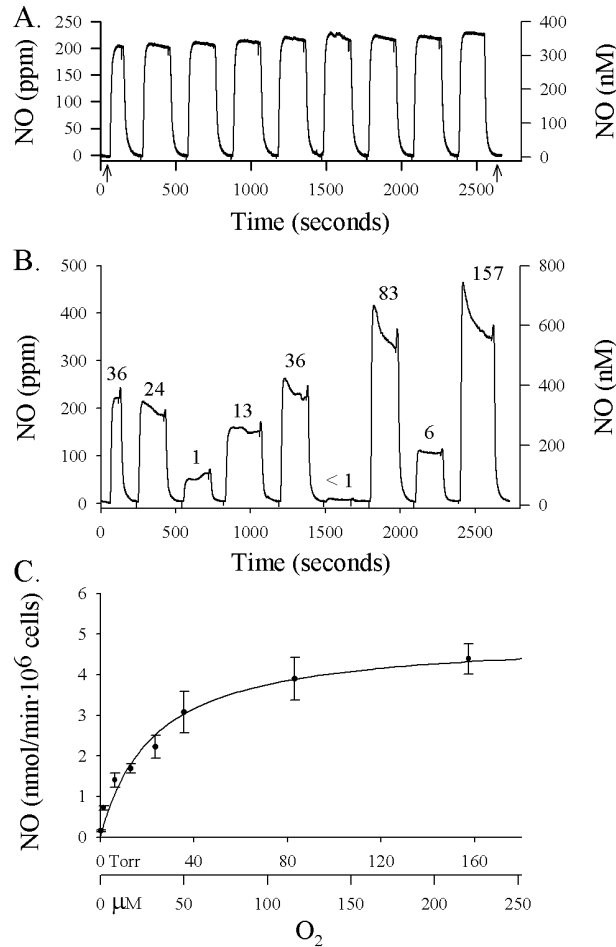
bypass. The bypass loop allowed for regular electrode baseline measurements. A syringe pump controlled the delivery of deoxygenated, deionized H<sub>2</sub>O equilibrated with 2000 ppm NO (balance N<sub>2</sub>) into a T connector (labeled T) inserted into the media stream from gas equilibrator 2. The addition of specific NO tensions (input NO) enabled calibration of the NO electrode and evaluation of cellular NO consumption. Figure adapted from Baumgardner and Otto (6).

**Figure 2.**



NO Consumption by Media. Oxygen dependence of the signal at the NO electrode was measured as a function of NO tension in minimal essential media (JBMEM) in the absence of cells. Each bar represents the mean (SD) of the NO probe signal (pA) for JBMEM at five input  $P_{NO}$  and six  $PO_2$  ( $n = 3$ ). Because the conversion of NO to its stable end products ( $NO_2$  and  $NO_3$ ) is  $O_2$  dependent, the results imply that NO consumption by the media is negligible.

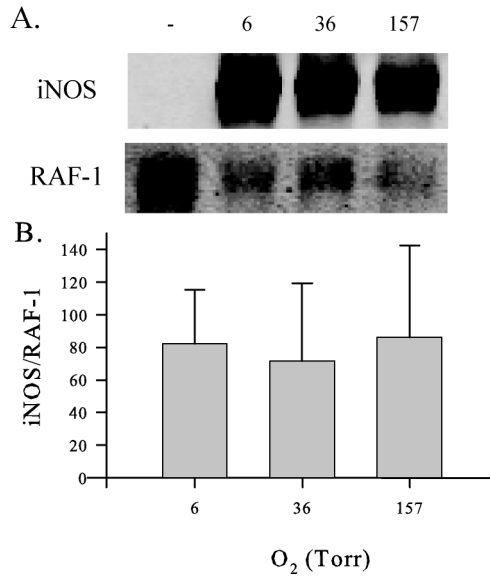
**Figure 3.**



Effect of  $PO_2$  on NO Production. A. Representative tracing of NO (ppm) released by LPS and  $IFN\gamma$  stimulated RAW 264.7 cells during rapid switching between 0 and 36 Torr  $O_2$ . Cells were repeatedly exposed to 0 Torr  $O_2$  for 2 minutes, then 36 Torr  $O_2$  for 3 minutes for a combined total of 40 minutes ( $n = 4$ ). Arrows indicate probe baseline, which was measured at the beginning and end of the experiments via the bypass loop. B. Representative tracing from one of five experiments in which LPS and  $IFN\gamma$  stimulated RAW 264.7 cells were exposed to eight  $O_2$  tensions ranging from < 1 to 157 Torr in a

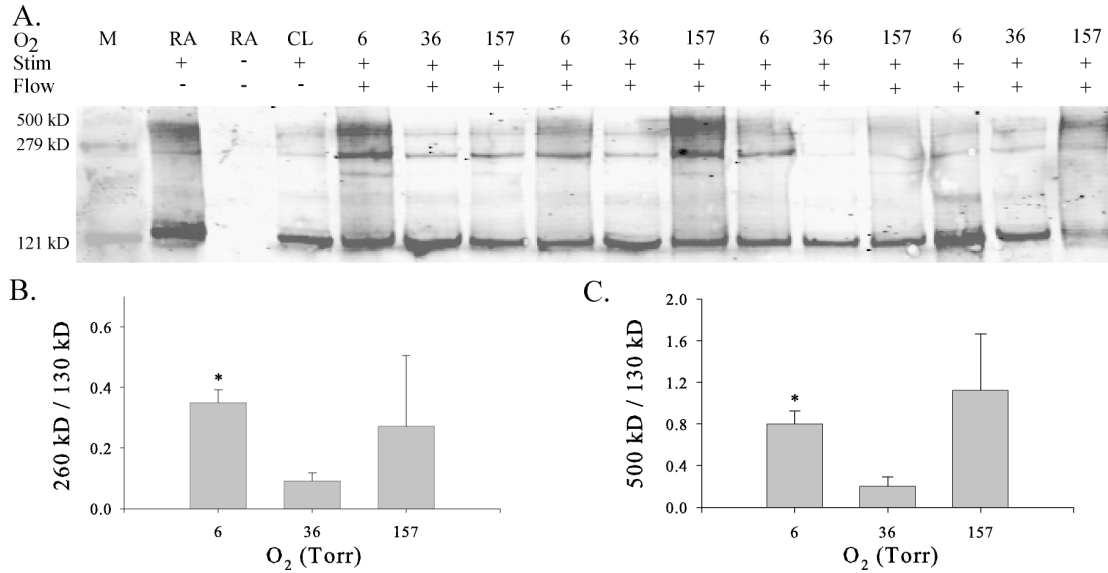
randomized order, while effluent NO (ppm) was measured electrochemically. In between each O<sub>2</sub> tension, cells were exposed to 0 Torr O<sub>2</sub>. The numerical values above each plateau represent the estimated mean cellular PO<sub>2</sub>. C. Michaelis-Menten plot. The calculated  $K_mO_2$  was 22 (SD 6) Torr. The calculated  $V_{max}$  was 4.9 (SD 0.4) nmol/min·10<sup>6</sup> cells.

**Figure 4.**



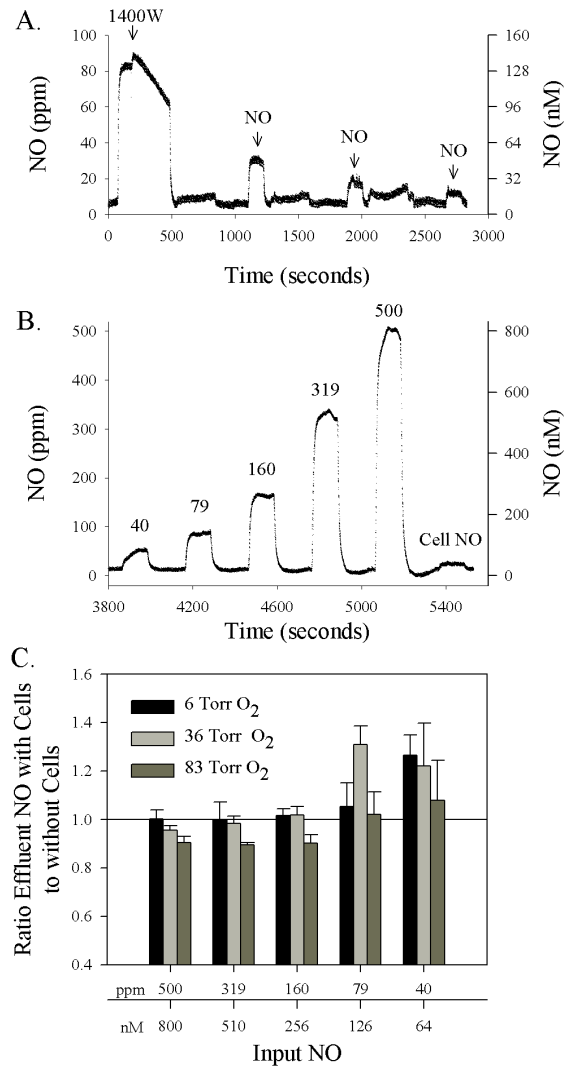
Effect of O<sub>2</sub> tension on iNOS protein concentration. Representative western blot of SDS-PAGE gel for inducible nitric oxide synthase (iNOS) in LPS and IFN $\gamma$  stimulated RAW 264.7 cells exposed to 6, 36, or 157 Torr O<sub>2</sub> for 40 minutes. iNOS signal was normalized to RAF-1, a constitutively expressed protein. The bar graph presents the mean (SD) of the iNOS to RAF-1 ratio at each PO<sub>2</sub> ( $n \geq 4$ ). (-) Unstimulated RAW 264.7 cells exposed to 36 Torr O<sub>2</sub> for 40 minutes.

**Figure 5.**



Effect of O<sub>2</sub> tension on iNOS dimerization. A. Western blot of low temperature SDS-PAGE gel for inducible nitric oxide synthase (iNOS) in LPS and IFN $\gamma$  stimulated RAW 264.7 cells exposed to 6, 36, or 157 Torr O<sub>2</sub> for 40 minutes. M = Hi-Mark pre-stained molecular weight marker (Invitrogen, Carlsbad CA). RA = RAW 264.7 cells grown in room air. CL = RAW 264.7 cells cultured in room air and treated with 10  $\mu$ M clotrimazole, an inhibitor of iNOS dimerization (232), for 30 minutes prior to and during stimulation with LPS and IFN $\gamma$  for 8 hours. Stim = RAW 264.7 cells were unstimulated (-) or stimulated (+) for 18 hours with LPS and IFN $\gamma$ . Flow = RAW 264.7 cells grown in culture dishes (-) or with forced convection (+). B. Bars represent the mean (SD) of the 260 kD to 130 kD ratio ( $n = 3$ ). \*  $p = 0.003$  compared to 36 Torr. C. Bars represent the mean (SD) of the 500 kD to 130 kD ratio ( $n = 3$ ). \*  $p = 0.008$  compared to 36 Torr.

**Figure 6.**

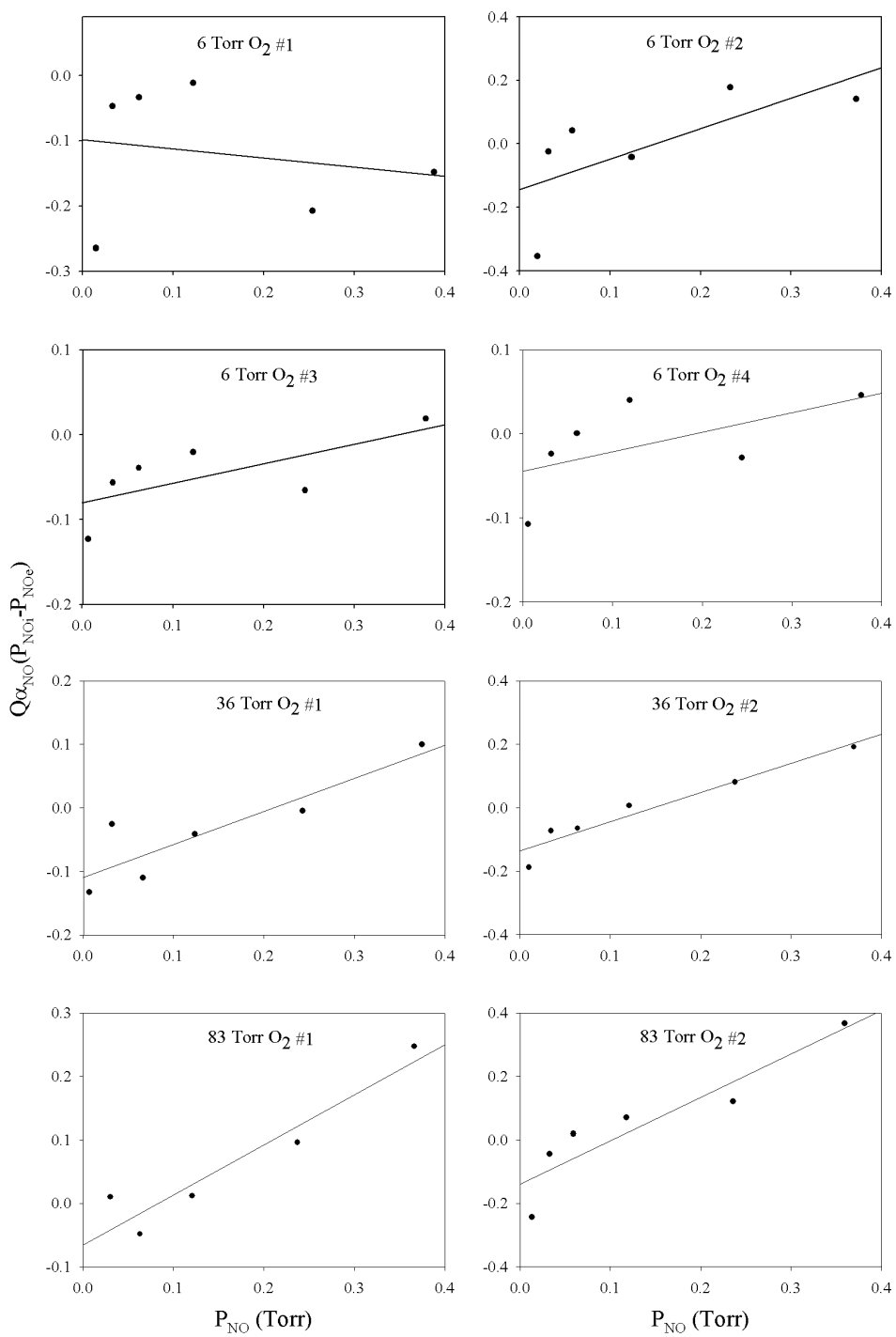


Effect of NO and O<sub>2</sub> tension on cellular NO consumption. A. Representative tracing of 1400W inhibition of NO produced by LPS and IFN $\gamma$  stimulated RAW 264.7 cells ( $n = 12$ ). Cells were switched from JBMEM to 100  $\mu$ M 1400W in JBMEM lacking L-arginine (labeled 1400W). Effluent P<sub>NO</sub> was measured approximately every 10 minutes for 2 minutes (labeled NO). B. Representative tracing showing effluent P<sub>NO</sub> measured during sequential exposure of 1400W-inhibited cells to 40, 79, 160, 319, and 500 ppm



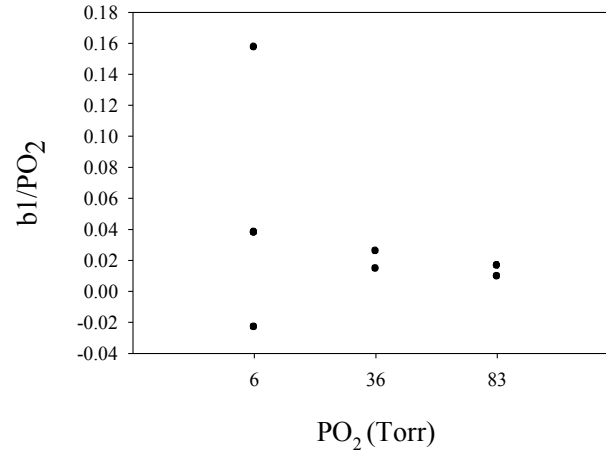
input  $P_{NO}$  as labeled, and 0 ppm NO (labeled Cell NO;  $n = 8$ ).  $O_2$  tension was 6 Torr. C. Cellular NO consumption by LPS and  $IFN\gamma$  stimulated RAW 264.7 cells treated with the iNOS inhibitor 1400W was measured as a function of  $O_2$  and NO tension. Each bar represents the mean (SD) of the ratio of the effluent  $P_{NO}$  with cells to the effluent  $P_{NO}$  without cells for five input  $P_{NO}$  and three  $PO_2$  ( $n \geq 2$ ). Reference line = 1. Ratios  $< 1$  = net NO consumption. Ratios  $> 1$  = net NO production.

Figure S1.



Dependence of cellular NO consumption on NO tension. Plots of  $Q_{\alpha_{NO}}(P_{NOi}-P_{NOe})$  versus  $P_{NO}$  for individual columns at 6, 36, or 83 Torr  $O_2$ . The lines represent the linear regression.

**Figure S2.**



Dependence of cellular NO consumption on PO<sub>2</sub>. Plot of b1/PO<sub>2</sub> versus PO<sub>2</sub> ( $n \geq 2$ ), where b1 = the best fit slope of the  $Q\alpha_{\text{NO}}(P_{\text{NOi}}-P_{\text{NOe}})$  versus  $P_{\text{NO}}$  data presented in Figure S1.

**Table 1.** NO Consumption in DMEM.

Component	% Consumption
DMEM (Gibco)	99.9
Gibco™ essential	72
amino acid mixture (1X)	
NaHCO <sub>3</sub> (3700 mg/L)	48
Glucose (4500 mg/L)	36
Glucose (1000 mg/L)	15
NaCl (6400 mg/L)	7
deionized H <sub>2</sub> O	0

Using the forced convection cell culture system and NO electrode, effluent NO was measured in DMEM and select components after a 29 second exposure to 80 ppm input NO in the absence of cells and O<sub>2</sub>. The signal generated by the exposure of deionized H<sub>2</sub>O at 0 Torr O<sub>2</sub> to 80 ppm NO was designated 0% consumption.

**Table 2.** Cell survival in DMEM and JBMEM.

Media	Time (hours)		
	2	6	18
DMEM (U)	95.1 (2.7)	97.4 (0.9)	90.2 (3.9)
DMEM (S)	94.8 (0.9)	94.5 (1.3)	ND
JBMEM (U)	91.2 (4.7)	90.9 (2.3)	88.0 (5.1)
JBMEM (S)	94.0 (0.4)	94.4 (0.5)	ND

RAW 264.7 cells were cultured for 2, 6, or 18 hours in DMEM or JBMEM with (S) or without (U) stimulation (1  $\mu\text{g/ml}$  LPS and 100 U/ml IFN $\gamma$  initiated 18 hours prior to seeding;  $n = 3$ ). Percent survival was measured via Trypan blue staining. Data are presented as mean (SD). ND = not determined.

## CHAPTER 2.

# **pO<sub>2</sub> Dependent NO Production Determines OPPC Activity in Macrophages**

Mary A. Robinson<sup>1,2,3</sup>, Stephen W. Tuttle<sup>1</sup>, Cynthia M. Otto<sup>2,3</sup>, and Cameron J. Koch<sup>1</sup>

<sup>1</sup>Department of Radiation Oncology, School of Medicine, University of Pennsylvania Philadelphia PA 19104; <sup>2</sup>Department of Clinical Studies-Philadelphia, School of Veterinary Medicine, University of Pennsylvania Philadelphia PA 19104; <sup>3</sup>Center for Sleep and Respiratory Neurobiology, University of Pennsylvania Philadelphia PA 19104.

Manuscript Submitted for Publication to Free Radical Biology and Medicine on April 9<sup>th</sup>, 2009.

## ABSTRACT

Stimulated macrophages produce nitric oxide (NO) via inducible nitric oxide synthase (iNOS) using molecular O<sub>2</sub>, L-arginine, and NADPH. Exposure of macrophages to hypoxia decreases NO production within seconds due to limitation of the reactant(s). Conflicting data exist regarding the effect of pO<sub>2</sub> on NADPH production via the oxidative pentose phosphate cycle (OPPC). Therefore, the present studies were developed to determine whether NADPH could be limiting for NO production under hypoxia. Production of NO metabolites (NO<sub>x</sub>) and OPPC activity by RAW 264.7 cells was significantly increased by stimulation with lipopolysaccharide (LPS) and interferon  $\gamma$  (IFN $\gamma$ ) at pO<sub>2</sub> ranging from 0.07% to 50%. OPPC activity exhibited a linear dependence on NO<sub>x</sub> production at pO<sub>2</sub> > 0.13%. Increased OPPC activity by stimulated RAW 264.7 cells was significantly reduced by 1400W, an iNOS inhibitor. OPPC activity was significantly increased by concomitant treatment of stimulated RAW 264.7 cells with chemical oxidants, hydroxyethyldisulfide or pimonidazole, at 0.07% and 50% O<sub>2</sub>, without decreasing NO<sub>x</sub> production. These results are the first to demonstrate the relationship between NO production and OPPC activity over a wide range of pO<sub>2</sub>, and to rule out limitations in OPPC activity as a mechanism by which NO production is decreased under hypoxia.



## INTRODUCTION

Nitric oxide (NO) production is a key component of the macrophage response during inflammation (33, 172). Macrophages stimulated by pathogen associated molecular patterns (PAMPs) produce NO from molecular O<sub>2</sub>, L-arginine, and NADPH via inducible nitric oxide synthase (iNOS) (245). NO production clearly depends on the partial pressure of O<sub>2</sub> (pO<sub>2</sub>) (179, 202, 218), and the estimated cellular K<sub>m</sub>O<sub>2</sub> (14 Torr (202) to 77 ± 1.4 Torr (179)) is within the physiological range (5 to 71 Torr (23, 37, 42, 124, 129, 263, 282)). Systemic and/or tissue hypoxia develops during several inflammatory diseases (42, 75, 122), extending the pO<sub>2</sub> range for tissue macrophages to even lower levels, and potentially limiting NO production *in vivo*. Acute exposures to hypoxia have been shown to rapidly (within seconds) and reversibly decrease NO production by PAMPs stimulated macrophages without decreasing iNOS protein or assembly (218), providing evidence for the dynamic regulation of NO production by substrate limitation. While molecular O<sub>2</sub> is clearly limiting, an effect of hypoxia on the electron donor NADPH represents a second potential mechanism that has not been investigated in macrophages.

NADPH is constitutively produced by NADP<sup>+</sup> dependent malic enzyme and isocitrate dehydrogenase. When NADPH oxidation exceeds the capacity of these enzymes to reduce the substrate, however, the increase in [NADP<sup>+</sup>] activates glucose-6-phosphate dehydrogenase (G6PD), the initial and rate limiting enzyme of the oxidative pentose phosphate cycle (OPPC) (68). An association between NADPH production by G6PD and the production of NO has previously been demonstrated in endothelial cells (156-158), an insulin-producing pancreatic beta cell line (RINm5F) (98), and

macrophages (57, 112, 180, 258). In macrophages, stimulation with PAMPs was found to elicit a parallel increase in OPPC activity (153, 177, 191) and NO production (57), by increasing G6PD activity and metabolic flux through the OPPC, rather than via the malic enzyme (58). Moreover, pharmacologic inhibition of OPPC activity or G6PD deficiency was shown to significantly impair NO production by stimulated macrophages (112, 180, 258).

Reduction of NADP<sup>+</sup> via the OPPC does not require molecular O<sub>2</sub>. Classical studies have measured increased [NADPH] in response to short term hypoxia due to the absence of metabolically-generated oxidizing agents (99, 127, 227, 259). More recently, however, [NADPH] was found to be significantly decreased in denuded bovine coronary arteries following brief exposure to hypoxia (~ 8 to 10 Torr, 20 minutes (100)). This effect was attributed to increased glycolytic flux, resulting in the redirection of substrate (glucose-6-phosphate) away from the OPPC. However, OPPC activity was not directly measured in these experiments. These results suggest NADPH availability may be limited during acute hypoxia in some tissues and/or cell types.

NADPH production via the OPPC maintains the cellular redox equilibrium (16). Therefore, to investigate whether OPPC activity was limited during acute hypoxia, the cells were simultaneously exposed to hydroxyethylthiol (HEDS) or pimonidazole (PIMO) to pharmacologically induce oxidative stress by two distinct mechanisms. HEDS is a low molecular weight, cell permeable disulfide that is reduced by exchange reactions with glutathione and other cellular thiols. These oxidized cellular thiols are subsequently reduced by NADPH-dependent glutathione and thioredoxin reductases (18, 26, 27).

PIMO is reduced by cytochrome P450 enzymes, which also utilize NADPH to provide reducing equivalents (264).

The primary goal of this study was to investigate the relationship between  $pO_2$  (0.07% to 50%), NO production, and OPPC activity in PAMPs stimulated and unstimulated macrophages (Figure 1). We chose to study RAW 264.7 cells due to the extensive literature on the  $pO_2$  dependence of NO production in these cells (179, 202, 218), and due to their abundant and persistent NO production (61). We hypothesized that 4 hours of hypoxia would decrease NO production and OPPC activity without affecting iNOS concentration or iNOS dimerization. Second, we hypothesized that  $pO_2$  would not affect the response of OPPC activity to chemically-induced oxidative stress via HEDS or PIMO. Our results suggest that  $pO_2$ , and not NADPH availability, affects NO production by PAMPs stimulated macrophages during acute hypoxia.

## METHODS

### Cell Culture

RAW 264.7 cells (American Type Culture Collection, Manassas, VA) were maintained at 37°C 5% CO<sub>2</sub> in DMEM (Invitrogen, Carlsbad, CA) supplemented with 10% FBS (HyClone, Logan, Utah) and 1% antibiotic/antimycotic (penicillin, streptomycin, amphotericin B; Invitrogen) for up to 10 passages. For experiments, 10<sup>6</sup> cells were plated on 20 mL glass vials (inner diameter ~ 24 mm), or 1.5 x 10<sup>6</sup> cells were spot plated on 50 mm glass dishes (143). Glass dishes and vials were cleaned and fired at 420°C, then treated with 75 mM sodium carbonate (Fisher, Fair Lawn, NJ) and 15% FBS for 1 hour at 37°C, treated with 0.2% gelatin (BioRad, Richmond, CA) for 20 minutes, and dried under UV light prior to plating the cells. Cells were then cultured overnight with 3 mL of MEM (Invitrogen, 11095) supplemented with penicillin, streptomycin, 15% FBS, non-essential amino acids, and 1 mM pyruvate. Stimulation of RAW 264.7 cells was performed by treating cells overnight (at least 18 hours) with 1 µg/mL LPS (*E. coli* O111:B4; Sigma) and 100 U/mL CHO-derived recombinant mouse IFN $\gamma$  (Cell Sciences, Canton, MA). Immediately prior to experiments, the media was replaced with 1 mL of low glucose (2 mM) MEM buffered with 25 mM HEPES (i.e. instead of sodium bicarbonate to prevent saturation of the filter paper with unlabeled CO<sub>2</sub> during the measurement) and containing 5% FBS, non-essential amino acids, 1% penicillin and streptomycin, and 2 mM glutamine. HEPES-buffered media pH was not affected by pO<sub>2</sub> or any of the other treatment conditions (data not shown). Where indicated, NO<sub>x</sub> production was inhibited by treating cells with 100 µM N-[[3-(aminomethyl)phenyl]methyl]-ethanimidamide, dihydrochloride (1400W; Cayman

Chemical, Ann Arbor, MI) in the absence of L-arginine for one and one half hours immediately prior to switching to low glucose media. To chemically induce oxidative stress, 2 mM hydroxyethylidisulfide (HEDS) or 2 mM pimonidazole (PIMO) were added to the low glucose media.

### **pO<sub>2</sub> Control with Thin Film Cell Culture**

RAW 264.7 cells were cultured at 0.07%, 0.13%, 0.24%, 0.61%, 2%, 10%, or 50% O<sub>2</sub> for 4 hours at 37°C in vials or dishes contained in leak proof aluminum chambers, which enabled precise control of headspace pO<sub>2</sub> as previously described (142-144, 259). Briefly, glass vials were capped with a rubber stopper containing a center well (Kimble Chase, Vineland, NJ) with a 1 × 0.5 cm Whatman GF/B glass-fiber filter soaked with 100 μL 5% KOH (259). A 25G 5/8 inch needle was inserted into the stopper to enable slow gas exchange during the evacuations and pressurizations for oxygen control, while limiting gas exchange under the constant pressure conditions during the subsequent incubation (259). Vials or dishes were placed in aluminum chambers and subjected to a series of gas exchanges with N<sub>2</sub> or O<sub>2</sub> to produce the desired headspace pO<sub>2</sub>. Chambers were warmed to 37°C and shaken continuously to ensure adequate gas exchange between the headspace and the media throughout the experiment (4 hours). The pO<sub>2</sub> in the chambers was measured at the end of the incubation period using a polarographic oxygen electrode. However, the pO<sub>2</sub> in the headspace of each vial was not directly accessible. Additionally, the depth of the medium layer in the vials did not conform to the “thin-layer” model that was originally developed in 50 mm glass dishes (143). Thus, in separate experiments, we added 100 μM EF5 to both dishes and vials, and assayed for

EF5 adducts using flow cytometry as previously described (141, 142) in order to directly assess cellular pO<sub>2</sub>. Note that in the experiments presented, pO<sub>2</sub> is defined as the % of oxygen in 1 atmosphere of dry gas at 37°C (i.e. 100% = 760 mm of Hg).

### **NO<sub>x</sub> Measurement**

Nitrite, nitrate, and nitrosothiols (NO<sub>x</sub>) were measured in media or cell lysates by injecting 20 µL into a reaction chamber containing a VCl<sub>3</sub>/HCl mixture (0.4 g VCl<sub>3</sub> in 50 mL 1 N HCl) heated to 90°C. The resulting NO was continuously flushed with helium into a Sievers Nitric Oxide Analyzer 280i (GE Analytical Instruments, Boulder, CO) for reaction with ozone and measurement via chemiluminescence. Quantification was performed by comparison to standards prepared with NaNO<sub>2</sub>.

### **Electrophoresis and Immunoblotting**

Cell lysates were prepared by washing cell monolayers with ice cold cell rinse (6.8 g/L NaCl, 400 mg/L KCl, 122 mg/L NaH<sub>2</sub>PO<sub>4</sub> anhydrous, 1 g/L glucose, 25 mM HEPES, pH 7.2), and then scraping cells into 0.4 mL ice cold protease-inhibitor containing hypotonic lysis buffer (1:1000 Protease Inhibitor Cocktail P8340 (Sigma-Aldrich, St. Louis, MO), 10 µM phenylmethylsulfonyl fluoride (Sigma-Aldrich) in dH<sub>2</sub>O). Lysates were subjected to 3 freeze/thaw cycles (-70°C). Cell lysate protein concentration was measured using the Biorad DC protein assay (Hercules, CA). Proteins (5 µg) were separated on a 7.5% Tris-HCl gel using SDS PAGE or low temperature SDS PAGE (LT SDS PAGE) as previously described (218), transferred to polyvinylidene fluoride (Immobilon<sup>TM</sup>-FL 0.45 µm; Millipore, Bedford, MA), and immunoblotted for

iNOS (1:2000; NOS2 M19 sc650, Santa Cruz Biotechnology, Inc., Santa Cruz, CA).  $\beta$  actin (1:20,000; Monoclonal anti- $\beta$  actin Clone AC-15 A5441, Sigma-Aldrich) was used as the loading control. Primary antibodies were immunocomplexed with IRDye<sup>TM</sup> 800 goat anti-rabbit or goat anti-mouse (1:10,000; Rockland, Gilbertsville, PA). Proteins were detected, documented, and analyzed using an Odyssey Imaging System and software (LiCor Biosciences, Lincoln, NE).

### **OPPC and TCA Activity**

RAW 264.7 cells were cultured in the presence of 2 mM glucose labeled in either the 1-<sup>14</sup>C or 6-<sup>14</sup>C position at a specific activity of 200  $\mu$ Ci/mmol glucose in 1 ml of bicarbonate-free MEM. At the completion of each experiment, the vials were removed from the aluminum chambers, the needle was removed from the rubber stopper, and cellular metabolism was stopped by injection of 100  $\mu$ L 6 N acetic acid into the media; the acidification step also releases CO<sub>2</sub> from the medium into the gas phase. <sup>14</sup>CO<sub>2</sub> was collected on a 5% KOH saturated filter overnight at room temperature. The filter was removed and the <sup>14</sup>CO<sub>2</sub> was counted with a Packard liquid scintillation counter. TCA activity leads to release of <sup>14</sup>CO<sub>2</sub> from either the 1-<sup>14</sup>C or 6-<sup>14</sup>C position of glucose, while OPPC activity causes release of <sup>14</sup>CO<sub>2</sub> only from the 1-<sup>14</sup>C position. Thus, OPPC activity was calculated using parallel vials and subtracting <sup>14</sup>CO<sub>2</sub> produced in the presence of 6-<sup>14</sup>C glucose from the <sup>14</sup>CO<sub>2</sub> produced in the presence of 1-<sup>14</sup>C glucose.

## **Statistics**

The apparent  $K_m$  and  $V_{max}$  values were calculated by SigmaPlot Enzyme Kinetics Module 1.1 using a Michaelis-Menten non-linear analysis. Comparison of means were tested by ANOVA for the effect of  $pO_2$  on measured values, and by two way ANOVA for the effect of  $pO_2$  and treatment on measured values. Data presented are mean  $\pm$  SD.



## RESULTS

### Control of Cellular pO<sub>2</sub>

Cellular pO<sub>2</sub> was regulated using a modified version of the Thin Film Culture Method developed in our laboratory (143). To ensure the modified method (i.e. glass vials with rubber stopper and needle) provided the same pO<sub>2</sub> at the cellular level, we compared the cellular pO<sub>2</sub> in glass dishes with the cellular pO<sub>2</sub> in glass vials via the measurement of EF5 protein adducts (Figure 2). The formation of EF5-protein adducts increases as the pO<sub>2</sub> decreases in a quantitative manner, thus permitting an accurate measurement of cellular pO<sub>2</sub> because the pO<sub>2</sub> is constant between the gas and liquid phases (143). The pO<sub>2</sub> dependence of EF5 binding for RAW 264.7 cells incubated on glass dishes was similar to results from other cultured cell lines (141). Importantly, the EF5 binding for cells in glass vials closely paralleled EF5 binding for cells on glass dishes (Figure 2).

### pO<sub>2</sub> dependence of NO<sub>x</sub> production

NO<sub>x</sub>, iNOS protein levels, and iNOS dimerization were measured using the thin film cell culture method and low glucose media required for the OPPC measurements. The results obtained in low glucose media were similar to previous cell culture systems (Figure 3 and references (202, 218)). Cumulative NO<sub>x</sub> released into the media by LPS and IFN $\gamma$ -stimulated RAW 264.7 cells fit a Michaelis-Menten kinetic model with a  $K_mO_2$  of  $0.66 \pm 0.12$  % ( $5 \pm 1$  Torr) and a  $V_{max}$  of  $25.2 \pm 1.0$  nmol/10<sup>6</sup> cells ( $R^2 = 0.91$ , Figure 3A). NO<sub>x</sub> measured in cell lysates from LPS and IFN $\gamma$ -stimulated RAW 264.7 cells exposed to 50% O<sub>2</sub> for 4 hours was  $3.5 \pm 1.1$  nmol/10<sup>6</sup> cells, 13% of NO<sub>x</sub> detected in the

media. In the absence of LPS and IFN $\gamma$  stimulation, RAW 264.7 cells did not produce detectable NO $_x$  (data not shown). pO $_2$  did not alter iNOS protein concentration (Figure 3B) or iNOS dimerization (Figure 3C). Stimulation of RAW 264.7 cells with LPS and IFN $\gamma$  decreased total protein isolated from the vials by 30%, consistent with previous reports (200, 218). pO $_2$  alone did not affect cell adhesion as visualized by light microscopy, or the amount of total protein isolated from the vials (data not shown).

### **pO $_2$ dependence of OPPC Activity**

Unstimulated RAW 264.7 OPPC activity exhibited a biphasic response to pO $_2$  (Figure 4A), with a decrease between 0.07% and 2% O $_2$  and a 2.5 fold increase between 10% and 50% O $_2$ . Stimulation of RAW 264.7 cells with LPS and IFN $\gamma$  for 18 hours significantly increased OPPC activity at all pO $_2$  ( $p < 0.001$ ). OPPC activity correlated directly with NO $_x$  production for pO $_2$  greater than 0.13% O $_2$  in LPS and IFN $\gamma$  stimulated cells (Figure 4B). Treatment of LPS and IFN $\gamma$  stimulated RAW 264.7 cells with 1400W, an iNOS inhibitor, completely inhibited NO $_x$  production (Table 1), and significantly decreased OPPC activity to levels observed without LPS and IFN $\gamma$  treatment ( $p < 0.001$ ; Figure 4A, Table 1). 1400W also decreased OPPC activity in unstimulated RAW 264.7 cells (Table 1) and unstimulated RAW 264.7 cells treated with PIMO (data not shown) at 50% O $_2$ , but not 2% and 0.07% O $_2$ , suggesting possible nonspecific effects of the treatment at 50% O $_2$ . Treatment of RAW 264.7 cells with LPS and IFN $\gamma$  decreased TCA activity (Table 1), consistent with NO $_x$ -mediated respiratory inhibition (reviewed by (40)). Treatment with 1400W, however, did not reverse the observed affect on TCA activity at any pO $_2$  (Table 1).

### **OPPC Challenge with HEDS and PIMO**

To further increase oxidative challenge, RAW 264.7 cells were treated with HEDS or PIMO, two chemical oxidants, which operate by distinct mechanisms. HEDS or PIMO both increased OPPC activity significantly in RAW 264.7 cells at either 0.07% O<sub>2</sub> and 50% O<sub>2</sub> ( $p < 0.001$ , Figure 5). Stimulation of RAW 264.7 cells with LPS and IFN $\gamma$  did not alter the magnitude of the increase in OPPC activity induced by HEDS or PIMO treatment. NO<sub>x</sub> production was measured during OPPC challenge to determine whether NO production was maintained despite chemical oxidant stress (i.e. to assess whether OPPC capacity was able to accommodate both processes). NO<sub>x</sub> production by LPS and IFN $\gamma$  stimulated RAW 264.7 cells was not affected by HEDS treatment at 0.07% O<sub>2</sub> or 50% O<sub>2</sub> (Figure 6). PIMO, a nitroimidazole, was detected by the nitric oxide analyzer (2 mM PIMO in media generated the equivalent signal of 3.6  $\mu$ M NaNO<sub>2</sub>). Even after correcting for this signal, however, NO<sub>x</sub> measurements were significantly increased in PIMO treated LPS and IFN $\gamma$  stimulated RAW 264.7 cells at 0.07% O<sub>2</sub> ( $p < 0.05$ ) and 50% O<sub>2</sub> ( $p < 0.001$ ), suggesting PIMO might be metabolized to nitrite, nitrate, or nitrosothiols (178).

## DISCUSSION

Increased NO<sub>x</sub> production and increased OPPC activity were observed over a wide range of pO<sub>2</sub> (0.07% to 50% O<sub>2</sub>) in LPS and IFN $\gamma$  stimulated RAW 264.7 cells, consistent with previous reports of a relationship between NO production and NADPH oxidation in atmospheric O<sub>2</sub> (57, 98, 112, 156-158, 180, 258). Moreover, inhibition of NO production significantly decreased OPPC activity at all pO<sub>2</sub> investigated, suggesting that the majority of the increased OPPC activity observed in stimulated RAW 264.7 cells was directly related to NO and/or reactive nitrogen species production. Hypoxia did not inhibit the ability of the OPPC to respond to chemically mediated oxidative stress induced by HEDS or PIMO, and HEDS did not inhibit NO<sub>x</sub> production in stimulated cells. These results demonstrate that OPPC activity is not limiting for NO production by stimulated RAW 264.7 cells irrespective of pO<sub>2</sub>.

The pO<sub>2</sub> dependence of NO<sub>x</sub> production was well fit by a Michaelis-Menten model, and the measured  $K_m$ O<sub>2</sub> (0.66% or 5 Torr) was within the range reported previously (5 Torr to 96 Torr) (1, 67, 179, 202, 214, 218). Despite substantial differences in experimental methodology, these data are consistent with our previous results using forced convection cell culture (22 Torr) (218), and our previous data from cell monolayers grown in dishes for 18 hours, after correction for iNOS activity and media depth (14 Torr) (202). The data are also consistent with measurements made by Rengasamy and Johns using RAW 264.7 cell lysates and a steady state system (5 Torr) (214). In contrast, rapid equilibrium studies with recombinant iNOS reported apparent  $K_m$ O<sub>2</sub> values of 93 Torr (1) and 96 Torr (67). At present, the reasons underlying the > 10 fold higher apparent  $K_m$ O<sub>2</sub> measured with recombinant iNOS are unclear. Regardless, the

range of pO<sub>2</sub> found *in vivo* (5 to 71 Torr (23, 37, 42, 75, 122, 124, 129, 263, 282)) has the potential to significantly and rapidly affect NO production, as suggested previously (1, 67, 179, 202, 214, 218).

The pO<sub>2</sub> dependence of NO<sub>x</sub> production was not due to changes in iNOS protein levels or iNOS dimerization, consistent with our previous studies of short-term hypoxia (40 minutes) (218). Multiple studies have documented the effects of long-term (18 to 24 hours) hypoxia on iNOS upregulation via HIF 1 $\alpha$  (126, 181, 182). Increased expression of iNOS protein due to hypoxia, however, requires incubations greater than or equal to 6 hours (4). The half-life of iNOS in atmospheric O<sub>2</sub> is approximately 1.6 hours (145), but the effect of hypoxia on stability of the protein has not been investigated. Based on the present study, we conclude that short-term hypoxia (i.e. < 4 hours) has negligible effects on the balance between transcription, translation, assembly, and degradation of iNOS.

Several previous studies have investigated the effects of short term hypoxia on NADPH and/or OPPC activity (99, 100, 127, 227, 259), but we have found no prior studies that examined the pO<sub>2</sub> dependence of OPPC activity in macrophages. Interestingly, OPPC activity in unstimulated RAW 264.7 cells exhibited a biphasic pO<sub>2</sub> dependence in contrast to our previous work in HT1080 (human fibrosarcoma) and A549 (human lung carcinoma) cells (259). One potential source of NADP<sup>+</sup> under hypoxia is the mitochondrial transhydrogenase. The decrease in mitochondrial respiration observed under severe hypoxia results in elevated glycolytic flux, to maintain [ATP]. Hypoxic glycolysis produces lactate and NAD<sup>+</sup>. Mitochondrial transhydrogenase couples reduction of NAD<sup>+</sup> to oxidation of NADPH (128). This reaction has been shown to increase under anaerobic conditions (241). We propose that the NADP<sup>+</sup> produced by the

mitochondrial transhydrogenase catalyzed reaction resulted in the stimulation of OPPC activity that we observed under hypoxia. While we are examining this hypothesis more thoroughly, it is important to note that the increase of OPPC activity between 2% and 0.07% for unstimulated RAW 264.7 cells under hypoxia, though statistically significant, is relatively small compared to the increase observed between 10% and 50% O<sub>2</sub>, or compared to the increase observed in LPS and IFN $\gamma$  stimulated cells.

Stimulation of RAW 264.7 cells with LPS and IFN $\gamma$  significantly increased OPPC activity at all pO<sub>2</sub>, thus extending previous reports for PAMPs stimulated macrophages in atmospheric O<sub>2</sub> (58, 153, 191, 192). These results are consistent with our results previously obtained in tumor cells (259), and conform with the classical view of decreased metabolic flux through the OPPC under hypoxia (99, 127, 227), whereby removal of O<sub>2</sub> leads to a reducing environment. For example, Scholz et al. measured an increase in NADPH fluorescence in rat liver within seconds of exposure to near anoxic pO<sub>2</sub>, and measured a new steady state within minutes (227). Treatment with the iNOS inhibitor, 1400W, significantly reversed the affect of LPS and IFN $\gamma$  stimulation at all pO<sub>2</sub>, suggesting the increase in OPPC activity was to accommodate NO production and/or the neutralization of reactive nitrogen mediated stress. Although NADPH may also be consumed by NADPH oxidase (149), or even by iNOS to produce superoxide (247), superoxide release by LPS and IFN $\gamma$  stimulated RAW 264.7 cells is reported to only occur within the first hour after stimulation (203), and to be only 6 % of NO production (11, 190).

OPPC activity correlated linearly with NO<sub>x</sub> production above 0.13% O<sub>2</sub>, with a slope of approximately 2, suggesting that for each molecule of NO<sub>x</sub> measured, 4

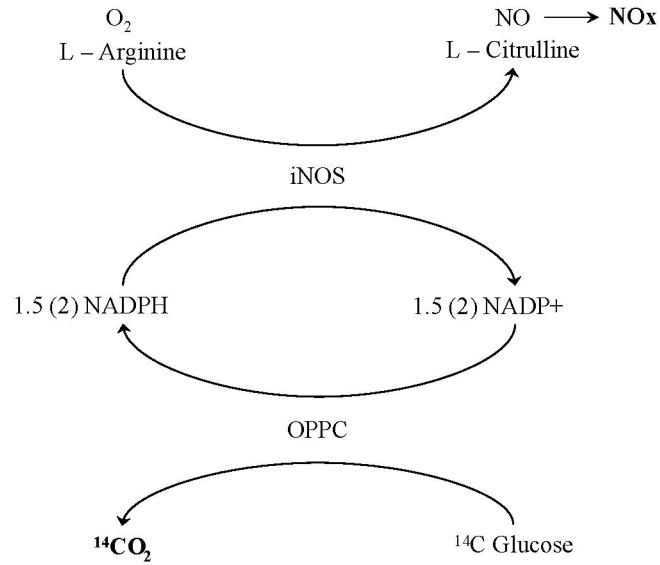
molecules of NADPH were consumed. NO production is reported to require 1.5 molecules of NADPH per NO molecule (reviewed by (247)), leaving a theoretical excess of 2.5 NADPH molecules. One possibility for this excess is that NADPH is required to maintain cellular redox equilibrium in the presence of reactive oxygen and nitrogen mediated stress (reviewed by (16, 73)). Another possibility is a limitation associated with our measurements: NO<sub>x</sub> does not account for all NO metabolites, or for the NO released into the gas phase of the vial. Since the thin film culture system is designed to keep the gas phase in equilibrium with the liquid phase, it is not technically possible to confine NO to the media. Because NO production was not measured via radiolabeled L-arginine, it is impossible to calculate the amount of NO released into the gas phase. Therefore, the absolute relationship between NO, NO<sub>x</sub> production, and NADPH consumption remains to be addressed by additional studies.

Because OPPC activity decreased with pO<sub>2</sub>, we investigated whether OPPC activity was limited by hypoxia. HEDS and PIMO are chemical oxidants that induce oxidative stress by mechanisms that are not dependent on pO<sub>2</sub> (18, 26, 27, 264). Thus, these compounds were used to challenge the OPPC in RAW 264.7 cells under hypoxia. Treatment with HEDS or PIMO significantly increased OPPC activity under all conditions tested including hypoxia. To further investigate the relationship between OPPC activity and NO<sub>x</sub> production, we measured NO<sub>x</sub> production in LPS and IFN $\gamma$  stimulated RAW 264.7 cells exposed to HEDS, and found that NO<sub>x</sub> production was maintained despite this chemical challenge to the OPPC. Therefore, we conclude that OPPC activity is not limiting for NO production in stimulated RAW 264.7 cells.

In summary, OPPC activity was increased following stimulation with LPS and IFN $\gamma$  at all pO<sub>2</sub> investigated in RAW 264.7 macrophages, a response which appears to be a direct consequence of NO production. OPPC activity under conditions of chemically mediated oxidative stress (i.e. HEDS or PIMO treatment) was not limited by hypoxia, nor was it limiting for NO production under any of the conditions investigated. Finally, we conclude that O<sub>2</sub> substrate limitation is the primary mechanism responsible for decreased NO production by LPS and IFN $\gamma$  stimulated macrophages exposed to acute hypoxia.

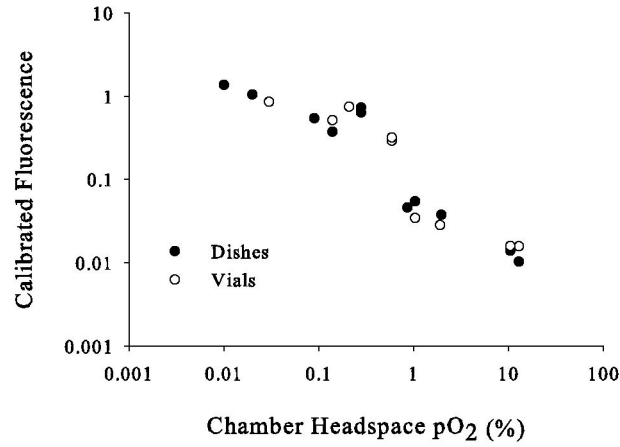


**Figure 1.**



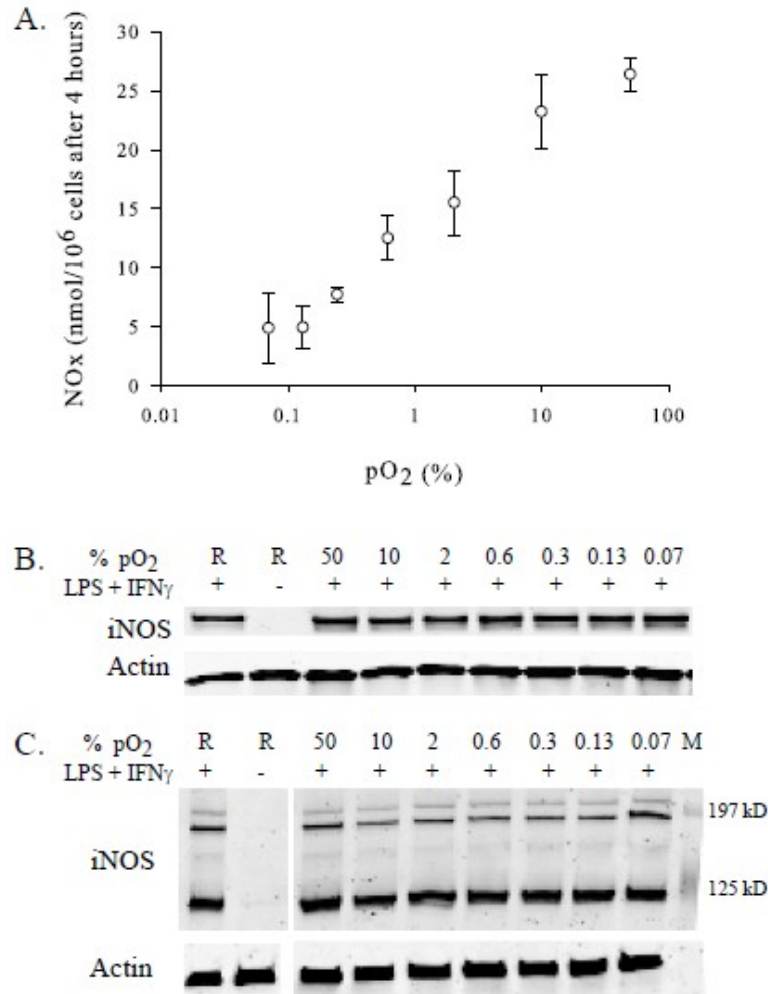
Schematic of the relationship investigated between NO<sub>x</sub> production and OPPC activity. The production of 1 molecule of NO consumes 1.5 NADPH molecules (247). The NO metabolites (NO<sub>x</sub>) measured in this study include nitrite, nitrate, and nitrosothiols in the extracellular media (see Methods). The OPPC produces 2 molecules of NADPH per molecule of CO<sub>2</sub> released. OPPC activity was measured as the production of <sup>14</sup>CO<sub>2</sub> from <sup>14</sup>C-labeled glucose minus the <sup>14</sup>CO<sub>2</sub> produced by the TCA cycle (see Methods).

**Figure 2.**



EF5 binding in Glass Dishes versus Vials. RAW 264.7 cells were cultured for 3 hours in the presence of 100  $\mu$ M EF5 at 0.03%, 0.14%, 0.21%, 0.59%, 1.04%, 1.91%, or 11.7% O<sub>2</sub>. RAW 264.7 cells were labeled with an EF5-specific Cy5 antibody and EF5 binding was measured by flow cytometry of a single cell suspension. Results across experiments were normalized to a positive control. Note that in the experiments presented, pO<sub>2</sub> is defined as the % of oxygen in 1 atmosphere of dry gas at 37°C (i.e. 100% = 760 mm of Hg).

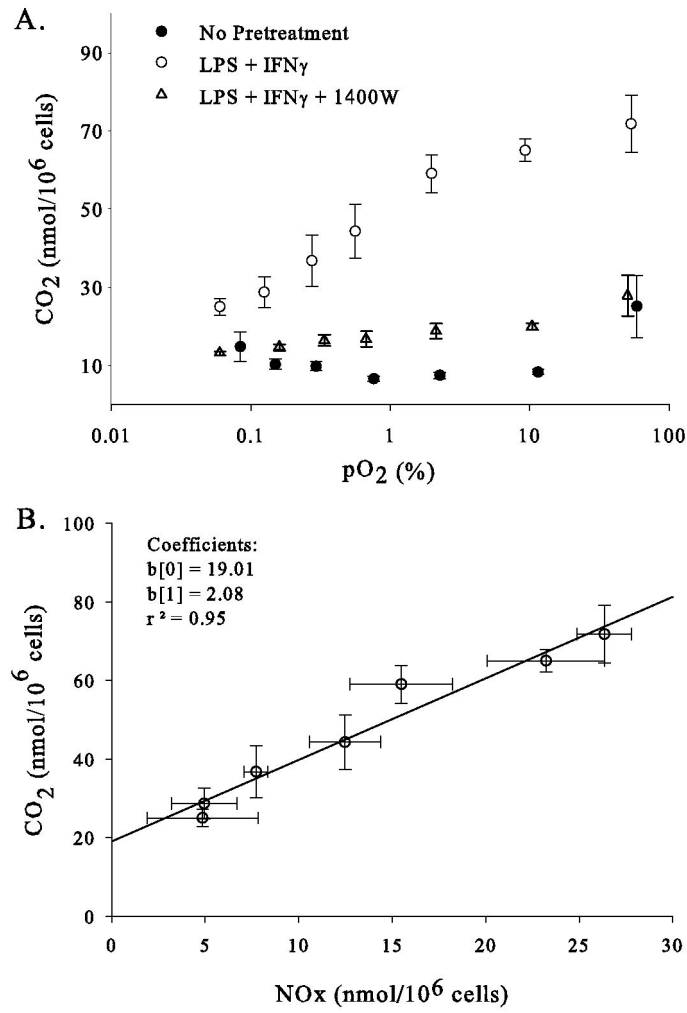
**Figure 3.**



NO<sub>x</sub> production, iNOS protein concentration, and iNOS dimerization in LPS and IFN<sub>γ</sub> stimulated RAW 264.7 cells cultured with Thin Film Cell Culture. LPS and IFN<sub>γ</sub> stimulated RAW 264.7 cells were exposed to 0.07%, 0.13%, 0.24%, 0.61%, 2%, 10%, or 50% O<sub>2</sub> (balance N<sub>2</sub>) for 4 hours using Thin Film Cell Culture. A. Media NO<sub>x</sub> were converted to NO via reaction with vanadium chloride and measured with a Sievers Nitric Oxide Analyzer (see Methods). Data presented are mean ± SD. (*n* ≥ 3). B, C. Representative western blots of an SDS-PAGE gel (B) and a low temperature SDS-PAGE gel (C) for iNOS and β actin. (*n* ≥ 3). (R) RAW 264.7 cells grown in atmospheric

O<sub>2</sub>. (+) RAW 264.7 cells treated with LPS and IFN $\gamma$  for at least 18 hours prior to exposure to the designated pO<sub>2</sub>. (-) RAW 264.7 cells not treated with LPS and IFN $\gamma$ .  
(M) BioRad Kaleidoscope Prestained Standards (BioRad, Hercules CA).

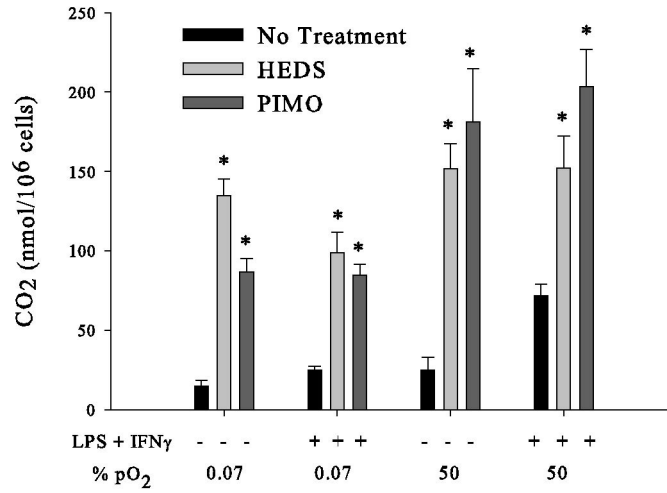
Figure 4.



Correlation between OPPC activity and NO<sub>x</sub> production. A. RAW 264.7 cells (closed circles), LPS and IFN $\gamma$  stimulated RAW 264.7 cells (open circles), or LPS and IFN $\gamma$  stimulated RAW 264.7 cells pretreated with the iNOS inhibitor, 1400W at 100  $\mu$ M (open triangles) were incubated with 1-<sup>14</sup>C glucose or 6-<sup>14</sup>C glucose in parallel experiments at 0.07%, 0.13%, 0.24%, 0.61%, 2%, 10%, or 50% O<sub>2</sub> (balance N<sub>2</sub>). Cumulative OPPC activity was calculated by subtracting <sup>14</sup>CO<sub>2</sub> produced in the presence of 6-<sup>14</sup>C glucose

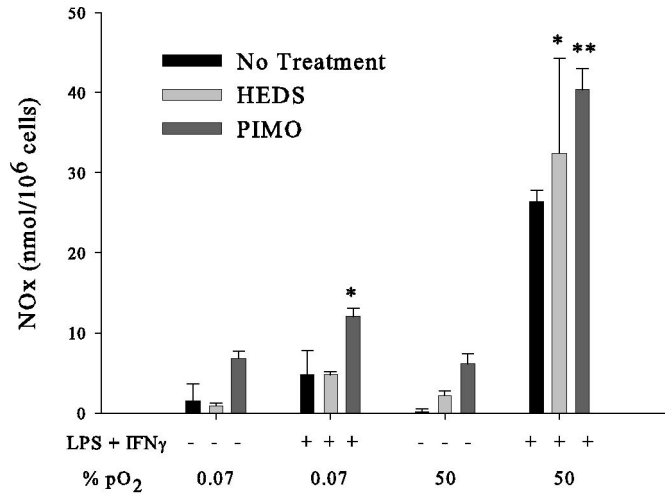
(TCA Activity) from  $^{14}\text{CO}_2$  produced in the presence of  $1\text{-}^{14}\text{C}$  glucose (OPPC Activity + TCA Activity). OPPC activity by LPS and  $\text{IFN}\gamma$  stimulated RAW 264.7 cells was significantly different from RAW 264.7 cells and LPS and  $\text{IFN}\gamma$  stimulated RAW 264.7 cells + 1400W at all  $\text{pO}_2$  ( $p < 0.001$ ). At this concentration (100  $\mu\text{M}$ ), 1400W did not completely inhibit the enhanced OPPC activity resulting from LPS and  $\text{IFN}\gamma$  stimulation. Data presented are mean  $\pm$  SD. ( $n \geq 4$ ) B. Linear regression of OPPC activity and NOx production (data shown in Figure 2).  $y = [b1]x + [b0]$

Figure 5.



OPPC Challenge with HEDS and PIMO. OPPC activity of RAW 264.7 cells and LPS and IFN $\gamma$  stimulated RAW 264.7 cells was measured during treatment with one of two chemical oxidants, HEDS (2 mM) or PIMO (2 mM), at 0.07% and 50% O<sub>2</sub> for 4 hours. (\*) Significant effect of HEDS or PIMO treatment on OPPC activity versus no treatment (p < 0.001). Data presented are mean  $\pm$  SD. (n = 4)

Figure 6.



NOx production during OPPC challenge with HEDS and PIMO. RAW 264.7 cells and LPS and IFN $\gamma$  stimulated RAW 264.7 cells were treated with 2 mM HEDS or 2 mM PIMO during a 4 hour exposure to 0.07% or 50% O<sub>2</sub>. Media NOx were converted to NO via reaction with vanadium chloride and measured with a Sievers Nitric Oxide Analyzer. PIMO data were corrected for the signal of PIMO in media (3.64 nmol). A statistically significant effect of HEDS or PIMO on NOx versus no treatment was calculated where indicated (\* p < 0.05, \*\* p < 0.001). Data presented are mean  $\pm$  SD. (n  $\geq$  3).



**Table 1.** Effect of 1400W on RAW 264.7 NOx Production, OPPC activity, and TCA activity.

		% pO <sub>2</sub>	0.07	0.07	2	2	50	50
		1400W	-	+	-	+	-	+
NOx nmol/10 <sup>6</sup> cells	NS		1.5 ± 2.1	ND	0.1 ± 1.1	ND	0.2 ± 0.3	ND
	S		4.9 ± 3.0 *	0.0 ± 0.5 †	15.5 ± 2.8 *	ND	26.4 ± 1.5 *	0.3 ± 1.3 †
OPPC nmol CO <sub>2</sub> /10 <sup>6</sup> cells	NS		14.7 ± 3.8 ‡	10.7 ± 1.7	7.4 ± 0.9	5.0 ± 1.9	25.1 ± 7.9 ‡	9.7 ± 1.0 §
	S		25.0 ± 2.2 a	13.1 ± 0.4 b	59.0 ± 4.8 a	18.8 ± 1.9 a,b	71.8 ± 7.3 a	27.9 ± 5.3 a,b
TCA nmol CO <sub>2</sub> /10 <sup>6</sup> cells	NS		0.3 ± 0.1	0.2 ± 0.02	1.7 ± 0.4	4.9 ± 0.4 c	4.1 ± 2.9	5.78 ± 2.9
	S		0.4 ± 0.1	0.3 ± 0.01	0.6 ± 0.04	0.3 ± 0.04 d	0.6 ± 0.04 d	0.3 ± 0.1 d

RAW 264.7 cells were stimulated (S), or not (NS), with 1 µg/mL LPS and 100 U/mL IFN $\gamma$  prior to exposure to 4 hours of 0.07%, 2%, or 10% O<sub>2</sub> with Thin Film Cell Culture. RAW 264.7 cells were treated with 100 µM 1400W (+), or not (-), for 1 ½ hours prior to Thin Film Cell Culture. (ND) = not determined. (\*) Effect of LPS and IFN $\gamma$  treatment on media NOx (0.07% p < 0.05; 2% and 50% p < 0.001). (†) Effect of 1400W treatment on media NOx (0.07% p < 0.01, 50% p < 0.001). (‡) Effect of pO<sub>2</sub> on RAW 264.7 OPPC activity (0.07% and 50% > 2%, p < 0.05). (§) Effect of 1400W treatment on RAW 264.7 cells OPPC activity (p < 0.001). (a) Effect of LPS and IFN $\gamma$  treatment on OPPC activity (p < 0.001). (b) Effect of 1400W treatment on OPPC activity by LPS and IFN $\gamma$  stimulated RAW 264.7 cells (p < 0.001). (c) Effect of 1400W on TCA activity (p < 0.05). (d) Effect of LPS and IFN $\gamma$  treatment on TCA activity (Without 1400W p < 0.01, With 1400W p < 0.001). Data presented are mean ± SD. (NOx n ≥ 3, OPPC n ≥ 4, TCA n ≥ 2).



**CHAPTER 3.**  
**EFFECT OF CHANGING EXTRACELLULAR L-ARGININE**  
**CONCENTRATION ON MACROPHAGE NO PRODUCTION**

Mary A. Robinson

Unpublished Data

## INTRODUCTION

L-arginine is a substrate for NO production by iNOS; the nitrogen in NO is derived from either of the guanidino nitrogens of L-arginine (120, 206). Pharmacological inhibition of iNOS can be obtained *in vivo* and *in vitro* with 1400W, an L-arginine analog that contains an amidine and an amine substituted for the guanidino groups (82). Once 1400W binds to the L-arginine binding site, it is slowly reversible with a dissociation constant ( $K_d$ ) of 7 nM (82). L-arginine competes directly with 1400W binding to iNOS with a binding constant ( $K_s$ ) of 2.2  $\mu$ M (82), similar to the iNOS apparent  $K_m$  for arginine (2.8  $\mu$ M (245)). The concentration of L-arginine in the cell culture media used for our studies was 300 (JBMEM) and 700  $\mu$ M (MEM). Therefore, in the studies describe in Chapters 1 and 2, incubations with 1400W were performed in media prepared without L-arginine to optimize inhibition kinetics. Inhibition of NO production by exposure to 1400W (100  $\mu$ M) in media prepared without L-arginine was measured directly in the forced convection cell culture system (Chapter 1, Figure 6B). To differentiate the effect of 1400W on NO production from the effect of changing the extracellular L-arginine concentration, NO production was also measured in real time during exposure to L-arginine deficient media. This experiment revealed some interesting kinetics of L-arginine removal and replacement.

## **METHODS**

RAW 264.7 cells (American Type Culture Collection, Manassas, VA) were cultured using the forced convection cell culture system described in Chapter 1 Methods (22). Cells were stimulated overnight (18 to 24 hours) with 1  $\mu\text{g/ml}$  LPS (*E. coli* O111:B4; Sigma) and 100 U/ml CHO-derived recombinant mouse IFN $\gamma$  (Cell Sciences, Canton, MA). Then, cells were perfused with a minimal essential media (JBMEM: 140 mM NaCl, 1.4 mM CaCl<sub>2</sub>, 5.3 mM KCl, 4.4 mM Dextrose, 25 mM HEPES, 0.3 mM L-arginine, and 0.1% heat-inactivated FBS (LONZA)) and NO production was measured with an NO electrode as described in Chapter 1 Methods. Once baseline NO production was established, the cells were perfused with L-arginine deficient media (JBMEM without L-arginine) for 1 hour. The cells were returned to L-arginine replete media, and the effect on NO production was measured. The pO<sub>2</sub> for these experiments was 36 Torr O<sub>2</sub>.

## RESULTS AND DISCUSSION

Perfusing the cells with L-arginine deficient media decreased NO production, but did not eliminate it (Figure 1). NO production achieved a new steady state within 15 minutes at approximately 20% of the initial NO production level. One hour later, when the cells were returned to L-arginine replete media, NO production immediately (within seconds) recovered to the initial measured level (Figure 1).

These results suggest that the majority of the L-arginine utilized for NO production by LPS and IFN $\gamma$  stimulated RAW 264.7 cells was transported into the cell, and are consistent with previous observations of extracellular L-arginine usage for NO production by some cell types and tissues (171, 294). They also indicate that transport into the cell was fast (within seconds), relative to the rate of intracellular L-arginine metabolism (minutes). MCAT-2B, a member of the cationic amino acid transporter family, is upregulated by LPS stimulation of macrophages (52, 53), making this transporter a possible candidate for mediating the L-arginine influx. The forced convection cell culture system could be a useful tool to investigate possible MCAT-2B involvement, and the potential requirement for extracellular L-arginine.

One limitation of this experiment is that the L-arginine deficient media contained 0.1% FBS. Plasma concentrations of L-arginine are typically 50 to 200  $\mu$ M (286), and could explain the residual NO production observed; residual NO production was  $\sim$  75 nM, and L-arginine concentration due to the addition of 0.1% FBS is estimated to be as high as 200 nM. However, intracellular conversion of L-citrulline to L-arginine via argininosuccinate synthase and argininosuccinate lyase is also possible (186, 187). These experiments need to be repeated in media without L-arginine or FBS to evaluate the

contribution of intracellular L-arginine supply to NO production by LPS and IFN $\gamma$  stimulated RAW 264.7 cells.

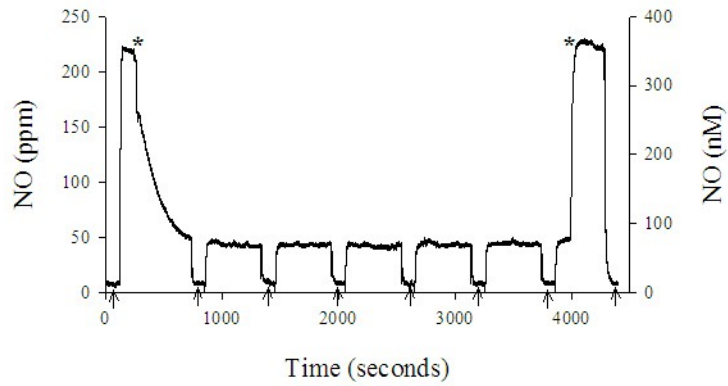
The effect of hypoxia on the kinetics of L-arginine transport and metabolism was not investigated. Hypoxia has also been shown to upregulate MCAT-2B mRNA (169), which would theoretically increase L-arginine influx. In contrast, both hypoxia (24 hours) alone and in combination with LPS has been shown to upregulate macrophage arginase (7, 169), which has been proposed to compete with iNOS for L-arginine as a substrate (48, 108, 250). Inhibition of arginase can increase NO production by stimulated macrophages, and vice versa (109). However, IFN $\gamma$  stimulation of RAW 264.7 cells did not induce arginase (270), and costimulation of RAW 264.7 cells with LPS and IFN $\gamma$  prevented arginase upregulation by an unknown mechanism (270). Thus, minimal arginase should have been present in RAW 264.7 cells following overnight stimulation with LPS and IFN $\gamma$  as described for this experiment and in Chapters 1 and 2.

The duration of hypoxia required to upregulate arginase, and the effect of combined stimulation with LPS, IFN $\gamma$ , and hypoxia on arginase expression and activity, have not been investigated. Because maximal arginase mRNA and protein upregulation by LPS (240, 270), cAMP (188), and dexamethasone (188) requires approximately 12 hours, it is unlikely that the hypoxic exposures used in our experiments (Chapter 1: 40 minutes; Chapter 2: 4 hours) were long enough to elicit an increase in arginase. Furthermore, L-arginine is required for iNOS dimerization, which was either increased (Chapter 1) or maintained (Chapter 2) with hypoxia in our experiments. Therefore, L-arginine availability for iNOS does not appear to be compromised by arginase in the experiments described in Chapters 1 and 2.

In summary, these data suggest that NO production predominantly depended on the continuous transport of extracellular L-arginine into the cell, and that the rate of transport was faster than the rate of utilization under these conditions. Although the effects of hypoxia on L-arginine transport and metabolism were not investigated, the maintenance of iNOS dimerization in Chapters 1 and 2 implied that L-arginine availability for iNOS was not affected by acute hypoxia. Further study of the mechanisms and kinetics of L-arginine transport and metabolism by macrophages in the forced convection cell culture system could help elucidate the physiology of L-arginine supply for NO production.



**Figure 1.**



Effect of Changing Extracellular L-Arginine Concentration on Macrophage NO production. Representative tracing of NO production by LPS and IFN $\gamma$  stimulated RAW 264.7 cells exposed to L-arginine deficient media (\* 240 seconds), and then returned to L-arginine replete media (\* 3980 seconds) using the forced convection cell culture system. NO production was continuously measured via an NO electrode; arrows on the x axis indicate probe baseline checkpoints. Data were baseline corrected. N = 2.

## DISCUSSION

### Acute Hypoxic Regulation of NO Production

The ability of macrophages to migrate to sites of infection, injury, and disease results in their exposure to multiple pO<sub>2</sub> [Physiological: 5 to 71 Torr (23, 32, 37, 42, 87, 88, 124, 129, 159, 253, 254, 263, 266, 281, 282); Pathophysiological: 0 to 20 Torr (37, 38, 69, 70, 72, 79, 111, 116, 118, 122, 130, 166, 194, 213, 236, 237)]. Thus, macrophages are required to operate over a much wider range of pO<sub>2</sub> than most cell types. The studies presented herein are the first to demonstrate the rapidity (seconds) at which NO production is affected by changes in pO<sub>2</sub>, the reversible nature of those changes, and confirm that these changes are occurring within the physiological and pathophysiological range. This rapid and reversible decrease in NO production following exposure to acute hypoxia ( $\leq 4$  hours) is due to O<sub>2</sub> substrate limitation, and not effects on iNOS concentration, iNOS dimerization, NADPH availability, or L-arginine availability.

No previous cell culture studies have investigated NO production during acute hypoxia for direct comparison to these results. The measured apparent  $K_m$ O<sub>2</sub> values (Chapter 1:  $22 \pm 6$  Torr (218), Chapter 2:  $5 \pm 1$  Torr), however, are within the range of values reported previously for long term hypoxic exposures ( $\geq 18$  hours) of LPS and IFN $\gamma$  stimulated macrophages (14 Torr (202),  $77 \pm 1.4$  Torr (179)), and for the isolated iNOS enzyme ( $5 \pm 0.6$  Torr (214), 93 Torr (1), 96 Torr (67)). They are also well within the range of pO<sub>2</sub> required for the regulation of NO production *in vivo* (0 to 71 Torr (23, 32, 37, 38, 42, 69, 70, 72, 79, 87, 88, 111, 116, 118, 122, 124, 129, 130, 159, 166, 194, 213, 236, 237, 253, 254, 263, 266, 281, 282)). The rapidity and reversibility of the

response within the physiological and pathophysiological  $pO_2$  range suggests that changes in tissue  $pO_2$  *in vivo* will significantly affect macrophage NO production, as has been suggested previously (1, 67, 179, 202, 214).

Two prior studies investigated the effects of long term hypoxic exposures on nitrite production by RAW 264.7 cells concurrently stimulated with LPS and  $IFN\gamma$  (179, 202). McCormick et al. measured an apparent  $K_mO_2$  for the headspace gas of  $10.8 \pm 2.0$  % ( $77 \pm 1.4$  Torr) (179). Otto and Baumgardner measured a similar  $pO_2$  dependence in a comparable system, but did not calculate an apparent  $K_mO_2$  from the nitrite data directly (202). Instead, they measured iNOS protein concentration and activity, and found that iNOS protein concentration and activity also decreased as  $pO_2$  decreased. Thus, the changes in nitrite were reflective of changes in the specific activity and/or the amount of active iNOS, as well as effects due to substrate limitation. After normalizing nitrite production to changes in iNOS activity, and accounting for the  $O_2$  diffusion gradient from the headspace gas to the cell surface, the estimated apparent  $K_mO_2$  at the cell surface was 14 Torr (202), similar to the apparent  $K_mO_2$  values measured in these studies of acute hypoxia (Chapter 1:  $22 \pm 6$  Torr (218), Chapter 2:  $5 \pm 1$  Torr).

Acute hypoxia did not affect iNOS protein concentration, and iNOS dimerization was either increased (Chapter 1) or maintained (Chapter 2). These results are consistent with a previous study showing that costimulation with LPS and hypoxia requires a minimum of 3 hours and 6 hours to affect iNOS mRNA and protein, respectively (4). Therefore, the key difference between the regulation of NO production by acute hypoxia and long term hypoxia appears to be the absence of sufficient time for acute hypoxia to influence iNOS mRNA and protein concentration. The mechanism for increased iNOS

dimerization observed in cells cultured with forced convection is not known. Regardless, decreased NO production despite increased iNOS dimerization further suggests that substrate limitation is the primary mechanism mediating decreased NO production during acute hypoxia.

O<sub>2</sub> substrate limitation, not decreased NADPH or L-arginine availability, is the primary mechanism mediating decreased NO production during acute hypoxia.

Macrophage OPPC activity linearly correlated with NO production at all pO<sub>2</sub>, consistent with previous studies in atmospheric O<sub>2</sub> (58, 153, 191, 192). OPPC activity was decreased during acute hypoxia due to the absence of NO production; treatment with 1400W, a specific iNOS inhibitor, significantly reduced OPPC activity in LPS and IFN $\gamma$  stimulated macrophages at all pO<sub>2</sub>. Chemically mediated oxidative stress (HEDS or PIMO) significantly increased OPPC activity under all conditions tested including hypoxia, and did not affect NO production (HEDS). These results are consistent with our measurements in tumor cells (259), and conform with the classical view of decreased metabolic flux through the OPPC under hypoxia (99, 127, 227), whereby removal of O<sub>2</sub> leads to a reducing environment. They additionally demonstrate that the absence of molecular O<sub>2</sub> is not limiting for OPPC activity.

The affect of hypoxia on L-arginine transport and metabolism was not measured directly. However, L-arginine is required for iNOS dimerization (20). Thus, the increase (Chapter 1) or maintenance (Chapter 2) of iNOS dimerization measured in these studies suggests L-arginine was not limiting. These results were expected, because the concentration of L-arginine in the media used for these studies (JBMEM: 300  $\mu$ M, MEM: 700  $\mu$ M) was much greater than the L-arginine apparent  $K_m$  (3  $\mu$ M) (245). Interestingly,

the removal of L-arginine also rapidly and reversibly decreased NO production to 20% of basal levels (Chapter 3). NO production decreased more slowly upon the removal of L-arginine (minutes) than upon the removal of O<sub>2</sub> (seconds), also suggesting the hypoxia mediated decrease in NO production was not due to limited L-arginine influx. In contrast, restoration of L-arginine immediately (seconds) enabled NO production to resume at levels equivalent to the initial measured level. The forced convection cell culture system promises to be a useful tool for studying the effect of changes in extracellular L-arginine transport on NO production.

In summary, changes in physiological and pathophysiological pO<sub>2</sub> rapidly and reversibly regulate macrophage NO production via O<sub>2</sub> substrate limitation. Acute hypoxia did not alter iNOS protein concentration, increased or maintained iNOS dimerization, and did not limit NADPH availability. Because long term hypoxic exposure mediates changes in NO production via effects on iNOS protein in addition to substrate limitation, identifying the degree and duration of hypoxia *in vivo* will be critical to assessing its influence on physiological and pathophysiological macrophage NO production.

### **Implications for Macrophage NO Physiology and Pathology**

Several macrophage phenotypes produce NO (14, 102, 210, 233, 234), and NO production is essential for eliminating certain types of bacterial and parasitic infections (6, 94, 96, 215, 265). However, tissue pO<sub>2</sub> varies widely, and tissues become hypoxic in the wound environment, and during many inflammatory diseases such as sepsis and cancer (116, 194, 213, 236). The studies presented herein suggest that NO production by

macrophages will be rapidly limited by low pO<sub>2</sub> *in vivo*. Additionally, changes in extracellular L-arginine could rapidly affect macrophage NO production *in vivo*.

The center of the wound environment is hypoxic and depleted of L-arginine (7, 225). NO production and L-arginine metabolism by wound macrophages are affected by hypoxia. During hypoxia, wound macrophages metabolize L-arginine by arginase instead of iNOS (7). This switch is thought to mediate the transition from the inflammatory phase of wound healing to the proliferative phase (99). However, once angiogenesis and revascularization restore O<sub>2</sub> to the wound, redirection of L-arginine back to iNOS may result in overlap of the inflammatory phase and the proliferative phase, as has been proposed previously (105). Spatial and temporal measurements of tissue pO<sub>2</sub>, NO production, and angiogenesis during wound healing would provide further insight into the sequence, duration, and overlap of these events.

Sepsis is by definition a systemic inflammatory response to infection (36), and can be thought of as a systemic wound. iNOS expressing macrophages in the heart, lung, liver, and kidney have been observed via immunohistochemistry during the first 24 hours in a rat endotoxemia model (44), which is similar to when of iNOS expressing macrophages appear in a localized wound (24 to 72 hours) (211). Also similar to the wound environment, septic patients become hypoxic (118), and L-arginine plasma concentrations decrease (78), albeit by different mechanisms. The results described herein suggest that macrophage NO production may be limited in septic patients due to decreased O<sub>2</sub> and L-arginine availability, as previously proposed (1, 7, 41, 62, 67, 94, 168, 179, 202, 214, 219). Spatial and temporal measurements of pO<sub>2</sub>, NO production, and L-arginine concentration and turnover in septic models and/or patients are necessary

to verify these results *in vivo*. If these findings are confirmed, diminished macrophage function as a result of hypoxia and L-arginine depletion could promote overwhelming infection, making it questionable as to whether specific iNOS inhibitors will provide therapeutic value for patients in septic shock. Preventing circulatory collapse, while enabling macrophages to fight off the infection, may be a more appropriate therapeutic strategy for patients in the later stages of sepsis.

Chronic inflammation and hypoxia correlate with tumor development and progression (37, 38, 69, 70, 79, 111, 162, 166). The results herein suggest that macrophage, and possibly tumor, NO production will be rapidly and reversibly limited within hypoxic areas. Similar to wound macrophages, TAM in a hypoxic environment may preferentially metabolize L-arginine via arginase (7). Arginase production of ornithine promotes cell growth, and may enable tumor growth (184). Furthermore, the results herein suggest that NO production could be restored once angiogenesis improves O<sub>2</sub> delivery to the tumor. Thus, spatial and temporal measurements of pO<sub>2</sub>, NO production, and ornithine production, and identification of the cell types involved, are needed to verify these results *in vivo*, and could further our understanding of how these factors contribute to tumor progression and metastasis.

## **Conclusions**

The pO<sub>2</sub> dependence of NO production occurs within the physiological and pathophysiological range. Acute hypoxia rapidly and reversibly decreases macrophage NO production. O<sub>2</sub> substrate limitation is responsible for decreased NO production during acute hypoxic exposures; no effects were attributable to changes in iNOS protein

concentration, iNOS dimerization, NADPH availability, or albeit indirectly, L-arginine availability. The primary differences observed between long term hypoxia and acute hypoxia appear to be the additional effects of long term hypoxia on iNOS mRNA and protein concentration. Modification of extracellular L-arginine concentration also rapidly and reversibly regulates macrophage NO production. Acute hypoxia did not appear to limit L-arginine availability. However, the effects of short and long term hypoxia on L-arginine transport and metabolism requires further investigation. Both tissue pO<sub>2</sub> and L-arginine concentration may significantly influence macrophage NO production and function *in vivo*. Further studies of the tissue microenvironment, and its effects on macrophage NO production, are required to understand its contribution to the pathogenesis of disease.



## **APPENDIX: HYPOXIC CELL CULTURE**

### **Challenges of Hypoxic Cell Culture**

Hypoxic cell culture is typically performed using an airtight chamber in which the gas phase overlying the media, or headspace gas, is tightly controlled. There are several limitations to this system that limit accurate and precise delivery of O<sub>2</sub> to the cells. When the media is not stirred, the poor solubility of O<sub>2</sub> in media forces investigators to use a long equilibration time to acquire hypoxic conditions (22). Diffusion of oxygen through the media is so slow, that the predicted pO<sub>2</sub> calculated based on diffusion alone (i.e. in the absence of convection currents) is 0 Torr at 1 mm below the media surface for a headspace gas of 40 Torr (22). Thus, convection currents, due to temperature gradients and vibrational changes in the environment, are responsible for the majority of the O<sub>2</sub> delivery to the cell monolayer. Since these currents depend on the environment, the resulting pO<sub>2</sub> at the cell monolayer is highly variable within and between cultures, as was confirmed in our laboratory (202). Another common problem experimenters face is that many of the materials commonly used for conventional cell culture absorb O<sub>2</sub> from room air and release substantial amounts into the media during “controlled” anoxia (242). These limitations were overcome using the two cell culture systems described below.

### **Forced Convection Cell Culture**

The forced convection cell culture system (Chapter 1, Figure 1) uses countercurrent exchange to equilibrate the media with a gas mixture before pumping the

media through a capillary tube containing the adherent cells (22). None of the materials used in this system absorb or release O<sub>2</sub>. Thus, accurate and precise amounts of O<sub>2</sub> can be delivered to the cells, and immediate changes between pO<sub>2</sub> can be performed. The outflow from this system immediately flows past two ports where various probes can be inserted. In these studies, a NO probe was used to record real-time NO production by the cells. The response time and sensitivity of the probe is such that physiologic changes in NO can be detected with as few as 1 X 10<sup>6</sup> cells in less than 5 seconds from its production. One disadvantage of this system is the limited number of cells (1 X 10<sup>6</sup>), and thus limited sample material (protein and RNA) available for analysis.

### **Thin Film Cell Culture**

The thin film cell culture system uses reduced media volume and constant mixing to accurately deliver O<sub>2</sub> to a cell monolayer (143). The headspace pO<sub>2</sub> is controlled by placing the glass dishes or vials into leak proof aluminum chambers, and subjecting them to a series of gas exchanges with N<sub>2</sub> or O<sub>2</sub> to produce the desired headspace pO<sub>2</sub> (142-144, 259). Chambers are warmed to 37°C and shaken continuously to ensure adequate gas exchange between the headspace and the media throughout the experiment. The pO<sub>2</sub> in the chambers is measured at the end of the incubation period using a polarographic O<sub>2</sub> electrode. Additionally, EF5, a nitroimidazole, can be used to verify that the cellular pO<sub>2</sub> is equivalent to the headspace pO<sub>2</sub> (141, 142). One disadvantage of this system is the slower equilibration time between the headspace pO<sub>2</sub> and the O<sub>2</sub> tension at the cell monolayer (~ 30 minutes).

## BIBLIOGRAPHY

1. Abu-Soud HM, Ichimori K, Nakazawa H, and Stuehr DJ. Regulation of inducible nitric oxide synthase by self-generated NO. *Biochemistry* 40: 6876-6881, 2001.
2. Abu-Soud HM, Rousseau DL, and Stuehr DJ. Nitric oxide binding to the heme of neuronal nitric-oxide synthase links its activity to changes in oxygen tension. *J Biol Chem* 271: 32515-32518, 1996.
3. Agani F, Puchowicz M, Chavez J, Pichiule P, and LaManna J. Role of nitric oxide in the regulation of HIF-1alpha expression during hypoxia. *Am J Physiol Cell Physiol* 283: C178-C186, 2002.
4. Agorreta J, Garayoa M, Montuenga LM, and Zulueta JJ. Effects of acute hypoxia and lipopolysaccharide on nitric oxide synthase-2 expression in acute lung injury. *Am J Respir Crit Care Med* 168: 287-296, 2003.
5. Akira S. Toll-like receptors and innate immunity. In: *Advances in Immunology* Academic Press, 2001, p. 1-56.
6. Alam MS, Zaki MH, Yoshitake J, Akuta T, Ezaki T, and Akaike T. Involvement of Salmonella enterica serovar Typhi RpoS in resistance to NO-mediated host defense against serovar Typhi infection. *Microbial Pathogenesis* 40: 116-125, 2006.
7. Albina J, Henry W, Jr, Mastrofrancesco B, Martin B, and Reichner J. Macrophage activation by culture in an anoxic environment. *J Immunol* 155: 4391-4396, 1995.
8. Albina JE, Cui S, Mateo RB, and Reichner JS. Nitric oxide-mediated apoptosis in murine peritoneal macrophages. *J Immunol* 150: 5080-5085, 1993.

9. Albina JE, Mills CD, Henry WL, Jr., and Caldwell MD. Regulation of macrophage physiology by L-arginine: role of the oxidative L-arginine deiminase pathway. *J Immunol* 143: 3641-3646, 1989.
10. Allen CB, Schneider BK, and White CW. Limitations to oxygen diffusion and equilibration in in vitro cell exposure systems in hyperoxia and hypoxia. *Am J Physiol Lung Cell Mol Physiol* 281: L1021-1027, 2001.
11. Amatore C, Arbault S, Bouton C, Drapier JC, Ghandour H, and Koh AC. Real-time amperometric analysis of reactive oxygen and nitrogen species released by single immunostimulated macrophages. *ChemBioChem* 9: 1472-1480, 2008.
12. Ambs S, Merriam WG, Bennett WP, Felley-Bosco E, Ogunfusika MO, Oser SM, Klein S, Shields PG, Billiar TR, and Harris CC. Frequent nitric oxide synthase-2 expression in human colon adenomas: Implications for tumor angiogenesis and colon cancer progression. *Cancer Res* 58: 334-341, 1998.
13. Archer SL, Freude KA, and Shultz PJ. Effect of graded hypoxia on the induction and function of inducible nitric oxide synthase in rat mesangial cells. *Circ Res* 77: 21-28, 1995.
14. Arimoto T, and Bing G. Up-regulation of inducible nitric oxide synthase in the substantia nigra by lipopolysaccharide causes microglial activation and neurodegeneration. *Neurobiology of Disease* 12: 35-45, 2003.
15. Arsham AM, Plas DR, Thompson CB, and Simon MC. Akt and hypoxia-inducible factor-1 independently enhance tumor growth and angiogenesis. *Cancer Res* 64: 3500-3507, 2004.

16. Arteel GE, Briviba K, and Sies H. Protection against peroxynitrite. *FEBS Letters* 445: 226-230, 1999.
17. Ashutosh K. Nitric oxide and asthma: a review. *Opin Pulm Med* 6: 21-25, 2000.
18. Ayene IS, Biaglow JE, Kachur AV, Stamato TD, and Koch CJ. Mutation in G6PD gene leads to loss of cellular control of protein glutathionylation: Mechanism and implication. *Journal of Cellular Biochemistry* 103: 123-135, 2008.
19. Bach EA, Aguet M, and Schreiber RD. The IFN $\gamma$  receptor: A paradigm for cytokine receptor signaling. *Annual Review of Immunology* 15: 563-591, 1997.
20. Baek KJ, Thiel BA, Lucas S, and Stuehr DJ. Macrophage nitric oxide synthase subunits. Purification, characterization, and role of prosthetic groups and substrate in regulating their association into a dimeric enzyme. *J Biol Chem* 268: 21120-21129, 1993.
21. Bakker J, Grover R, McLuckie A, Holzapfel L, Andersson J, Lodato R, Watson D, Grossman S, Donaldson J, and Takala J. Administration of the nitric oxide synthase inhibitor N-G-methyl-L-arginine hydrochloride (546C88) by intravenous infusion for up to 72 hours can promote the resolution of shock in patients with severe sepsis: Results of a randomized, double-blind, placebo-controlled multicenter study (study no. 144-002). *Crit Care Med* 32: 1-12, 2004.
22. Baumgardner J, and Otto C. In vitro intermittent hypoxia: challenges for creating hypoxia in cell culture. *Respiratory Physiology and Neurobiology* 136: 131-139, 2003 Jul 16.

23. Baumgartl H, Zimmelka W, and Lubbers D. Evaluation of PO<sub>2</sub> profiles to describe the oxygen pressure field within the tissue. *Comparative Biochemistry and Physiology Part A: Physiology* 132: 75-85, 2002.
24. Bentley AM, Otto CM, and Shofer FS. Comparison of dogs with septic peritonitis: 1988 - 1993 versus 1999 - 2003. *Journal of Veterinary Emergency & Critical Care* 17: 391-398, 2007.
25. Beutler BA. TLRs and innate immunity. *Blood* 113: 1399-1407, 2009.
26. Biaglow JE, Ayene IS, Koch CJ, Donahue J, Stamato TD, Mieyal JJ, and Tuttle SW. Radiation response of cells during altered protein thiol redox. *Radiation Research* 159: 484-494, 2003.
27. Biaglow JE, Ayene IS, Tuttle SW, Koch CJ, Donahue J, and Mieyal JJ. Role of vicinal protein thiols in radiation and cytotoxic responses. *Radiation Research* 165: 307-317, 2006.
28. Bjornheden T, Levin M, Evaldsson M, and Wiklund O. Evidence for hypoxic areas within the arterial wall in vivo. *Arterioscler Thromb Vasc Biol* 19: 870-876, 1999.
29. Blanchette J, Jaramillo M, and Olivier M. Signalling events involved in interferon-gamma-inducible macrophage nitric oxide generation. *Immunology* 108: 513-522, 2003.
30. Blough NV, and Zafiriou OC. Reaction of superoxide with nitric oxide to form peroxonitrite in alkaline aqueous solution. *Inorg Chem* 24: 3502-3504, 1985.

31. Blouin CC, Page EL, Soucy GM, and Richard DE. Hypoxic gene activation by lipopolysaccharide in macrophages: implication of hypoxia-inducible factor 1a. *Blood* 103: 1124-1130, 2004.
32. Boegehold MA, and Johnson PC. Periarteriolar and tissue PO<sub>2</sub> during sympathetic escape in skeletal muscle. *Am J Physiol Heart Circ Physiol* 254: H929-936, 1988.
33. Bogdan C. Nitric oxide and the immune response. *Nat Immunol* 2: 907-916, 2001.
34. Bostrom P, Magnusson B, Svensson P, Wiklund O, Boren J, Carlsson LMS, Stahlman M, Olofsson S, and Hulten LM. Hypoxia converts human macrophages into triglyceride-loaded foam cells. *Arterioscler Thromb Vasc Biol* 26: 1871-1876, 2006.
35. Bove PF, and van der Vliet A. Nitric oxide and reactive nitrogen species in airway epithelial signaling and inflammation. *Free Radical Biology and Medicine* 41: 515-527, 2006.
36. Brady CA, and Otto CM. Systemic inflammatory response syndrome, sepsis, and multiple organ dysfunction. *Vet Clinics North America: Small Animal Practice* 31: 1147-1162, 2001.
37. Braun RD, Lanzen JL, Snyder SA, and Dewhirst MW. Comparison of tumor and normal tissue oxygen tension measurements using OxyLite or microelectrodes in rodents. *Am J Physiol Heart Circ Physiol* 280: H2533-2544, 2001.
38. Brizel DM, Scully SP, Harrelson JM, Layfield LJ, Bean JM, Prosnitz LR, and Dewhirst MW. Tissue oxygenation predicts for the likelihood of distant metastases in human soft tissue sarcoma. *Cancer Res* 56: 941-943, 1996.

39. Brodsky SV, Morrishow AM, Dharia N, Gross SS, and Goligorsky MS. Glucose scavenging of nitric oxide. *Am J Physiol Renal Physiol* 280: F480-F486, 2001.
40. Brown GC. Nitric oxide and mitochondria. *Frontiers in Bioscience* 12: 1024-1033, 2007.
41. Bruins MJ, Lamers WH, Meijer AJ, Soeters PB, and Deutz NEP. In vivo measurement of nitric oxide production in porcine gut, liver and muscle during hyperdynamic endotoxaemia. *Br J Pharmacol* 137: 1225-1236, 2002.
42. Buerk DG, and Nair P. PtiO<sub>2</sub> and CMRO<sub>2</sub> changes in cortex and hippocampus of aging gerbil brain. *J Appl Physiol* 74: 1723-1728, 1993.
43. BATTERY L, Springall D, Chester A, Evans T, Standfield E, Parums D, Yacoub M, and Polak J. Inducible nitric oxide synthase is present within human atherosclerotic lesions and promotes the formation and activity of peroxynitrite. *Laboratory Investigation* 75: 77-85, 1996.
44. BATTERY LDK, Evans TJ, Springall DR, Carpenter A, Cohen J, and Polak JM. Immunochemical localization of inducible nitric oxide synthase in endotoxin-treated rats. *Laboratory Investigation* 71: 755-764, 1994.
45. Caplan M, Hedlund E, Hill N, and MacKendrick W. The role of endogenous nitric oxide and platelet-activating factor in hypoxia-induced intestinal injury in rats. *Gastroenterology* 106: 346-352, 1994.
46. Carlin RE, Ferrario L, Boyd JT, Camporesi EM, McGraw DJ, and Hakim TS. Determinants of nitric oxide in exhaled gas in the isolated rabbit lung. *American Journal of Respiratory & Critical Care Medicine* 155: 922-927, 1997.



47. Caulfield JL, Singh SP, Wishnok JS, Deen WM, and Tannenbaum SR. Bicarbonate inhibits N-nitrosation in oxygenated nitric oxide solutions. *Journal of Biological Chemistry* 271: 25859-25863, 1996.
48. Chang C-I, Liao JC, and Kuo L. Arginase modulates nitric oxide production in activated macrophages. *Am J Physiol Heart Circ Physiol* 274: H342-348, 1998.
49. Charles IG, Palmer RMJ, Hickery MS, Bayliss MT, Chubb AP, Hall VS, Moss DW, and Moncada S. Cloning, characterization, and expression of a cDNA encoding an inducible nitric oxide synthase from the human chondrocyte. *PNAS* 90: 11419-11423, 1993.
50. Chen J-H, Lin H-H, Chiang T-A, Hsu J-D, Ho H-H, Lee Y-C, and Wang C-J. Gaseous nitrogen oxide promotes human lung cancer cell line A549 migration, invasion, and metastasis via iNOS-mediated MMP-2 production. *Toxicol Sci* 106: 364-375, 2008.
51. Christova T, and Templeton DM. Effect of hypoxia on the binding and subcellular distribution of iron regulatory proteins. *Mol Cell Biochem* 301: 21-32, 2007.
52. Closs EI. Expression, regulation and function of carrier proteins for cationic amino acids. *Current Opinion in Nephrology & Hypertension* January 11: 99-107, 2002.
53. Closs EI, Scheld J-S, Sharafi M, and Forstermann U. Substrate supply for nitric oxide synthase in macrophages and endothelial cells: Role of cationic amino acid transporters. *Mol Pharmacol* 57: 68-74, 2000.

54. Cobb JP, Hotchkiss RS, Swanson PE, Chang K, Qiu Y, Laubach VE, Karl IE, and Buchman TG. Inducible nitric oxide synthase (iNOS) gene deficiency increases the mortality of sepsis in mice. *Surgery* 126: 438-442, 1999.
55. Cobb JP, Natanson C, Quezado ZM, Hoffman WD, Koev CA, Banks S, Correa R, Levi R, Elin RJ, Hosseini JM, and et a. Differential hemodynamic effects of L-NMMA in endotoxemic and normal dogs. *Am J Physiol Heart Circ Physiol* 268: H1634-1642, 1995.
56. Colakogullari M, Ulukaya E, Yilmaztepe A, Ocakoglu G, Yilmaz M, Karadag M, and Tokullugil A. Higher serum nitrate levels are associated with poor survival in lung cancer patients. *Clinical Biochemistry* 39: 898-903, 2006.
57. Corraliza IM, Campo ML, Fuentes JM, Camposportuguez S, and Soler G. Parallel Induction of nitric oxide and glucose-6-phosphate dehydrogenase in activated bone marrow derived macrophages. *Biochemical and Biophysical Research Communications* 196: 342-347, 1993.
58. Costa Rosa LF, Curi R, Murphy C, and Newsholme P. Effect of adrenaline and phorbol myristate acetate or bacterial lipopolysaccharide on stimulation of pathways of macrophage glucose, glutamine and O<sub>2</sub> metabolism. Evidence for cyclic AMP-dependent protein kinase mediated inhibition of glucose-6-phosphate dehydrogenase and activation of NADP<sup>+</sup>-dependent 'malic' enzyme. *Biochem J* 310: 709-714, 1995.
59. D'Angio C, and Finkelstein J. Oxygen regulation of gene expression: A study in opposites. *Molecular Genetics and Metabolism* 71: 371-380, 2000.

60. Dalton DK, and al. e. Multiple defects in immune-cell function in mice with disrupted interferon-gamma genes. *Science* 259: 1739-1742, 1993.
61. Daniliuc S, Bitterman H, Rahat M, Kinarty A, Rosenzweig D, and Nitza L. Hypoxia inactivates inducible nitric oxide synthase in mouse macrophages by disrupting its interaction with alpha-actinin-4. *J Immunol* 171: 3225-3232, 2003.
62. Desmukh DR, Ghole VS, Marescau B, and De Deyn PP. Effect of endotoxemia on plasma and tissue levels of nitric oxide metabolites and guanidino compounds. *Arch Physiol Biochem* 105: 32-37, 1997.
63. Dlaska M, and Weiss G. Central role of transcription factor NF-IL6 for cytokine and iron-mediated regulation of murine inducible nitric oxide synthase expression. *J Immunol* 162: 6171-6177, 1999.
64. Dombrovskiy V, Martin A, Sunderram J, and Paz HL. Rapid increase in hospitalization and mortality rates for severe sepsis in the United States: A trend analysis from 1993 to 2003. *Critical Care Medicine* 35: 1244-1250, 2007.
65. Drapier JC, and Hibbs JB, Jr. Differentiation of murine macrophages to express nonspecific cytotoxicity for tumor cells results in L-arginine-dependent inhibition of mitochondrial iron-sulfur enzymes in the macrophage effector cells. *J Immunol* 140: 2829-2838, 1988.
66. Drapier JC, Hirling H, Wietzerbin J, Kaldy P, and Kuhn LC. Biosynthesis of nitric oxide activates iron regulatory factor in macrophages. *EMBO Journal* 12: 3643-3649, 1993.

67. Dweik R, Laskowski D, Abu-Soud H, Kaneko F, Hutte R, Stuehr D, and Erzurum S. Nitric oxide regulation in the lung: Regulation by oxygen through a kinetic mechanism. *J Clin Invest* 101: 660-666, 1998.
68. Eggleston LV, and Krebs HA. Regulation of the pentose phosphate cycle. *Biochem J* 138: 425-435, 1974.
69. Evans SM, Du KL, Chalian AA, Mick R, Zhang PJ, Hahn SM, Quon H, Lustig R, Weinstein GS, and Koch CJ. Patterns and levels of hypoxia in head and neck squamous cell carcinomas and their relationship to patient outcome. *Int J Radiat Oncol Biol Phys* 69: 1024-1031, 2007.
70. Evans SM, Fraker DL, Hahn SM, Gleason K, Jenkins WT, Jenkins K, Hwang WT, Zhang PD, Mick R, and Koch CJ. EF5 binding and clinical outcome in human soft tissue sarcomas. *Int J Radiat Oncol Biol Phys* 64: 922-927, 2006.
71. Felley-Bosco E. Role of nitric oxide in genotoxicity: Implication for carcinogenesis. *Cancer and Metastasis Reviews* 17: 25-37, 1998.
72. Ferreira C, Chagas A, Carvalho M, Dantas A, Jatene M, Bento de Souza L, and Lemos da Luz P. Influence of hypoxia on nitric oxide synthase activity and gene expression in children with congenital heart disease. A novel pathophysiological adaptive mechanism. *Circulation* 103: 2272-2276, 2001.
73. Finkel T, and Holbrook NJ. Oxidants, oxidative stress and the biology of ageing. *Nature* 408: 239-247, 2000.
74. Ford PC, Wink DA, and Stanbury DM. Autoxidation kinetics of aqueous nitric oxide. *FEBS Letters* 326: 1-3, 1993.

75. Foster GE, Poulin MJ, and Hanly PJ. Intermittent hypoxia and vascular function: implications for obstructive sleep apnoea. *Experimental Physiology* 92: 51-65, 2007.
76. Fowler A, Hamman R, Zerbe G, Benson K, and Hyers T. Adult respiratory distress syndrome. Prognosis after onset. *Am Rev Respir Dis* 132: 472-478, 1985.
77. Freeman BD, Zeni F, Banks SM, Eichacker PQ, Bacher JD, Garvey EP, Tuttle JV, Jurgensen CH, Natanson C, and Danner RL. Response of the septic vasculature to prolonged vasopressor therapy with N-omega-monomethyl-L-arginine and epinephrine in canines. *Crit Care Med* 26: 877-886, 1998.
78. Freund H, Atamian S, Holroyde J, and Fischer JE. Plasma amino acids as predictors of the severity and outcome of sepsis. *Ann Surg* 190: 571-576, 1979.
79. Fyles AW, Milosevic M, Wong R, Kavanagh MC, Pintili M, Chapman W, Levin W, Manchul L, Keane TJ, and Hill RP. Oxygenation predicts radiation response and survival in patients with cervix cancer. *Radioth Oncol* 48: 149-156, 1998.
80. Gao J, Morrison DC, Parmely TJ, Russell SW, and Murphy WJ. An interferon-gamma -activated Site (GAS) is necessary for full expression of the mouse iNOS gene in response to interferon-gamma and lipopolysaccharide. *J Biol Chem* 272: 1226-1230, 1997.
81. Gardner PR, Martin LA, Hall D, and Gardner AM. Dioxygen-dependent metabolism of nitric oxide in mammalian cells. *Free Radical Biology and Medicine* 31: 191-204, 2001.
82. Garvey EP, Oplinger JA, Furfine ES, Kiff RJ, Laszlo F, Whittle BJR, and Knowles RG. 1400W is a slow, tight binding, and highly selective inhibitor of

- inducible nitric oxide synthase *in vitro* and *in vivo*. *J Biol Chem* 272: 4959-4963, 1997.
83. Gauthier N, Lohm S, Touzery C, Chantome A, Perette B, Reveneau S, Brunotte F, Juillerat-Jeanneret L, and Jeannin J-F. Tumour-derived and host-derived nitric oxide differentially regulate breast carcinoma metastasis to the lungs. *Carcinogenesis* 25: 1559-1565, 2004.
84. Geissmann F, Jung S, and Littman DR. Blood monocytes consist of two principal subsets with distinct migratory properties. *Immunity* 19: 71-82, 2003.
85. Giovanelli J, Campos K, and Kaufman S. Tetrahydrobiopterin, a cofactor for rat cerebellar nitric oxide synthase does not function as a reactant in the oxygenation of arginine. *PNAS* 88: 7091-7095, 1991.
86. Gole M, Souza J, Choi I, Hertkorn C, Malcolm S, Roust III R, Finkel B, Lanken P, and Ischiropoulos H. Plasma proteins modified by tyrosine nitration in acute respiratory distress syndrome. *Am J Physiol Lung Cell Mol Physiol* 278: L961-L967, 2000.
87. Golub AS, Barker MC, and Pittman RN. Microvascular oxygen tension in the rat mesentery. *Am J Physiol Heart Circ Physiol* 294: H21-28, 2008.
88. Golub AS, and Pittman RN. PO<sub>2</sub> measurements in the microcirculation using phosphorescence quenching microscopy at high magnification. *Am J Physiol Heart Circ Physiol* 294: H2905-2916, 2008.
89. Gomez-Jimenez J, Salgado A, Mourelle M, Martin M, Segura R, Peracaula R, and Moncada S. L-arginine: Nitric oxide pathway in endotoxemia and human septic shock. *Critical Care Medicine* 23: 253-258, 1995.

90. Gow A, Thom S, and Ischiropoulos H. Nitric oxide and peroxynitrite-mediated pulmonary cell death. *Am J Physiol* 274: L112-L118, 1998.
91. Gow AJ, Chen Q, Hess DT, Day BJ, Ischiropoulos H, and Stamler JS. Basal and stimulated protein S-nitrosylation in multiple cell types and tissues. *J Biol Chem* 277: 9637-9640, 2002.
92. Gow AJ, Farkouh CR, Munson DA, Posencheg MA, and Ischiropoulos H. Biological significance of nitric oxide-mediated protein modifications. *Am J Physiol Lung Cell Mol Physiol* 287: L262-268, 2004.
93. Gow AJ, and Ischiropoulos H. Nitric oxide chemistry and cellular signaling. *Journal of Cellular Physiology* 187: 277-282, 2001.
94. Granger D, Hibbs Jr. J, Perfect J, and Durack D. Metabolic fate of L-arginine in relation to microbistatic capability of murine macrophages. *J Clin Invest* 85: 264-273, 1990.
95. Griscavage JM, Wilk S, and Ignarro LJ. Inhibitors of the proteasome pathway interfere with induction of nitric oxide synthase in macrophages by blocking activation of transcription factor NF-kappaB. *Proc Natl Acad Sci* 93: 3308-3312, 1996.
96. Groote MAD, and Fang FC. NO inhibitions: Antimicrobial properties of nitric oxide. *Clinical Infectious Diseases* 21: S162-S165, 1995.
97. Grover R, Zaccardelli D, Colice G, Guntupalli K, Watson D, and Vincent J. An open-label dose escalation study of the nitric oxide synthase inhibitor, N-G-methyl-L-arginine hydrochloride (546C88), in patients with septic shock. *Critical Care Medicine* 27: 913-922, 1999.

98. Guo L, Zhang Z, Green K, and Stanton RC. Suppression of Interleukin-1 $\beta$ -induced nitric oxide production in RINm5F cells by inhibition of glucose-6-phosphate dehydrogenase. *Biochemistry* 41: 14726-14733, 2002.
99. Gupte SA, Okada T, McMurtry IF, and Oka M. Role of pentose phosphate pathway-derived NADPH in hypoxic pulmonary vasoconstriction. *Pulmonary Pharmacology & Therapeutics* 19: 303-309, 2006.
100. Gupte SA, and Wolin MS. Hypoxia promotes relaxation of bovine coronary arteries through lowering cytosolic NADPH. *Am J Physiol Heart Circ Physiol* 290: H2228-2238, 2006.
101. Haddad I, Zhu S, Ischiropoulos H, and Matalon S. Nitration of surfactant protein A results in decreased ability to aggregate lipids. *Am J Physiol* 270: L281-L288, 1996.
102. Hagemann T, Biswas SK, Lawrence T, Sica A, and Lewis CE. Regulation of macrophage function in tumors: the multifaceted role of NF- $\kappa$ B. *Blood* 113: 3139-3146, 2009.
103. Hara MR, Agrawal N, Kim SF, Cascio MB, Fujimuro M, Ozeki Y, Takahashi M, Cheah JH, Tankou SK, Hester LD, Ferris CD, Hayward SD, Snyder SH, and Sawa A. S-nitrosylated GAPDH initiates apoptotic cell death by nuclear translocation following Siah1 binding. *Nat Cell Biol* 7: 665-674, 2005.
104. He BP, Wang JJ, Zhang X, Wu Y, Wang M, Bay B, and Chang AY. Differential reactions of microglia to brain metastasis of lung cancer. *Mol Med* 12: 161-170, 2006.



105. Henry G, and Garner WL. Inflammatory mediators in wound healing. *Surgical Clinics of North America* 83: 483-507, 2003.
106. Hentze MW, and Kühn LC. Molecular control of vertebrate iron metabolism: mRNA-based regulatory circuits operated by iron, nitric oxide, and oxidative stress. *Proceedings of the National Academy of Sciences of the United States of America* 93: 8175-8182, 1996.
107. Hesse M, Modolell M, La Flamme AC, Schito M, Fuentes JM, Cheever AW, Pearce EJ, and Wynn TA. Differential regulation of nitric oxide synthase-2 and arginase-1 by type 1/type 2 cytokines in vivo: Granulomatous pathology is shaped by the pattern of L-arginine metabolism. *J Immunol* 167: 6533-6544, 2001.
108. Hey C, Boucher J-L, Vadon-Le Goff S, Ketterer G, Wessler I, and Racke K. Inhibition of arginase in rat and rabbit alveolar macrophages by N-omega-hydroxy-D,L-inosipicine, effects on L-arginine utilization by nitric oxide synthase. *Br J Pharmacol* 121: 395-400, 1997.
109. Hibbs JJB, Taintor RR, Vavrin Z, and Rachlin EM. Nitric oxide: A cytotoxic activated macrophage effector molecule. *Biochemical and Biophysical Research Communications* 157: 87-94, 1988.
110. Hillier SC, Graham JA, Hanger CC, Godbey PS, Glenny RW, and Wagner WW, Jr. Hypoxic vasoconstriction in pulmonary arterioles and venules. *Journal of Applied Physiology* 82: 1084-1090, 1997.
111. Hockel M, Knoop C, Schlenger K, Vorndran B, Knapstein PG, and Vaupel P. Intratumoral pO<sub>2</sub> histography as predictive assay in advance cancer of the uterine cervix. *Adv Exptl Med Biol* 345: 445-450, 1994.

112. Hothersall JS, Gordge M, and Noronha-Dutra AA. Inhibition of NADPH supply by 6-aminonicotinamide: effect on glutathione, nitric oxide and superoxide in J774 cells. *FEBS Letters* 434: 97-100, 1998.
113. Hu P, Ischiropoulos H, Beckman J, and Matalon S. Peroxynitrite inhibition of oxygen consumption and sodium transport in alveolar type II cells. *Am J Physiol* 266: L628-L634, 1994.
114. Huang LE, Willmore WG, Gu J, Goldberg MA, and Bunn HF. Inhibition of hypoxia-inducible factor 1 activation by carbon monoxide and nitric oxide. Implications for oxygen sensing and signaling. *J Biol Chem* 274: 9038-9044, 1999.
115. Huie RE, and Padmaja S. The reaction of NO with superoxide. *Free Rad Res Comm* 18: 195-199, 1993.
116. Hunt TK, Twomey P, Zederfeldt B, and Dunphy JE. Respiratory gas tensions and pH in healing wounds. *Am J Surg* 114: 302-307, 1967.
117. Hussein Z, Beerah M, Grover R, Jordan B, Jeffs R, Donaldson J, Zaccardelli D, Colice G, Guntupalli K, Watson D, and Vincent J. Pharmacokinetics of the nitric oxide synthase inhibitor L-N-G-methylarginine hydrochloride in patients with septic shock. *Clinical Pharmacology and Therapeutics* 65: 1-9, 1999.
118. Ince C, and Sinaasappel M. Microcirculatory oxygenation and shunting in septic shock. *Crit Care Med* 27: 1369-1377, 1999.
119. Ip MSM, Lam B, Chan L-Y, Zheng L, Tsang KWT, Fung PCW, and Lam W-K. Circulating nitric oxide is suppressed in obstructive sleep apnea and is reversed by

- nasal continuous positive airway pressure.. *Am J Respir Crit Care Med* 162: 2166-2171, 2000.
120. Iyengar R, Stuehr DJ, and Marletta MA. Macrophage synthesis of nitrite, nitrate, and N-nitrosamines: precursors and role of the respiratory burst. *Proceedings of the National Academy of Sciences of the United States of America* 84: 6369-6373, 1987.
  121. Jackson P, Haddad P, and Dilli S. Determination of nitrate and nitrite in cured meats using high-performance liquid chromatography. *Journal of Chromatography* 295: 471-478, 1984.
  122. James PE, Thomas MP, and Jackson SK. Tissue oxygenation in sepsis; new insights from *in vivo* EPR. *NMR in Biomedicine* 17: 319-326, 2004.
  123. Janeway CA, and Medzhitov R. Innate immune recognition. *Annual Review of Immunology* 20: 197, 2002.
  124. Jiang J, Nakashima T, Liu KJ, Goda F, Shima T, and Swartz HM. Measurement of PO<sub>2</sub> in liver using EPR oximetry. *J Appl Physiol* 80: 552-558, 1996.
  125. Johnston M. Hypoxic and ischemic disorders of infants and children. Lecture for 38<sup>th</sup> meeting of Japanese Society of Child Neurology, Tokyo, Japan, July 1996. *Brain & Development* 19: 235-239, 1997.
  126. Jung F, Palmer LA, Zhou N, and Johns RA. Hypoxic regulation of inducible nitric oxide synthase via hypoxia inducible factor-1 in cardiac myocytes. *Circ Res* 86: 319-325, 2000.

127. Kahraman S, and Fiskum G. Anoxia-induced changes in pyridine nucleotide redox state in cortical neurons and astrocytes. *Neurochemical Research* 32: 799-806, 2007.
128. Kaplan NO, Swartz MN, Frech ME, and Ciotti MM. Phosphorylative and nonphosphorylative pathways of electron transfer in rat liver mitochondria. *Proc Natl Acad Sci* 42: 481-487, 1956.
129. Kaufman DL, and Mitchell JA. Intrauterine oxygen tension during the oestrous cycle in the hamster: patterns of change. *Comparative Biochemistry and Physiology Part A: Physiology* 107: 673-678, 1994.
130. Kerger H, Saltzman DJ, Menger MD, Messmer K, and Intaglietta M. Systemic and subcutaneous microvascular Po<sub>2</sub> dissociation during 4-h hemorrhagic shock in conscious hamsters. *Am J Physiol Heart Circ Physiol* 270: H827-836, 1996.
131. Keynes RG, Griffiths C, and Garthwaite J. Superoxide-dependent consumption of nitric oxide in biological media may confound *in vitro* experiments. *Biochemistry Journal* 369: 399-406, 2003.
132. Kharitonov S, Rajakulasingam K, O'Connor B, Durham S, and Barnes P. Nasal nitric oxide is increased in patients with asthma and allergic rhinitis and may be modulated by nasal glucocorticoids. *Journal of Allergy and Clinical Immunology* 99: 58-64, 1997.
133. Kilbourn R, Gross S, Jubran A, Adams J, Griffith O, Levi R, and Lodato R. NG-methyl-L-arginine inhibits tumor necrosis factor-induced hypotension: Implications for the involvement of nitric oxide. *Proc Natl Acad Sci USA* 87: 3629-3632, 1990.

134. Kilbourn RG, Jubran A, Gross SS, Griffith OW, Levi R, Adams J, and Lodato R. Reversal of endotoxin-mediated shock by N-G-methyl-L-arginine, an inhibitor of nitric oxide synthesis. *Biochem Biophys Res Commun* 172: 1132-1138, 1990.
135. Kilbourn RG, Owen-Schaub LB, Cromeens DM, Gross SS, Flaherty MJ, Santee SM, Alak AM, and Griffith OW. NG-methyl-L-arginine, an inhibitor of nitric oxide formation, reverses IL-2-mediated hypotension in dogs. *J Appl Physiol* 76: 1130-1137, 1994.
136. Kim N, Vardi Y, Padma-Nathan H, Daley J, Goldstein I, and Saenz de Tejada I. Oxygen tension regulates the nitric oxide pathway. Physiological role in penile erection. *J Clin Invest* 91: 437-442, 1993.
137. Kim SF, Huri DA, and Snyder SH. Inducible nitric oxide synthase binds, S-nitrosylates, and activates cyclooxygenase-2. *Science* 310: 1966-1970, 2005.
138. Kimura H, Weisz A, Kurashima Y, Hashimoto K, Ogura T, D'Acquisto F, Addeo R, Makuuchi M, and Esumi H. Hypoxia response element of the human vascular endothelial growth factor gene mediates transcriptional regulation by nitric oxide: control of hypoxia-inducible factor-1 activity by nitric oxide. *Blood* 95: 189-197, 2000.
139. Kimura T, Nakayama K, Penninger J, Kitagawa M, Harada H, Matsuyama T, Tanaka N, Kamijo R, Vilček J, Mak TW, and Taniguchi T. Involvement of the IRF-1 transcription factor in antiviral responses to interferons. *Science* 264: 1921-1924, 1994.
140. Kobayashi A, Hashimoto S, Kooguchi K, Kitamura Y, Onodera H, Urata Y, and Ashihara T. Expression of inducible nitric oxide synthase and inflammatory

- cytokines in alveolar macrophages of ARDS following sepsis. *Chest* 113: 1632-1639, 1998.
141. Koch CJ. Importance of antibody concentration in the assessment of cellular hypoxia by flow cytometry: EF5 and pimonidazole. *Radiation Research* 169: 677-688, 2008.
142. Koch CJ. Measurement of absolute oxygen levels in cells and tissues using oxygen sensors and 2-nitroimidazole EF5. *Methods in Enzymology* 352: 3-31, 2002.
143. Koch CJ. A thin-film culturing technique allowing rapid gas-liquid equilibration (6 sec) with no toxicity to mammalian cells. *Radiation Research* 97: 434-442, 1984.
144. Koch CJ, Stobbe CC, and Bump EA. The effect on the Km for radiosensitization at 0 degree C of thiol depletion by diethylmaleate pretreatment: quantitative differences found using the radiation sensitizing agent misonidazole or oxygen. *Radiation Research* 98: 141-153, 1984.
145. Kolodziejki PJ, Koo J-S, and Eissa NT. Regulation of inducible nitric oxide synthase by rapid cellular turnover and cotranslational down-regulation by dimerization inhibitors. *PNAS* 101: 18141-18146, 2004.
146. Kroger A, Koster M, Schroeder K, Hauser Hr, and Mueller PP. Review: Activities of IRF-1. *Journal of Interferon & Cytokine Research* 22: 5-14, 2002.
147. Kwon N, Nathan C, and Stuehr D. Reduced biopterin as a cofactor in the generation of nitrogen oxides by murine macrophages. *J Biol Chem* 264: 20496-20501, 1989.

148. Kwon NS, Nathan CF, Gilker C, Griffith OW, Matthews DE, and Stuehr DJ. L-citrulline production from L-arginine by macrophage nitric oxide synthase. The ureido oxygen derives from dioxygen. *J Biol Chem* 265: 13442-13445, 1990.
149. Lambeth JD. NOX enzymes and the biology of reactive oxygen. *Nat Rev Immunol* 4: 181-189, 2004.
150. Lancaster JR. Nitroxidative, nitrosative, and nitrative stress: Kinetic predictions of reactive nitrogen species chemistry under biological conditions. *Chem Res Toxicol* 19: 1160-1174, 2006.
151. Laszlo F, and Whittle BJR. Actions of isoform-selective and non-selective nitric oxide synthase inhibitors on endotoxin-induced vascular leakage in rat colon. *European Journal of Pharmacology* 334: 99-102, 1997.
152. Laubach V, Shesely E, Smithies O, and Sherman P. Mice lacking inducible nitric oxide synthase are not resistant to lipopolysaccharide-induced death. *PNAS* 92: 10688-10692, 1995.
153. Lazdins JK, Kuhner AL, David JR, and Karnovsky ML. Alteration of some functional and metabolic characteristics of resident mouse peritoneal macrophages by lymphocyte mediators. *J Exp Med* 148: 746-758, 1978.
154. Le Cras T, Xue C, Rengasamy A, and Johns R. Chronic hypoxia upregulates endothelial and inducible NO synthase gene and protein expression in the rat lung. *Am J Physiol* 270: L164-L170, 1996.
155. Leone AM, Palmer RM, Knowles RG, Francis PL, Ashton DS, and Moncada S. Constitutive and inducible nitric oxide synthases incorporate molecular oxygen into both nitric oxide and citrulline. *J Biol Chem* 266: 23790-23795, 1991.

156. Leopold JA, Cap A, Scribner AW, Stanton RC, and Loscalzo J. Glucose-6-phosphate dehydrogenase deficiency promotes endothelial oxidant stress and decreases endothelial nitric oxide bioavailability. *FASEB J* 15: 1771-1773, 2001.
157. Leopold JA, Dam A, Maron BA, Scribner AW, Liao R, Handy DE, Stanton RC, Pitt B, and Loscalzo J. Aldosterone impairs vascular reactivity by decreasing glucose-6-phosphate dehydrogenase activity. *Nat Med* 13: 189-197, 2007.
158. Leopold JA, Zhang Y-Y, Scribner AW, Stanton RC, and Loscalzo J. Glucose-6-phosphate dehydrogenase overexpression decreases endothelial cell oxidant stress and increases bioavailable nitric oxide. *Arterioscler Thromb Vasc Biol* 23: 411-417, 2003.
159. Levy B, Pinard E, Michel J, Tedgui A, and Seylaz J. Transmural gradient of tissue gas tensions in the canine left ventricular myocardium during coronary clamping and reactive hyperemia. *Pflugers Arch* 407: 388-395, 1986.
160. Li H, and Forstermann U. Nitric oxide in the pathogenesis of vascular disease. *J Pathol* 190: 244-254, 2000.
161. Liaudet L, Rosselet A, Schaller M, Markert M, Perret C, and Feihl F. Nonselective versus selective inhibition of inducible nitric oxide synthase in experimental endotoxic shock. *The Journal of Infectious Diseases* 177: 127-132, 1998.
162. Lin W, and Karin M. A cytokine-mediated link between innate immunity, inflammation, and cancer. *J Clin Invest* 117: 1175-1183, 2007.



163. Liu SF, and Malik AB. NF- $\kappa$ B activation as a pathological mechanism of septic shock and inflammation. *Am J Physiol Lung Cell Mol Physiol* 290: L622-645, 2006.
164. Liu X, Miller MJS, Joshi MS, Thomas DD, and Lancaster JR, Jr. Accelerated reaction of nitric oxide with O<sub>2</sub> within the hydrophobic interior of biological membranes. *PNAS* 95: 2175-2179, 1998.
165. Liu Y, Christou H, Morita T, Laughner E, Semenza GL, and Kourembanas S. Carbon monoxide and nitric oxide suppress the hypoxic induction of vascular endothelial growth factor gene via the 5' enhancer. *J Biol Chem* 273: 15257-15262, 1998.
166. Ljungkvist ASE, Bussink J, Kaanders JHAM, and van der Kogel AJ. Dynamics of tumor hypoxia measured with bioreductive hypoxic cell markers. *Radiation Research* 167: 127-145, 2007.
167. Lopez A, Lorente J, Steingrub J, Bakker J, McLuckie A, Willatts S, Brockway M, Anzueto A, Holzapfel L, Breen D, Silverman MS, Takala J, Donaldson J, Arneson C, Grove G, Grossman S, and Grover R. Multiple-center, randomized, placebo-controlled, double-blind study of the nitric oxide synthase inhibitor 546C88: Effect on survival in patients with septic shock. *Crit Care Med* 32: 21-30, 2004.
168. Lortie MJ, Ishizuka S, Schwartz DA, and Blantz RC. Bioactive products of arginine in sepsis: tissue and plasma composition after LPS and iNOS blockade. *Am J Physiol Cell Physiol* 278: C1191-C1199, 2000.

169. Louis CA, Reichner JS, Henry WL, Jr., Mastrofrancesco B, Gotoh T, Mori M, and Albina JE. Distinct arginase isoforms expressed in primary and transformed macrophages: regulation by oxygen tension. *Am J Physiol Regul Integr Comp Physiol* 274: R775-782, 1998.
170. Lowenstein CJ, Alley EW, Raval P, Snowman AM, Snyder SH, Russell SW, and Murphy WJ. Macrophage nitric oxide synthase gene: two upstream regions mediate induction by interferon gamma and lipopolysaccharide. *Proceedings of the National Academy of Sciences of the United States of America* 90: 9730-9734, 1993.
171. MacKenzie A, and Wadsworth RM. Extracellular L-arginine is required for optimal NO synthesis by eNOS and iNOS in the rat mesenteric artery wall. *British Journal of Pharmacology* 139: 1487, 2003.
172. MacMicking J, Xie Q-w, and Nathan C. Nitric oxide and macrophage function. *Annual Review of Immunology* 15: 323-350, 1997.
173. Marshall HE, and Stamler JS. Nitrosative stress-induced apoptosis through inhibition of NF-kappaB. *J Biol Chem* 277: 34223-34228, 2002.
174. Martin E, Nathan C, and Xie QW. Role of interferon regulatory factor 1 in induction of nitric oxide synthase. *J Exp Med* 180: 977-984, 1994.
175. Martin GS, Mannino DM, Eaton S, and Moss M. The epidemiology of sepsis in the United States from 1979 through 2000. *N Engl J Med* 348: 1546-1554, 2003.
176. Matejovic M, Krouzecky A, Martinkova V, Rokyta R, Kralova H, Treska V, Radermacher P, and Novak I. Selective inducible nitric oxide synthase inhibition during long-term hyperdynamic porcine bacteremia. *Shock* 21: 458-465, 2004.

177. Mateo RB, Reichner JS, Mastrofrancesco B, Kraft-Stolar D, and Albina JE. Impact of nitric oxide on macrophage glucose metabolism and glyceraldehyde-3-phosphate dehydrogenase activity. *Am J Physiol Cell Physiol* 268: C669-675, 1995.
178. McClelland RA, Panicucci R, and Rauth AM. Electrophilic intermediate in the reactions of a 2-(hydroxylamino)imidazole. A model for biological effects of reduced nitroimidazoles. *J Am Chem Soc* 107: 1762-1763, 1985.
179. McCormick CC, Li WP, and Calero M. Oxygen tension limits nitric oxide synthesis by activated macrophages. *Biochem J* 350: 709-716, 2000.
180. Mei JJM, Hursting SD, Perkins SN, and Phang JM. p53-independent inhibition of nitric oxide generation by cancer preventive interventions in ex vivo mouse peritoneal macrophages. *Cancer Letters* 129: 191-197, 1998.
181. Melillo G, Musso T, Sica A, Taylor LS, Cox GW, and Varesio L. A hypoxia-responsive element mediates a novel pathway of activation of the inducible nitric oxide synthase promoter. *J Exp Med* 182: 1683-1693, 1995.
182. Melillo G, Taylor L, Brooks A, Cox G, and Varesio L. Regulation of inducible nitric oxide synthase expression in IFN-gamma- treated murine macrophages cultured under hypoxic conditions. *J Immunol* 157: 2638-2644, 1996.
183. Merce J, Tournoy A, X. L, Mangalaboyi J, Fourrier F, Goudemand J, Gosselin B, Vallet B, and Chopin C. Effects of N-sup-omega-nitro-L-arginine methyl ester on the endotoxin-induced disseminated intravascular coagulation in porcine septic shock. *Crit Care Med* 25: 452-459, 1997.

184. Mills CD. Macrophage arginine metabolism to ornithine/urea or nitric oxide/citrulline: A life or death issue. *Crit Rev Immunol* 21: 399-426, 2001.
185. Montgomery A, Stager M, Carrico C, and Hudson L. Causes of mortality in patients with the adult respiratory distress syndrome. *Am Rev Respir Dis* 132: 485-489, 1985.
186. Morris SM. Regulation of arginine availability and its impact on NO synthesis. In: *Nitric oxide: biology and pathobiology*, edited by Ignarro LJ. San Diego: Academic Press, 2000, p. 187-197.
187. Morris SM, Jr, and Billiar TR. New insights into the regulation of inducible nitric oxide synthesis. *Am J Physiol Endocrinol Metab* 266: E829-839, 1994.
188. Morris SM, Jr., Kepka-Lenhart D, and Chen L-C. Differential regulation of arginases and inducible nitric oxide synthase in murine macrophage cells. *Am J Physiol Endocrinol Metab* 275: E740-747, 1998.
189. Musial A, and Eissa NT. Inducible Nitric-oxide synthase is regulated by the proteasome degradation pathway. *J Biol Chem* 276: 24268-24273, 2001.
190. Nalwaya N, and Deen WM. Nitric oxide, oxygen, and superoxide formation and consumption in macrophage cultures. *Chemical Research in Toxicology* 18: 486-493, 2005.
191. Nathan CF, Karnovsky ML, and David JR. Alterations of macrophage functions by mediators from lymphocytes. *J Exp Med* 133: 1356-1376, 1971.
192. Nessel CC, Henry WL, Jr., Mastrofrancesco B, Reichner JS, and Albina JE. Vestigial respiratory burst activity in wound macrophages. *Am J Physiol Regul Integr Comp Physiol* 276: R1587-1594, 1999.

193. Nicholson SC, Hahn RT, Grobmyer SR, Brause JE, Hafner A, Potter S, Devereux RB, and Nathan CF. Echocardiographic and survival studies in mice undergoing endotoxic shock: Effects of genetic ablation of inducible nitric oxide synthase and pharmacologic antagonism of platelet-activating factor. *Journal of Surgical Research* 86: 198-205, 1999.
194. Ninikoski J, Heughan C, and Hunt TK. Oxygen and carbon dioxide tensions in experimental wounds. *Surg Gynecol Obstet* 133: 1003-1007, 1971.
195. Nishi K, Oda T, Takabuchi S, Oda S, Fukuda K, Adachi T, Semenza GL, Shingu K, and Hirota K. LPS induces hypoxia-inducible factor 1 activation in macrophage-differentiated cells in a reactive oxygen species-dependent manner. *Antioxidants & Redox Signal* 10: 983-995, 2008.
196. Numagami Y, Zubrow A, Mishra O, and Delivoria-Papadopoulos M. Lipid free radical generation and brain cell membrane alteration following nitric oxide synthase inhibition during cerebral hypoxia in the newborn piglet. *J Neurochem* 69: 1542-1547, 1997.
197. Ochoa J, Udekwu A, Billiar T, Curran R, Cerra F, Simmons R, and Peitzman A. Nitrogen oxide levels in patients after trauma and during sepsis. *Ann Surg* 214: 621-626, 1991.
198. Offner PJ, Robertson FM, and Pruitt BA. Effects of nitric oxide synthase inhibition on regional blood flow in a porcine model of endotoxic shock. *J Trauma* 39: 338-343, 1995.
199. Okamoto I, Abe M, Shibata K, Shimizu N, Sakata N, Katsuragi T, and Tanaka K. Evaluating the role of inducible nitric oxide synthase using a novel and selective

- nitric oxide inhibitor in septic lung injury produced by cecal ligation and puncture. *Am J Respir Crit Care Med* 162: 716-722, 2000.
200. Osawa Y, Lee HT, Hirschman CA, Xu D, and Emala CW. Lipopolysaccharide-induced sensitization of adenylyl cyclase activity in murine macrophages. *Am J Physiol Cell Physiol* 290: C143-C151, 2006.
201. Otto C, Vijayasathy C, Fox J, and Baumgardner J. Hypoxic culture inhibits inducible nitric oxide synthase dimerization. *Shock* 15: 91, 2001.
202. Otto CM, and Baumgardner JE. Effect of culture PO<sub>2</sub> on macrophage (RAW 264.7) nitric oxide production. *Am J Physiol Cell Physiol* 280: C280-287, 2001.
203. Palazzolo-Ballance AM, Suquet C, and Hurst JK. Pathways for intracellular generation of oxidants and tyrosine nitration by a macrophage cell line. *Biochemistry* 46: 7536-7548, 2007.
204. Palmer LA, Gaston B, and Johns RA. Normoxic stabilization of hypoxia-inducible factor-1 expression and activity: Redox-dependent effect of nitrogen oxides. *Mol Pharmacol* 58: 1197-1203, 2000.
205. Palmer LA, Semenza GL, Stoler MH, and Johns RA. Hypoxia induces type II NOS gene expression in pulmonary artery endothelial cells via HIF-1. *Am J Physiol Lung Cell Mol Physiol* 274: L212-219, 1998.
206. Palmer RMJ, Ashton DS, and Moncada S. Vascular endothelial cells synthesize nitric oxide from L-arginine. *Nature* 333: 664-666, 1988.
207. Pervin S, Singh R, Hernandez E, Wu G, and Chaudhuri G. Nitric oxide in physiologic concentrations targets the translational machinery to increase the

- proliferation of human breast cancer cells: Involvement of mammalian target rapamycin/eIF4E pathway. *Cancer Res* 67: 289-299, 2007.
208. Pollard JW. Trophic macrophages in development and disease. *Nat Rev Immunol* 9: 259-270, 2009.
209. Presta A, Siddhanta U, Wu C, Sennequier N, Huang L, Abu-Soud H, Erzurum S, and Stuehr D. Comparative functioning of dihydro- and tetrahydropterins in supporting electron transfer, catalysis, and subunit dimerization in inducible nitric oxide synthase. *Biochemistry* 37: 298-310, 1998.
210. Ransohoff RM, and Perry VH. Microglial physiology: Unique stimuli, specialized responses. *Annual Review of Immunology* 27: 119-145, 2009.
211. Reichner J, Meszaros A, Louis C, Henry Jr W, Mastrofrancesco B, Martin B, and Albina J. Molecular and metabolic evidence for restricted expression of inducible nitric oxide synthase in healing wounds. *Am J Pathol* 154: 1097-1104, 1999.
212. Reiter TA. NO\* chemistry: a diversity of targets in the cell. *Redox Report* 11: 194-206, 2006.
213. Remensnyder JP, and Majno G. Oxygen gradients in healing wounds. *Am J Pathol* 52: 301-323, 1968.
214. Rengasamy A, and Johns RA. Determination of Km for oxygen of nitric oxide synthase isoforms. *J Pharmacol Exp Ther* 276: 30-33, 1996.
215. Rhee KY, Erdjument-Bromage H, Tempst P, and Nathan CF. S-nitroso proteome of Mycobacterium tuberculosis: Enzymes of intermediary metabolism and antioxidant defense. *PNAS* 102: 467-472, 2005.

216. Robinson M, Baumgardner JE, Fox J, and Otto CM. Abstract: Oxygen substrate limitation regulates nitric oxide production by cytokine-stimulated macrophages. *Shock* 23: P156, 2005.
217. Robinson M, Baumgardner JE, Fox J, and Otto CM. The kinetics of nitric oxide production by activated hypoxic macrophages. *Proceedings of the American Thoracic Society* 2: A747, 2005.
218. Robinson MA, Baumgardner JE, Good VP, and Otto CM. Physiological and hypoxic O<sub>2</sub> tensions rapidly regulate NO production by stimulated macrophages. *Am J Physiol Cell Physiol* 294: C1079-1087, 2008.
219. Roland CR, Nakafusa Y, and Flye MW. Gadolinium chloride inhibits lipopolysaccharide-induced mortality and in vivo prostaglandin E<sub>2</sub> release by splenic macrophages. *Gastrointest Surg* 3: 301-307, 1999.
220. Ross M, and Iadecola C. Nitric oxide synthase expression in cerebral ischemia: Neurochemical, immunocytochemical, and molecular approaches. *Methods in Enzymology* 269: 408-426, 1996.
221. Saetre T, Hovig T, Roger M, Gundersen Y, and Aasen AO. Hepatocellular damage in porcine endotoxemia: beneficial effects of selective versus non-selective nitric oxide synthase inhibition? *Scand J Clin Lab Invest* 61: 503-512, 2001.
222. Sandau KB, Fandrey J, and Brune B. Accumulation of HIF-1alpha under the influence of nitric oxide. *Blood* 97: 1009-1015, 2001.
223. Sandau KB, Zhou J, Kietzmann T, and Brune B. Regulation of the hypoxia-inducible factor 1alpha by the inflammatory mediators nitric oxide and tumor



- necrosis factor-alpha in contrast to desferroxamine and phenylarsine oxide. *J Biol Chem* 276: 39805-39811, 2001.
224. Sarih M, Souvannavong V, and Adam A. Nitric oxide synthase induces macrophage death by apoptosis. *Biochemical and Biophysical Research Communications* 191: 503-508, 1993.
225. Sato K, Rodman D, and McMurtry I. Hypoxia inhibits increased ETB receptor-mediated NO synthesis in hypertensive rat lungs. *Am J Physiol (Lung Cell Mol Physiol)* 276: L511-L581, 1999.
226. Satriano J. Arginine pathways and the inflammatory response: Interregulation of nitric oxide and polyamines: Review article. *Amino Acids* 26: 321-329, 2004.
227. Scholz R, Thurman RG, Williamson JR, Chance B, and Bucher T. Flavin and pyridine nucleotide oxidation-reduction changes in perfused rat liver. I. Anoxia and subcellular localization of fluorescent flavoproteins. *J Biol Chem* 244: 2317-2324, 1969.
228. Seidenfeld J, Pohl D, Bell R, Harris G, and Johanson Jr. W. Incidence, site, and outcome of infections in patients with adult respiratory distress syndrome. *Am Rev Respir Dis* 134: 12-16, 1986.
229. Semenza G. HIF-1: mediator of physiological and pathophysiological responses to hypoxia. *J Appl Physiol* 88: 1474-1480, 2000.
230. Semenza GL. HIF-1 and mechanisms of hypoxia sensing. *Current Opinion in Cell Biology* 13: 167-171, 2001.
231. Semenza GL. Hypoxia-inducible factor 1 and cancer pathogenesis. *IUBMB Life* 60: 591-597, 2008.

232. Sennequier N, Wolan D, and Stuehr DJ. Antifungal imidazoles block assembly of inducible NO synthase into an active dimer. *J Biol Chem* 274: 930-938, 1999.
233. Serbina NV, Salazar-Mather TP, Biron CA, Kuziel WA, and Pamer EG. TNF/iNOS-producing dendritic cells mediate innate immune defense against bacterial infection. *Immunity* 19: 59-70, 2003.
234. Shen S, Yu S, Binek J, Chalimoniuk M, Zhang X, Lo S, Hannink M, Wu J, Fritsche K, Donato R, and Sun GY. Distinct signaling pathways for induction of type II NOS by IFN $\gamma$  and LPS in BV-2 microglial cells. *Neurochemistry International* 47: 298-307, 2005.
235. Sica A, and Bronte V. Altered macrophage differentiation and immune dysfunction in tumor development. *J Clin Invest* 117: 1155-1166, 2007.
236. Silver IA. The measurement of oxygen tension in healing tissue. *Progr Resp Res* 3: 124-135, 1969.
237. Sinaasappel M, van Iterson M, and Ince C. Microvascular oxygen pressure in the pig intestine during haemorrhagic shock and resuscitation. *J Physiol (Lond)* 514: 245-253, 1999.
238. Sogawa K, Numayama-Tsuruta K, Ema M, Abe M, Abe H, and Fujii-Kuriyama Y. Inhibition of hypoxia-inducible factor 1 activity by nitric oxide donors in hypoxia. *PNAS* 95: 7368-7373, 1998.
239. Sono M, Stuehr DJ, Ikeda-Saito M, and Dawson JH. Identification of nitric oxide synthase as a thiolate-ligated heme protein using magnetic circular dichroism spectroscopy. *J Biol Chem* 270: 19943-19948, 1995.

240. Sonoki T, Nagasaki A, Gotoh T, Takiguchi M, Takeya M, Matsuzaki H, and Mori M. Coinduction of nitric-oxide synthase and arginase I in cultured rat peritoneal macrophages and rat tissues *in vivo* by lipopolysaccharide. *J Biol Chem* 272: 3689-3693, 1997.
241. Stein AM, Kaplan NO, and Ciotti MM. Pyridine Nucleotide Transhydrogenase. VII. Determination of the reactions with coenzyme analogues in mammalian tissues. *J Biol Chem* 234: 979-986, 1959.
242. Stevens E. Use of plastic materials in oxygen-measuring systems. *J Appl Physiol* 72: 801-804, 1992.
243. Stoclet J, Martinez M, Ohlmann P, Chasserot S, Schott C, Kleschyov A, Schneider F, and Andriantsitohaina R. Induction of nitric oxide synthase and dual effects of nitric oxide and cyclooxygenase products in regulation of arterial contraction in human septic shock. *Circulation* 100: 107-112, 1999.
244. Strand OA, Leone AM, Giercksky K, Skovlund E, and Kirkeboen KA. N-G-monomethyl-L-arginine improves survival in a pig model of abdominal sepsis. *Crit Care Med* 26: 1490-1499, 1998.
245. Stuehr D, Cho H, Kwon N, Weise M, and Nathan C. Purification and characterization of the cytokine-induced macrophage nitric oxide synthase: An FAD- and FMN-containing flavoprotein. *Proc Natl Acad Sci USA* 88: 7773-7777, 1991.
246. Stuehr DJ, and Nathan CF. Nitric oxide. A macrophage product responsible for cytostasis and respiratory inhibition in tumor target cells. *J Exp Med* 169: 1543-1555, 1989.

247. Stuehr DJ, Santolini J, Wang Z-Q, Wei C-C, and Adak S. Update on mechanism and catalytic regulation in the NO synthases. *J Biol Chem* 279: 36167-36170, 2004.
248. Suchyta M, Orme Jr. J, and Morris A. The changing face of organ failure in ARDS. *Chest* 124: 1871-1879, 2003.
249. Szabo C, Southan G, and Thiemermann C. Beneficial effects and improved survival in rodent models of septic shock with S-methylisothiurea sulfate, a potent and selective inhibitor of inducible nitric oxide synthase. *PNAS* 91: 12472-12476, 1994.
250. Tenu J-P, Lepoivre M, Moali C, Brollo M, Mansuy D, and Boucher J-L. Effects of the new arginase inhibitor N[omega]-hydroxy-nor-arginine on NO synthase activity in murine macrophages. *Nitric Oxide* 3: 427-438, 1999.
251. Thomas DD, Liu X, Kantrow SP, and Lancaster JR, Jr. The biological lifetime of nitric oxide: Implications for the perivascular dynamics of NO and O<sub>2</sub>. *PNAS* 98: 355-360, 2001.
252. Titheradge M. Nitric oxide in septic shock. *Biochemica et Biophysica Acta* 1411: 437-455, 1999.
253. Torres Filho I, Kerger H, and Intaglietta M. pO<sub>2</sub> measurements in arteriolar networks. *Microvascular Research* 51: 202-212, 1996.
254. Towell ME, Lysak I, Layne EC, and Bessman SP. Tissue oxygen tension in rabbits measured with a galvanic electrode. *J Appl Physiol* 41: 245-250, 1976.
255. Toyokuni S. Role of iron in carcinogenesis: Cancer as a ferrototoxic disease. *Cancer Sci* 100: 9-16, 2009.

256. Trager K, Radermacher P, Rieger KM, Grover R, Vlatten A, Iber T, Adler J, Georgieff M, and Santak B. Norepinephrine and N-G-monomethyl-L-arginine in hyperdynamic septic shock in pigs: Effects on intestinal oxygen exchange and energy balance. *Crit Care Med* 28: 2007-2014, 2000.
257. Trager K, Radermacher P, Rieger KAREN M, Vlatten A, Vogt J, Iber T, Adler J, Wachter U, Grover R, Georgieff M, and Santak B. Norepinephrine and Nomega - monomethyl-L-arginine in porcine septic shock. Effects on hepatic O<sub>2</sub> exchange and energy balance. *Am J Respir Crit Care Med* 159: 1758-1765, 1999.
258. Tsai K-J, Hung I-J, Chow CK, Stern A, Chao SS, and Chiu DT-Y. Impaired production of nitric oxide, superoxide, and hydrogen peroxide in glucose 6-phosphate-dehydrogenase-deficient granulocytes. *FEBS Letters* 436: 411-414, 1998.
259. Tuttle SW, Maity A, Oprysko PR, Kachur AV, Ayene IS, Biaglow JE, and Koch CJ. Detection of reactive oxygen species via endogenous oxidative pentose phosphate cycle activity in response to oxygen concentration: Implications for the mechanism of HIF-1alpha stabilization under moderate hypoxia. *J Biol Chem* 282: 36790-36796, 2007.
260. Tzeng E, Billiar T, Robbins P, Loftus M, and Stuehr D. Expression of human inducible nitric oxide synthase in a tetrahydrobiopterin (H4B)-deficient cell line: H4B promotes assembly of enzyme subunits into an active dimer. *Proc Natl Acad Sci USA* 92: 11771-11775, 1995.

261. Vakkala M, Kahlos K, Lakari E, Paakko P, Kinnula V, and Soini Y. Inducible nitric oxide synthase expression, apoptosis, and angiogenesis in *in situ* and invasive breast carcinomas. *Clin Cancer Res* 6: 2408-2416, 2000.
262. Van der Vliet A, Eiserich J, Kaur H, Cross C, and Halliwell B. Nitrotyrosine as biomarker for reactive nitrogen species. *Methods in Enzymology* 269: 175-184, 1996.
263. Vanderkooi JM, Erecinska M, and Silver IA. Oxygen in mammalian tissue: methods of measurement and affinities of various reactions. *Am J Physiol Cell Physiol* 260: C1131-1150, 1991.
264. Varnes M, Tuttle SW, and Biaglow JE. Nitroheterocyclic metabolism in mammalian cells: Stimulation of hexose monophosphate shunt. *Biochem Pharmacol* 33: 1671-1677, 1984.
265. Vincendeau P, and Daulouede S. Macrophage cytostatic effect on *Trypanosoma muscoli* involves an L- arginine-dependent mechanism. *J Immunol* 146: 4338-4343, 1991.
266. Vollmar B, Conzen PF, Kerner T, Habazettl H, Vierl M, Waldner H, and Peter K. Blood flow and tissue oxygen pressures of liver and pancreas in rats: Effects of volatile anesthetics and of hemorrhage. *Anesthesia & Analgesia* 75: 421-430, 1992.
267. Walker G, Pfeilschifter J, and Kunz D. Mechanisms of suppression of inducible nitric oxide synthase (iNOS) expression in interferon (IFN)-gamma -stimulated RAW 264.7 cells by dexamethasone. Evidence for glucocorticoid-induced

- degradation of iNOS protein by calpain as a key step in post-transcriptional regulation. *J Biol Chem* 272: 16679-16687, 1996.
268. Walker G, Pfeilschifter J, Otten U, and Kunz D. Proteolytic cleavage of inducible nitric oxide synthase (iNOS) by calpain I. *Biochimica et Biophysica Acta (BBA) - General Subjects* 1568: 216-224, 2001.
269. Wang F, Sekine H, Kikuchi Y, Takasaki C, Miura C, Heiwa O, Shuin T, Fujii-Kuriyama Y, and Sogawa K. HIF-1[alpha]-prolyl hydroxylase: molecular target of nitric oxide in the hypoxic signal transduction pathway. *Biochemical and Biophysical Research Communications* 295: 657-662, 2002.
270. Wang WW, Jenkinson CP, Griscavage JM, Kern RM, Arabolos NS, Byrns RE, Cederbaum SD, and Ignarro LJ. Co-induction of arginase and nitric oxide synthase in murine macrophages activated by lipopolysaccharide. *Biochemical and Biophysical Research Communications* 210: 1009-1016, 1995.
271. Washburn E editor. *International Critical Tables of Numerical Data, Physics, Chemistry, and Technology*. Knovel, 1926-1930; 2003, p. 259.
272. Watson D, Grover R, Anzueto A, Lorente J, Smithies M, Bellomo R, Guntupalli K, Grossman S, Donaldson J, and Le Gall J. Cardiovascular effects of the nitric oxide synthase inhibitor N-G-methyl-L-arginine hydrochloride (546C88) in patients with septic shock: Results of a randomized, double-blind, placebo-controlled multicenter study (study no. 144-002). *Crit Care Med* 32: 13-20, 2004.
273. Weathersby PK, and Homer LD. Solubility of inert gases in biological fluids and tissues: a review. *Undersea Biomedical Research* 7: 277-296, 1980.

274. Wenger RH. Cellular adaptation to hypoxia: O<sub>2</sub>-sensing protein hydroxylases, hypoxia inducible transcription factors, and O<sub>2</sub>-regulated gene expression. *FASEB J* 16: 1151-1162, 2002.
275. Werner E, Gorren A, Heller R, Werner-Felmayer G, and Mayer B. Tetrahydrobiopterin and nitric oxide: Mechanistic and pharmacological aspects. *Exp Biol Med* 228: 1291-1302, 2003.
276. Werner E, Werner-Felmayer G, Fuchs D, Hausen A, Reibnegger G, Yim J, Pfleiderer W, and Wachter H. Tetrahydrobiopterin biosynthetic activities in human macrophages, fibroblasts, THP-1, and T 24 cells: GTP-cyclohydrolase I is stimulated by interferon-gamma, and 6-pyruvoyl tetrahydropterin synthase and sepiapterin reductase are constitutively present. *J Biol Chem* 265: 3189-3192, 1990.
277. Werner E, Werner-Felmayer G, Fuchs D, Hausen A, Reibnegger G, Yim J, and Wachter H. Impact of tumour necrosis factor-alpha and interferon-gamma on tetrahydrobiopterin synthesis in murine fibroblasts and macrophages. *Biochem J* 280: 709-714, 1991.
278. Werner E, Werner-Felmayer G, Weiss G, and Wachter H. Stimulation of tetrahydrobiopterin synthesis by cytokines in human and in murine cells. In: *Chemistry and Biology of Pteridines and Folates*, edited by Ayline Jea. New York: Plenum Press, 1993, p. 203-209.
279. West JB. *Respiratory physiology: the essentials*. Philadelphia, PA: Lippincott Williams & Wilkins, 2005.



280. Wiener CM, Booth G, and Semenza GL. In vivo expression of mRNAs encoding hypoxia-inducible factor 1. *Biochemical and Biophysical Research Communications* 225: 485-488, 1996.
281. Wilson DF. Quantifying the role of oxygen pressure in tissue function. *Am J Physiol Heart Circ Physiol* 294: H11-13, 2008.
282. Wilson DF, Lee WMF, Makonnen S, Finikova O, Apreleva S, and Vinogradov SA. Oxygen pressures in the interstitial space and their relationship to those in the blood plasma in resting skeletal muscle. *J Appl Physiol* 101: 1648-1656, 2006.
283. Wink DA, Ridnour LA, Hussain SP, and Harris CC. The reemergence of nitric oxide and cancer. *Nitric Oxide* 19: 65-67, 2008.
284. Wink DA, Vodovotz Y, Laval J, Laval F, Dewhirst MW, and Mitchell JB. The multifaceted roles of nitric oxide in cancer. *Carcinogenesis* 19: 711-721, 1998.
285. Witte MB, and Barbul A. General principles of wound healing. *Surgical Clinics of North America* 77: 509-528, 1997.
286. Wu G, and Morris SM. Arginine metabolism: nitric oxide and beyond. *Biochem J* 336: 1-17, 1998.
287. Xie Q-w, Leung M, Fuortes M, Sassa S, and Nathan C. Complementation analysis of mutants of nitric oxide synthase reveals that the active site requires two hemes. *PNAS* 93: 4891-4896, 1996.
288. Xie QW, Whisnant R, and Nathan C. Promoter of the mouse gene encoding calcium-independent nitric oxide synthase confers inducibility by interferon gamma and bacterial lipopolysaccharide. *J Exp Med* 177: 1779-1784, 1993.

289. Xiong Y, Karupiah G, Hogan SP, Foster PS, and Ramsay AJ. Inhibition of allergic airway inflammation in mice lacking nitric oxide synthase 2. *J Immunol* 162: 445-452, 1999.
290. Xue C, and Johns R. Upregulation of nitric oxide synthase correlates temporally with onset of pulmonary vascular remodeling in the hypoxic rat. *Hypertension* 28: 743-753, 1996.
291. Yamaguchi H, Kidachi Y, Umetsu H, and Ryoyama K. L-NAME inhibits tumor cell progression and pulmonary metastasis of r / m HM-SFME-1 cells by decreasing NO from tumor cells and TNF- $\alpha$  from macrophages. *Molecular and Cellular Biochemistry* 312: 103-112, 2008.
292. Yamamoto Y, Henrich M, Snipes RL, and Kummer W. Altered production of nitric oxide and reactive oxygen species in rat nodose ganglion neurons during acute hypoxia. *Brain Research* 961: 1-9, 2003.
293. Yamasaki K, Edington HDJ, McClosky C, Tzeng E, Lizonova A, Kovcsdl I, Steed DL, and Billiar TR. Reversal of impaired wound repair in iNOS-deficient mice by topical adenoviral-mediated iNOS gene transfer. *J Clin Invest* 101: 967-971, 1998.
294. Zani BG, and Bohlen HG. Transport of extracellular L-arginine via cationic amino acid transporter is required during in vivo endothelial nitric oxide production. *Am J Physiol Heart Circ Physiol* 289: H1381-H1390, 2005.
295. Ziegler M. Sleep disorders and the failure to lower nocturnal blood pressure. *Current Opinion in Nephrology and Hypertension* 12: 97-102, 2003.

296. Zulueta JJ, Sawhney R, Kayyali U, Fogel M, Donaldson C, Huang H, Lanzillo JJ, and Hassoun PM. Modulation of inducible nitric oxide synthase by hypoxia in pulmonary artery endothelial cells. *Am J Respir Cell Mol Biol* 26: 22-30, 2002.